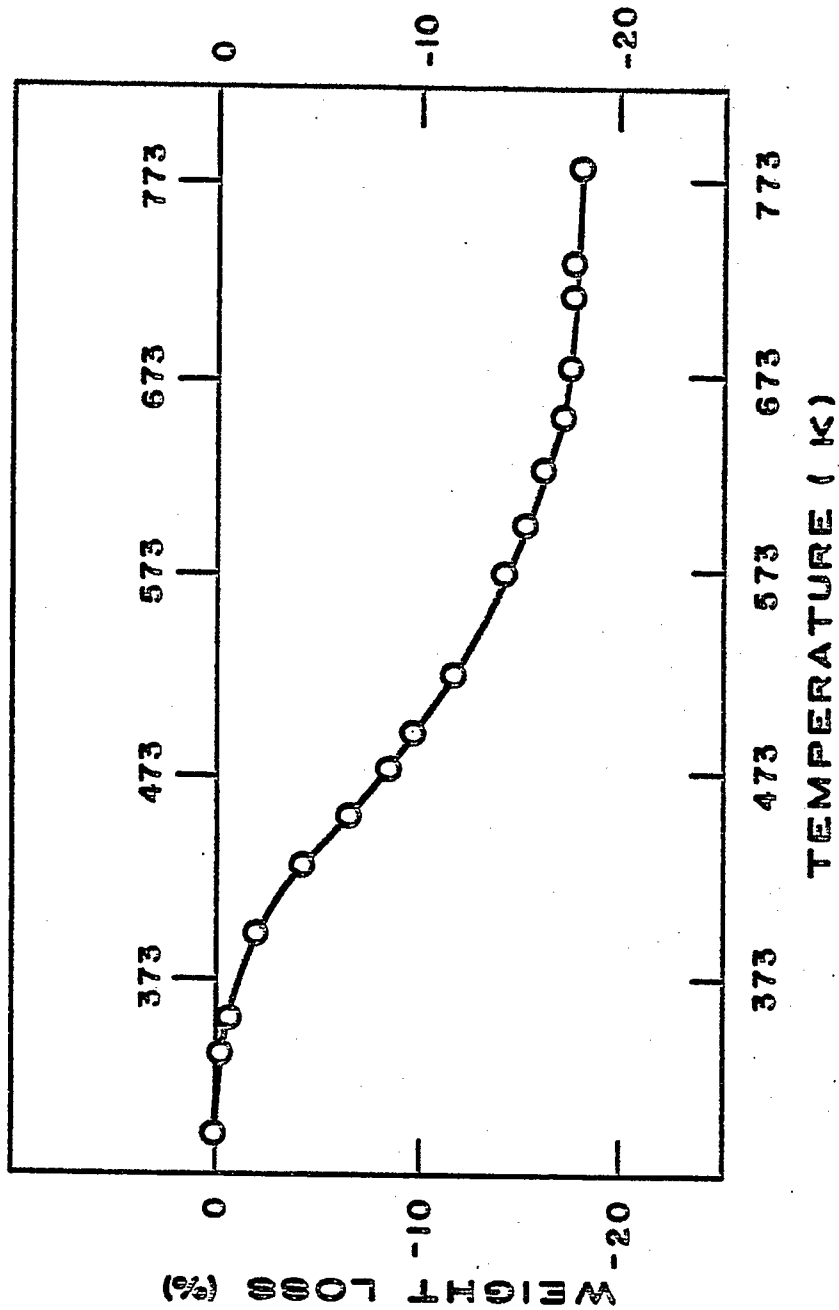
WEIGHT LOSS (%)
0
-10
-20
373
473
573
673
773
TEMPERATURE (K)

Figure 37

Reduction of Raney Catalysts at 648 K

Hydrogen Atmosphere

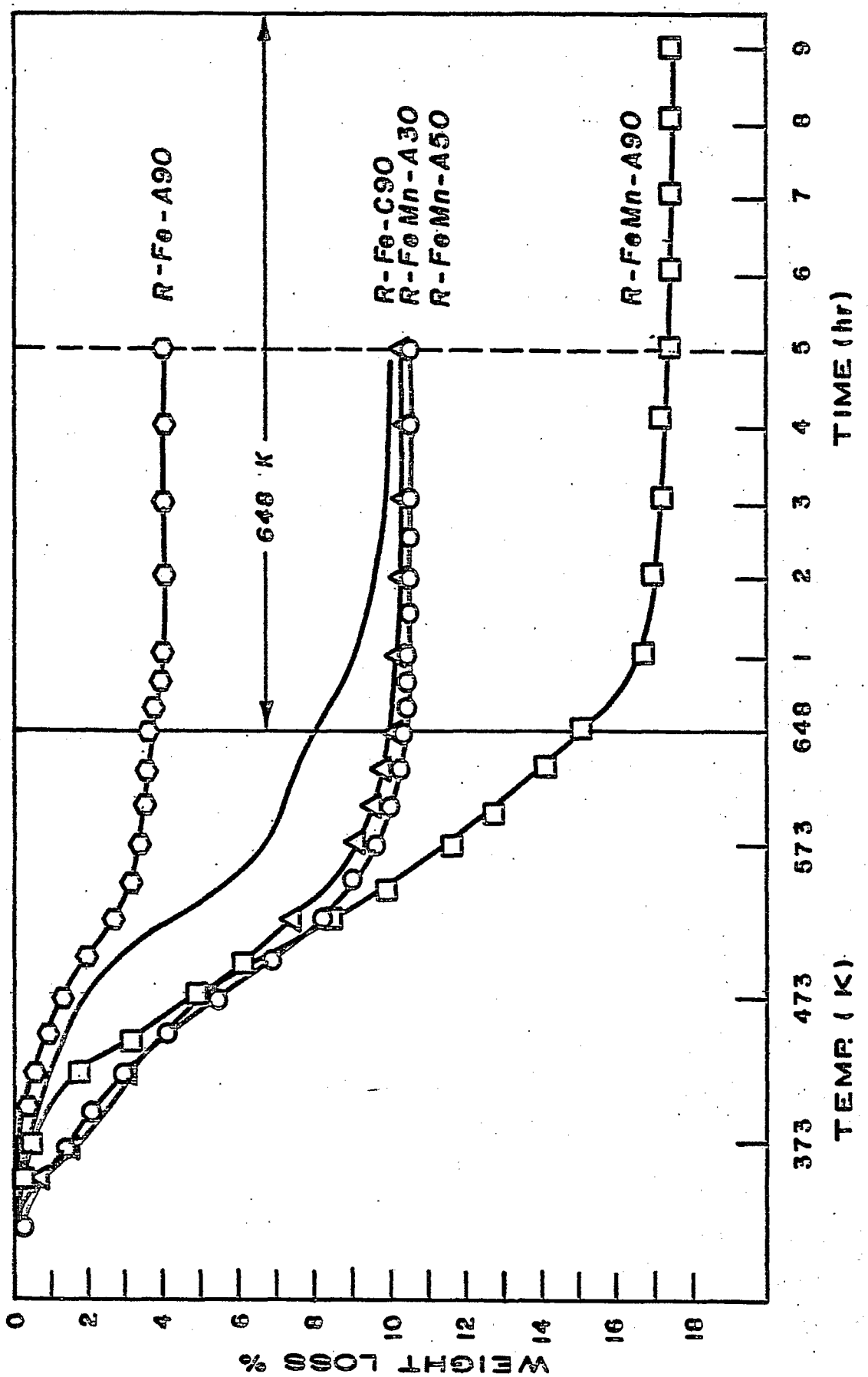
R-Fe-A90
R-Fe-C90
R-FeMn-A30
R-FeMn-A50
R-FeMn-A90
648 K
WEIGHT LOSS %
0
2
4
6
8
10
12
14
16
18
TEMP. (K)
373
473
573
648
TIME (hr)
1
2
3
4
5
6
7
8
9

Catalyst Screening Test

A series of preliminary experiments were conducted for the catalyst screening test. First, the relative response factors of the components in the product from the hydrogenation of carbon monoxide were determined with a gas chromatograph to make a quantitative analysis of the product and the results are contained in Appendix E.

Secondly, the flowrate of the reactant gas mixture (H_2/CO = 2.0) was calibrated at the reaction condition (pressure = 1465 KPa) with a mass flowmeter controller to find a proper flowrate of the reactant gas for a desired space velocity from a calibration chart (Appendix F). A series of exploratory fixed-bed experiments were carried out to find a proper range of process variables for the catalyst screening test such as temperature, pressure, and space velocity. The hydrogen-to-carbon monoxide ratio of the reactant gas was fixed at 2.0, under which condition the deposition of carbon was expected to be negligible. The range of process variables was determined to achieve a differential reaction condition, that is, the conversion of carbon monoxide was low enough to ensure a nearly isothermal condition, to minimize the product inhibition effect on the reaction, and to prevent catalyst deactivation. The results of the exploratory fixed-bed experiments are contained in Appendix F.

Based on the above tests the following reaction conditions were chosen as standard conditions for the catalyst screening investigation:

H_2/CO: 2.0

Reaction temperature: 423 to 473 K

Reactor pressure: 1465 KPa (200 psig)

Space velocity: 3.0 $cm^3 g^{-1} s^{-1}$.

All the Raney catalysts (iron and iron-manganese) were reduced at 648 K for 5 hours and the precipitated catalysts (iron and iron-manganese) were reduced at 673 K for 5 hours in flowing hydrogen. The reduction condition for each type of catalyst was chosen based on the thermogravimetric reduction study. The initial induction time, during which the catalyst activity and selectivity were stabilized, was found to be dependent on the catalyst type. Therefore, each catalyst tested was pretreated in the carbon monoxide and hydrogen mixture gas at the reaction condition (temperature = 423 K) until it showed a stable activity and selectivity prior to each activity test.

Screening Test with the Raney Iron Catalysts

Catalyst activity. A series of catalyst activity screening tests has been carried out with the Raney iron catalysts at the standard reaction condition.

The catalyst activities, in terms of carbon monoxide conversion, and product selectivities are listed in Table 11. The variation of carbon monoxide conversion with temperature for Raney iron catalysts prepared by the alloy addition and by the caustic addition method are presented in Figures 38 and 39, respectively. The Raney iron catalyst prepared at 363 K (R-Fe-A90) exhibited the highest activity, in terms of carbon monoxide conversion, in the temperature range of 423 to 443 K, whereas at 453 K the Raney iron catalyst prepared at 323 K exhibited higher activity than the R-Fe-A90 catalyst. This change in the order of catalytic activity with

Table 11

Fixed-Bed Evaluation of Iron Catalysts

Pressure = 1465 KPa (200 psig); $H_2/CO = 2.0$;

Space Velocity = 3.0 $cm^3 g^{-1} s^{-1}$

Catalyst Type	Temp. (K)	Conversion (%)	Product Carbon Atom Selectivity (%)				
			C_1	C_2-C_4	C_5^+	ROH[a]	CO_2
R-Fe-A25	423	1.1	33.5	46.7	13.9	1.0	4.8
	433	2.4	35.3	43.5	12.2	2.7	6.4
	443	4.5	30.1	41.8	15.6	3.3	9.3
	453	9.8	26.5	39.1	14.7	2.5	17.2
R-Fe-A50	423	1.2	45.5	36.5	12.1	1.0	5.0
	433	2.3	31.1	44.3	13.9	2.3	7.9
	443	5.1	28.9	41.1	14.3	3.1	12.8
	453	14.2	20.2	37.9	15.0	1.3	25.6
R-Fe-A90	423	1.3	34.2	40.3	17.5	3.9	4.1
	433	3.3	35.9	39.2	16.0	2.4	6.5
	443	5.4	31.4	39.7	15.9	3.6	9.4
	453	11.5	26.2	37.6	16.2	3.2	16.7
R-Fe-A90[b]	423	1.7	25.9	40.5	14.7	15.2	3.7
	433	3.5	29.2	42.5	18.7	2.3	7.2
	443	6.6	26.3	41.4	14.6	8.2	10.1
	453	10.2	25.1	41.8	14.9	1.7	16.5
ppt Fe	423	1.0	45.7	33.6	10.0	6.4	4.3
	433	2.0	39.4	37.5	14.3	5.3	3.5
	443	3.7	36.8	38.6	15.1	3.8	5.6
	453	7.4	34.9	37.3	15.3	3.5	9.1

Table 11 - Continued

Catalyst Type	Temp. (K)	Conversion (%)	Product Carbon Atom Selectivity (%)				
			C_1	C_2-C_4	C_{5+}	ROH[a]	CO_2
R-Fe-C25	423	1.3	31.9	44.6	14.9	4.9	3.7
	433	2.9	31.0	42.4	16.7	4.4	5.4
	443	5.8	29.0	40.1	15.2	7.3	8.3
	453	10.6	26.3	38.4	16.4	5.6	13.3
R-Fe-C50	423	1.3	32.9	44.4	14.3	4.4	4.0
	433	3.4	30.6	41.6	18.2	3.6	6.0
	443	6.3	29.9	41.1	15.0	4.7	9.2
R-Fe-C90	423	1.5	37.4	38.2	15.4	3.8	5.2
	433	2.5	31.3	43.2	17.8	0.7	7.0
	443	7.4	27.9	40.6	15.9	2.0	13.6
R-Fe-C90 (10%)	423	0.8	53.6	34.9	18.3	0.9	2.3
	433	1.4	35.6	44.6	14.6	0.8	4.5
	443	3.3	31.2	42.5	16.3	2.6	7.4
	453	5.1	30.5	42.5	15.4	1.4	10.2

[a]Alcohols.

[b]Alloy from Alpha Products.

Figure 38

Activity of Raney Iron Catalyst for
Carbon Monoxide Conversion

Catalyst: Prepared by Alloy Addition Technique

Pressure = 1465 KPa; H_2/CO = 2.0;

Space Velocity = 3.0 $cm^3g^{-1}s^{-T}$

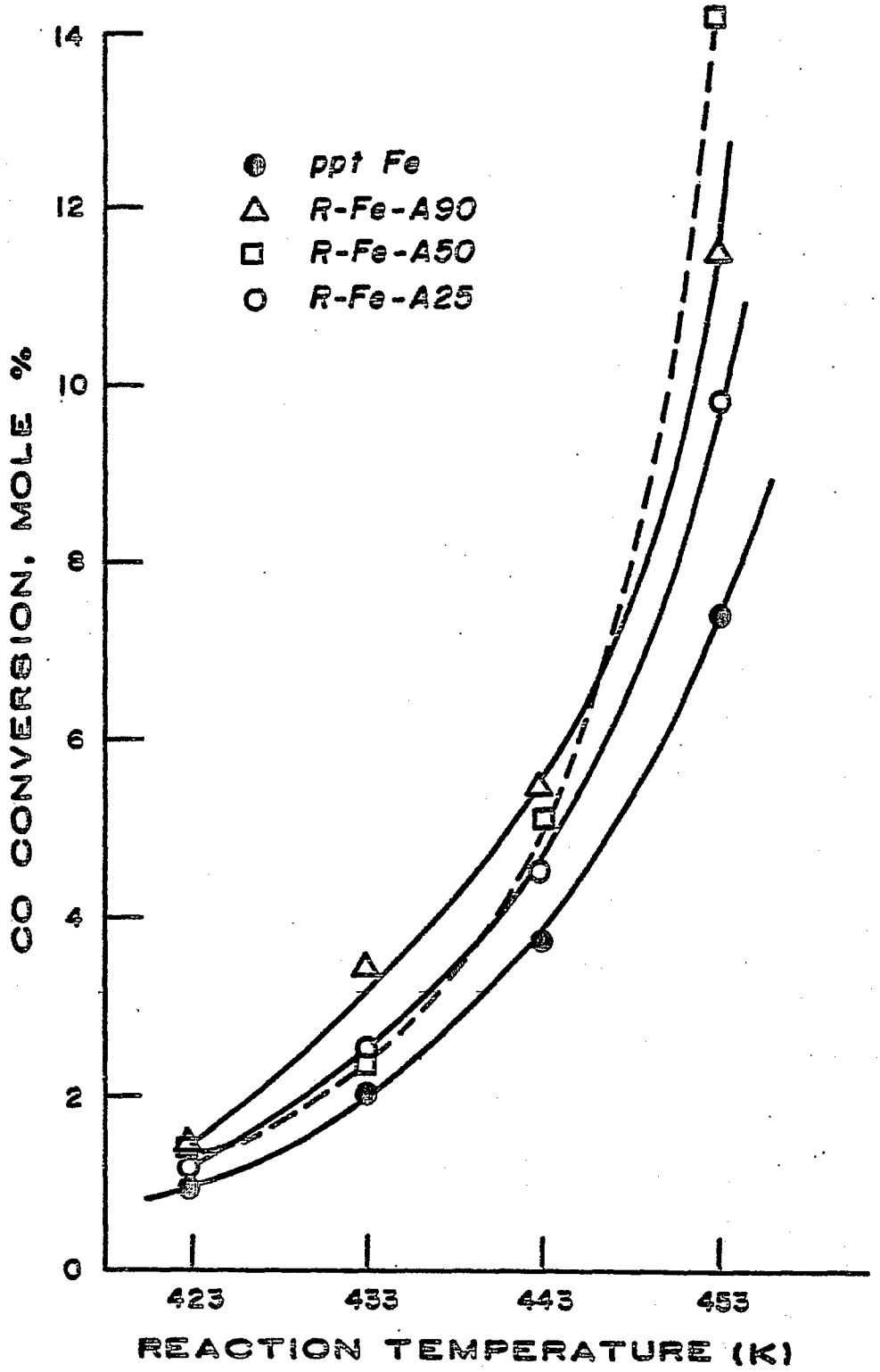
ppt Fe
R-Fe-A90
R-Fe-A50
R-Fe-A25
CO CONVERSION, MOLE %
0
2
4
6
8
10
12
14
423
433
443
453
REACTION TEMPERATURE (K)

Figure 39

Activity of Raney Iron Catalyst for
Carbon Monoxide Conversion

Catalyst: Prepared by Caustic Addition Technique

Pressure = 1465 KPa; $H_2/CO = 2.0$;

Space Velocity = 3.0 $cm^3 g^{-1} s^{-1}$

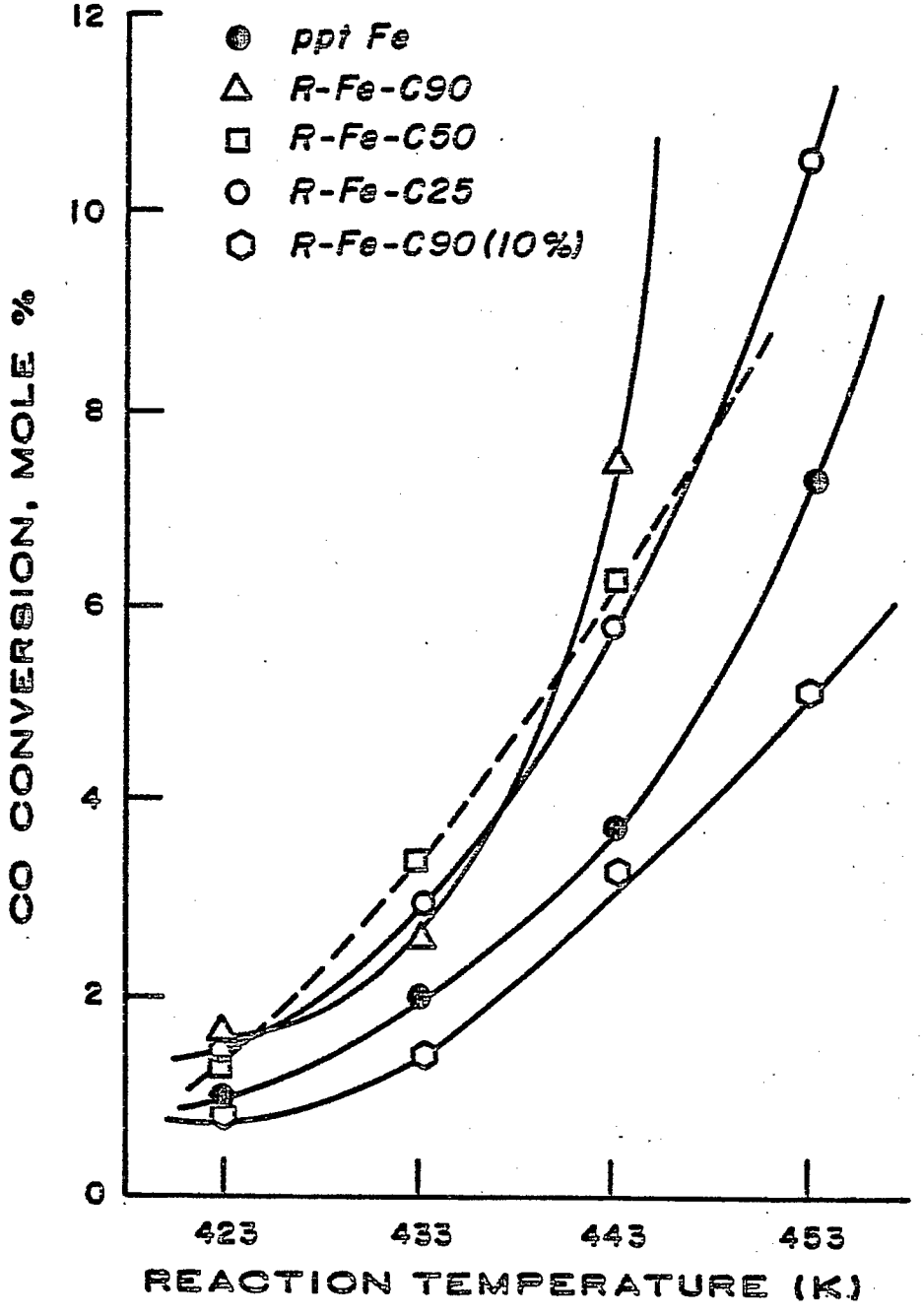
ppt Fe
R-Fe-C90
R-Fe-C50
R-Fe-C25
R-Fe-C90(10%)
CO CONVERSION, MOLE %
0
2
4
6
8
10
12
423
433
443
453
REACTION TEMPERATURE (K)

reaction temperature was also observed with the Raney iron catalysts prepared by caustic addition (Figure 39).

At the test conditions all the Raney iron catalysts exhibited higher activity than the precipitated iron catalyst, irrespective of the preparation method, except for the Raney iron catalyst prepared with the 10% NaOH solution [(R-Fe-A90 (10%)].

The catalyst activity data for the Raney iron catalysts in Table 11 have been analyzed using the following general rate expression:

$$r = r_o f (P_{H_2} , P_{CO}) = A \exp(-E_1/RT) \; f (P_{H_2} , P_{CO}) \qquad (71)$$

where r is the rate of conversion of carbon monoxide (mol/sec), A is the pre-exponential factor, E_1 is activation energy (KJ/mole), P_{H_2} and P_{CO} are the partial pressure of hydrogen and carbon monoxide, respectively, f is a function of P_{H_2} and P_{CO}, and r_o is A $\exp(-E_1/RT)$. Since the catalysts have been tested at the standard test condition, f (P_{H_2} , P_{CO}) becomes a constant term, especially at low levels of carbon monoxide conversion. This assumption is justified in the following discussion.

Anderson[45] expressed the function f (P_{H_2} , P_{CO}) for the hydrogenation of carbon monoxide over iron catalysts as follows:

$$f (P_{H_2} , P_{CO}) = \frac{P_{H_2}}{1 + b_o \exp(-E_2/RT) \; P_{H_2O} / P_{CO}} \qquad (72)$$

where E_2 is the activation energy (J/mol), and b_o is the pre-exponential factor. According to Atwood and Bennett,[46] b_o = 0.164 and

E_2 = 502 J/mol for iron catalysts under the reaction condition similar to the standard reaction condition used for this study: a reactor pressure of 2.0 MPa, a H_2/CO ratio of 2.0, and a reactor temperature of 523 - 588 K. At the highest carbon monoxide conversion achieved with a Raney iron catalyst, P_{H_2O} / P_{CO} was estimated to be about 0.04. At the highest carbon monoxide conversion the term, $b_o \exp(-E_2/RT)$ P_{H_2O} / P_{CO}, was about 0.05. Therefore, Equation (72) can be approximated by Equation (73), which is the same equation obtained by Dry[40] for carbon monoxide hydrogenation over iron catalysts:

$$f(P_{H_2}, P_{CO}) = P_{H_2} . \qquad (73)$$

According to Atwood and Bennett,[46] the usage ratio of H_2/CO was quite constant, 0.75, over a wide range of carbon monoxide conversion, which was far below the H_2/CO reactant ratio of 2.0. The partial pressure of hydrogen, P_{H_2}, would be a constant value in a differential reactor, which was the case for the screening tests done with the Raney iron catalysts.

The constancy of the term was confirmed as follows: Taking the logarithm of Equation (71), we obtain

$$\ln r = \ln A - \frac{E_1}{RT} + \ln f (P_{H_2}, P_{CO}) . \qquad (74)$$

Activation energies were obtained from the Arrhenius plot, ln r vs. 1/T, for all the catalysts. Rearrangement of Equation (71) gives:

$$r \exp (E_1/RT) = A f (P_{H_2}, P_{CO}) . \qquad (75)$$

The constancy of the term, f (P_{H_2} , P_{CO}), has been confirmed by comparing values of the left-hand side of this equation for each catalyst at different reaction temperatures. In the case of R-Fe-A50 catalyst, which showed the highest activity at 453 K, the left-hand term, r exp(E_1/RT), was quite constant, 2.1 ($\pm$ 0.3) x 10^{14}, in the temperature range investigated.

The apparent activation energies for carbon monoxide conversion and the ln (Af) values were obtained from the Arrhenius plots by linear regression. Typical arrhenius plots are presented for iron catalysts in Figure 40. The reaction rates of carbon monoxide conversion were obtained in the following manner:

$$r_{CO} = (N^o_{CO})(sv)(3600\ s\ h^{-1})\ (x) \qquad (76)$$

where r_{CO} is the reaction rate of carbon monoxide conversion (mol g^{-1} hr^{-1}), N^o_{CO} is the concentration of carbon monoxide in the reactant mixture gas (mol/cm^3), x is the conversion of carbon monoxide, and sv is the space velocity ($cm^3 g^{-1} s^{-1}$). The number of moles of carbon monoxide in the reactant gas was calculated using ideal gas law, which is valid for mixtures of carbon monoxide and hydrogen below pressures of about 4 MPa.[44]

The activation energies and the ln (Af) values for the Raney iron catalysts are listed in Table 12. The activation energy ranged from 96 to 139 KJ/mol, which was in the same range of values obtained by previous workers for iron catalysts [Anderson (44), Bennet (46); 84 KJ/mol, Vannice (47); 113 KJ/mol]. The relative activities of the Raney iron catalysts are listed in Table 12. The normalized rates of

Figure 40

Arrhenius Plots for Carbon Monoxide Conversion over Iron Catalysts

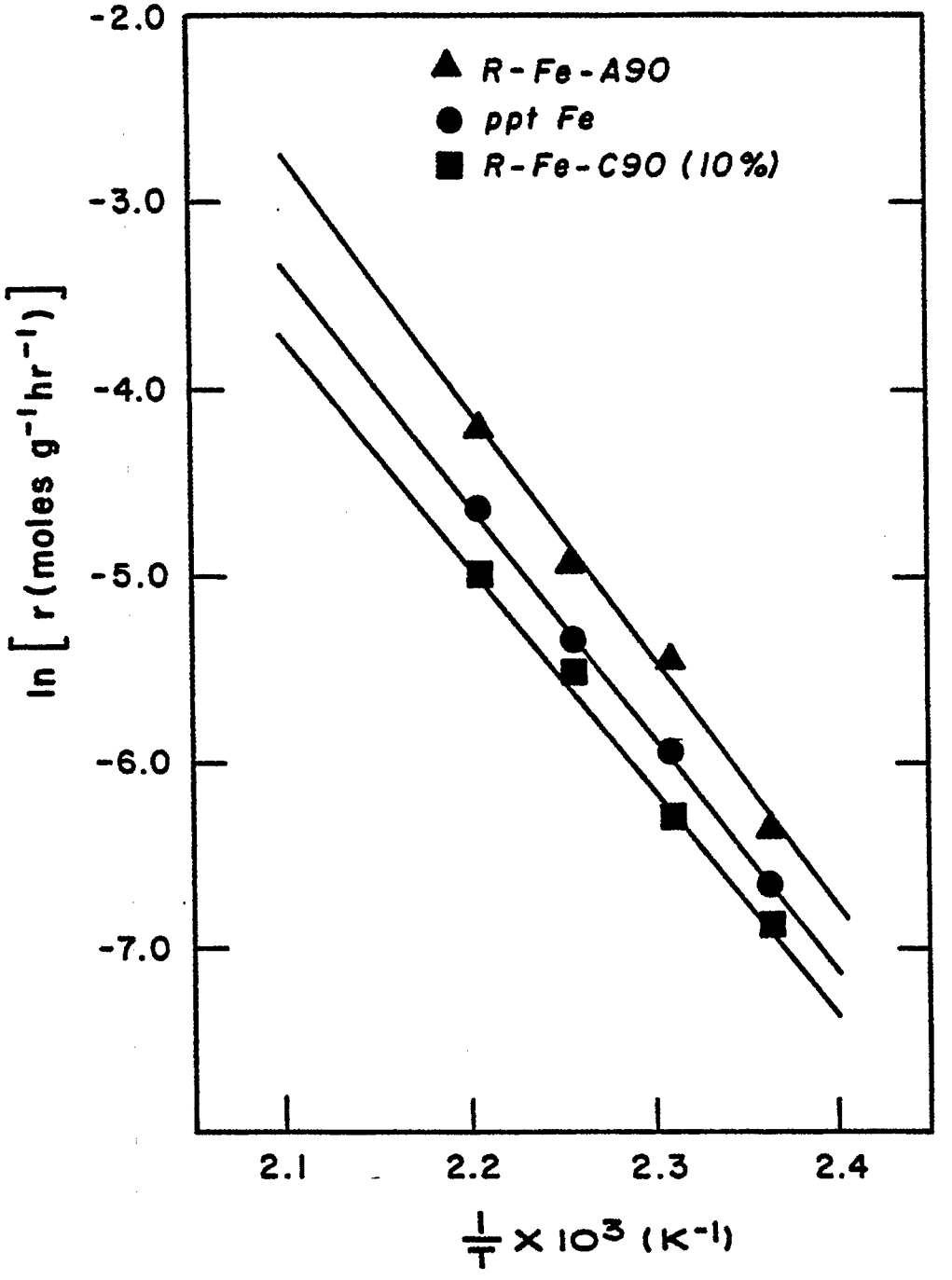
R-Fe-A90
ppt Fe
R-Fe-C90 (10%)
-2.0
-3.0
-4.0
-5.0
-6.0
-7.0
ln [r (moles g⁻¹hr⁻¹)]
2.1
2.2
2.3
2.4
1/T x 10³ (K⁻¹)

Table 12

Activation Energy and Relative Activity of Raney Iron Catalysts

Catalyst Type	E (KJ/mol)	ln (Af)	Relative Activity at Temperature, K					
			423	433	443	453	463	473
			(1.0)	(2.01)	(3.88)	(7.28)	(13.29)	(23.83)
ppt Fe	105.4	23.3	1.0	1.0	1.0	1.0	1.0	1.0
R-Fe-C90	123.4	28.8	1.37	1.54	1.73	1.93	2.14	2.36
R-Fe-C50	123.0	28.6	1.38	1.55	1.72	1.91	2.11	2.32
R-Fe-C25	111.3	25.3	1.35	1.41	1.46	1.52	1.57	1.62
R-Fe-C90 (10%)	102.1	22.2	0.79	0.77	0.76	0.74	0.73	0.72
R-Fe-A90	112.1	25.6	1.39	1.46	1.52	1.58	1.64	1.71
R-Fe-A50	139.3	33.0	1.06	1.13	1.31	1.52	1.74	2.00
R-Fe-A25	114.6	26.1	1.10	1.17	1.24	1.31	1.39	1.46
R-Fe-A90[a]	95.8	21.2	1.80	1.69	1.60	1.51	1.43	1.36

[a]Alloy from Alpha Products.

carbon monoxide conversion over Raney iron catalysts were calculated relating to the rate over the precipitated iron catalyst at each reaction temperature. Some of the relative activity values were obtained by extrapolation of the Arrhenius plots. The numbers in parentheses are the relative activity values of the precipitated iron catalyst obtained by taking the reaction rate at 423 K as 1.0.

The relative activity of the precipitated iron increased about two times for each 10 K increase in reaction temperature, which is the case for a typical homogeneous reaction. This fact, combined with the knowledge that the activation energy values lie within a reasonable range, indicated that the carbon monoxide conversion reaction was free of any significant intraparticle transport limitations at the standard reaction condition. If this were not the case, the activation energy would be much lower than 84 KJ/mol since the apparent activation energy is half of the sum of the true activation energy and the activation energy for diffusion, usually much lower than 40 KJ/mol, in a situation where the intraparticle mass transport limitation prevails.[160] The absence of any interphase and intraparticle transport limitations is discussed in detail in Appendix G.

The relative activity of a Raney iron catalyst increased with temperature, when the activation energy over the Raney iron catalyst was higher than that over the precipitated iron catalyst, 105 KJ/mol, and vice versa. The most noticeable increase was observed with the R-Fe-A50 catalyst, for which the activation energy was highest among the Raney iron catalysts tested.

When comparing the activities of different Raney iron catalysts prepared at different leaching temperatures, the

activities of Raney iron catalysts prepared at a low temperature (298 K) were lower than those of Raney iron catalysts prepared at higher temperatures (323 and 363 K), irrespective of the preparation mode, that is, alloy or caustic addition. The catalyst prepared with the 10% NaOH solution exhibited lower activity than that prepared with the 20% NaOH solution at the same leaching temperature as can be seen from the data of R-Fe-C90 and R-Fe-C90 (10%) in Table 12. At the same leaching temperature the caustic addition method yielded a Raney iron catalyst with slightly higher activity than the one prepared by the alloy addition method.

No correlation could be found between the BET surface area and the relative activities of the Raney iron catalysts. A better correlation could have been made by determining the number of active sites for the reaction on each catalyst from a study of selective chemisorption of carbon monoxide and hydrogen which was out of the scope of this study. It needs to be pointed out that a criterion for selecting a catalyst depends on the specific purpose of the use of the catalyst. As has been discussed by Butt, et al.,[161] there are several criteria when a standard activity test is carried out to select a most desirable catalyst for a given reaction:

i) temperature required for a given conversion
ii) temperature for a given product quality
iii) space velocity required for a given conversion
iv) conversion achieved
v) reaction rate
vi) rate constants and parameters extracted from kinetic studies.

Among the above the second, for example, obviously has more to do with selectivity, while those criteria based on conversion may be quite misleading under certain circumstances. The last two measures of activity seem to be most appropriate for this study. The others, which compare the catalyst activity at a single parameter such as temperature, conversion, and space velocity, will mislead the results as evidenced by the fact that the order of catalyst activity changes depending on the reaction temperature as shown in Figure 38 and Figure 39.

The reaction rate data for carbon monoxide conversion have also been analyzed by a first-order kinetic equation which also correlated the rate data reasonably well. The activation energy for carbon monoxide conversion over each Raney iron catalyst obtained from the Arrhenius plot was found to agree within $\pm$ 4 KJ/mol with the values listed in Table 12.

The reaction rate of each product formed (C_1-C_4 hydrocarbons and CO_2) has been analyzed in the same manner as was done for the carbon monoxide conversion rate. The rate of formation of each product was obtained by multiplying the rate of carbon monoxide conversion (mol $g^{-1}hr^{-1}$) to each product selectivity (carbon atom mole %) and divided by the number of carbon atoms in each molecule.

The Arrhenius plots for hydrocarbon synthesis from carbon monoxide hydrogenation over a Raney iron (R-Fe-A90) and a precipitated iron catalyst are presented in Figure 41. The reaction rate for hydrocarbon formation decreased in the following order: $CH_4 > C_2H_6 > C_2H_4 > C_3H_6 > C_4H_8 > C_3H_8 \sim C_4H_{10}$. The activation energy and the ln (Af) value obtained from the Arrhenius plot for each product from

Figure 41

Arrhenius Plots for Hydrocarbon Formation over Iron Catalysts

C_1: Methane

C_2: Ethane

C_3: Propane

C_4: Butane

CO: Carbon Monoxide

$C_2^=$: Ethylene

$C_3^=$: Propylene

$C_4^=$: Butene

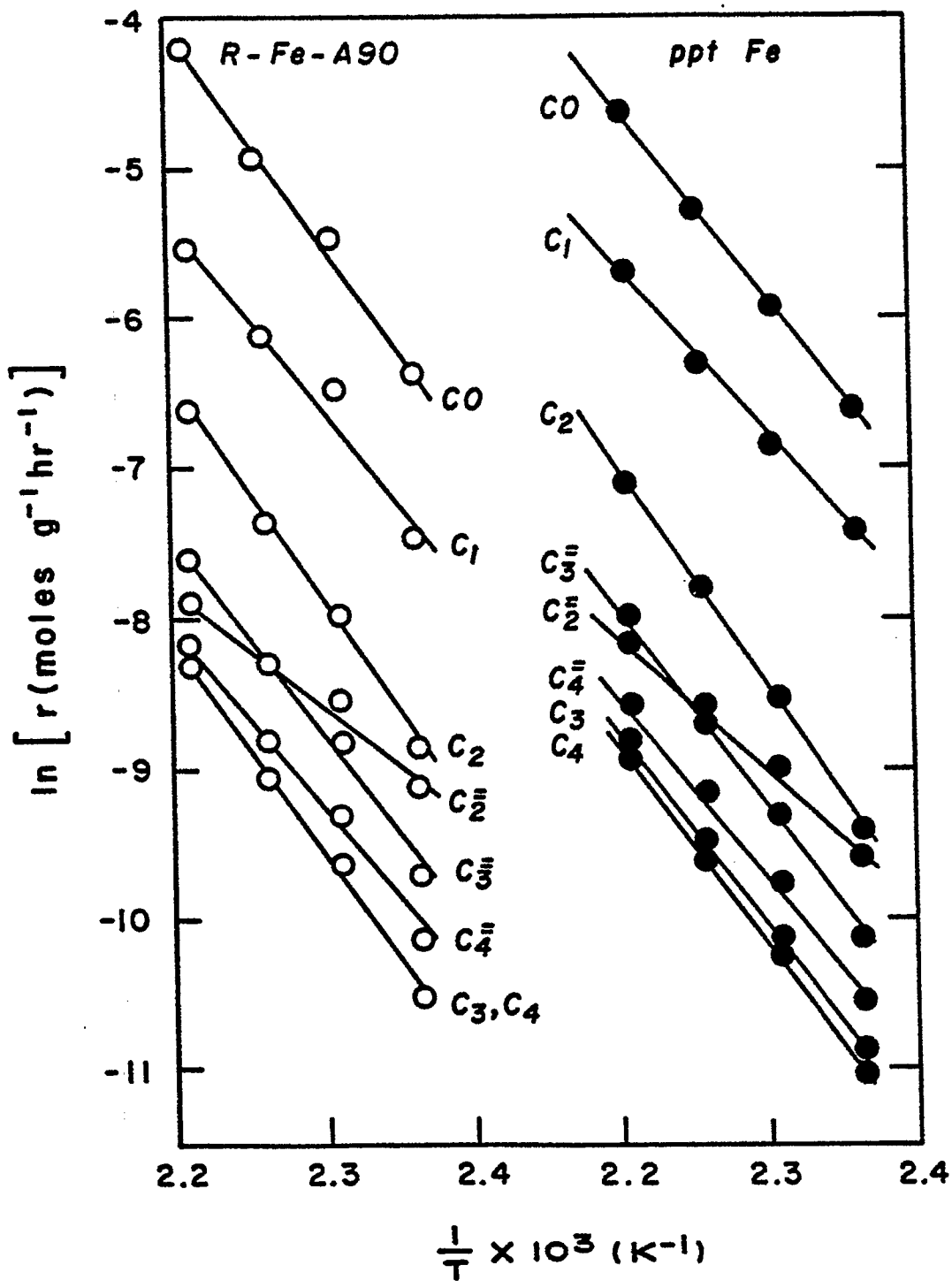
R-Fe-A90
ppt Fe
CO
C1
C2
C2=
C3=
C4=
C3,C4
ln [r(moles g-1 hr-1)]
-4
-5
-6
-7
-8
-9
-10
-11
2.2
2.3
2.4
1/T x 10^3 (K-1)

carbon monoxide hydrogenation is listed in Table 13. The activation energies for each product formed over Raney iron catalysts were in the following ranges: CH_4 = 73 - 116 KJ/mol, C_2H_4 = 61 - 98 KJ/mol, C_2H_6 = 115 - 157 KJ/mol, C_3H_6 = 100 - 131 KJ/mol, C_3H_8 = 97 - 140 KJ/mol, C_4H_8 = 94 - 123 KJ/mol, C_4H_{10} = 100 - 144 KJ/mol, and CO_2 = 149 - 217 KJ/mol.

It is noteworthy that the range of activation energy for ethylene formation was low relative to the range of activation energies for other hydrocarbons and the range of activation energy for carbon dioxide formation was much higher than those for all the hydrocarbons.

Product selectivity. The product selectivity for the Raney iron catalyst depended on the preparation conditions as well as on the reaction temperatures as indicated in Table 11. The methane selectivities of the Raney iron catalysts prepared by the alloy addition and by the caustic addition technique are presented in Figures 42 and 43, respectively.

The methane selectivity decreased with increasing temperature for a given catalyst. The precipitated iron catalyst showed higher methane selectivity than any of the Raney iron catalysts. At 453 K the methane selectivity of the precipitated iron was 35%, while the methane selectivity of the Raney iron catalysts ranged from 20 to 30%.

The C_2-C_4 hydrocarbon selectivities are presented in Figure 44. At the lowest reaction temperature, 423 K, the C_2-C_4 selectivity was quite different for the different catalysts. It ranged from 33 to 48% (product carbon atom mole%). However, the C_2-C_4 selectivity

Table 13

Kinetic Parameters for Product Formation over Raney Iron Catalysts

Catalyst Type	Methane		Ethylene		Ethane		Propylene	
	E[b]	ln Af	E	ln Af	E	ln Af	E	ln Af
ppt Fe	91.6	18.6	72.8	10.4	130.5	26.9	113.0	21.6
R-Fe-C90	100.8	21.3	79.5	12.8	156.9	34.8	129.7	27.1
R-Fe-C50	115.5	25.4	79.5	12.7	136.4	29.2	117.2	23.7
R-Fe-C25	101.7	21.4	69.9	10.1	119.2	24.4	105.4	20.4
R-Fe-C90 (10%)	73.2	13.2	72.8	10.5	137.7	28.7	113.0	21.8
R-Fe-A90	97.9	20.5	62.8	8.1	128.0	26.7	111.3	22.0
R-Fe-A50	90.4	18.3	98.3	15.0	139.3	29.8	131.4	27.4
R-Fe-A25	100.8	21.1	71.8	10.4	119.2	24.3	106.3	20.5
R-Fe-A90[a]	93.3	19.2	60.7	7.8	114.6	23.2	100.0	19.0

Table 13 - Continued

Catalyst Type	Propane		1-Butene		Butane		CO_2	
	E[b]	ln Af	E	ln Af	E	ln Af	E	ln Af
ppt Fe	111.7	20.8	104.6	19.0	115.1	21.4	148.5	32.2
R-Fe-C90	126.8	25.6	123.4	24.7	132.2	26.7	197.9	46.9
R-Fe-C50	114.2	22.2	114.6	22.3	118.0	22.9	187.4	43.8
R-Fe-C25	100.4	18.3	101.7	18.5	122.6	24.0	179.9	41.5
R-Fe-C90 (10%)	109.2	20.0	107.9	19.7	114.2	21.0	182.4	41.2
R-Fe-A90	111.3	21.2	101.7	18.6	114.6	21.8	185.8	43.2
R-Fe-A50	139.7	29.1	120.5	23.5	143.5	29.7	216.7	52.0
R-Fe-A25	103.8	19.0	100.8	18.1	108.8	20.0	181.6	42.0
R-Fe-A90[a]	97.1	17.5	93.7	16.5	100.4	18.0	173.6	40.0

[a]Alloy from Alpha Products.

[b]KJ/mol.

Figure 42

Methane Selectivity of Raney Iron Catalyst

Catalyst: Prepared by Alloy Addition Technique

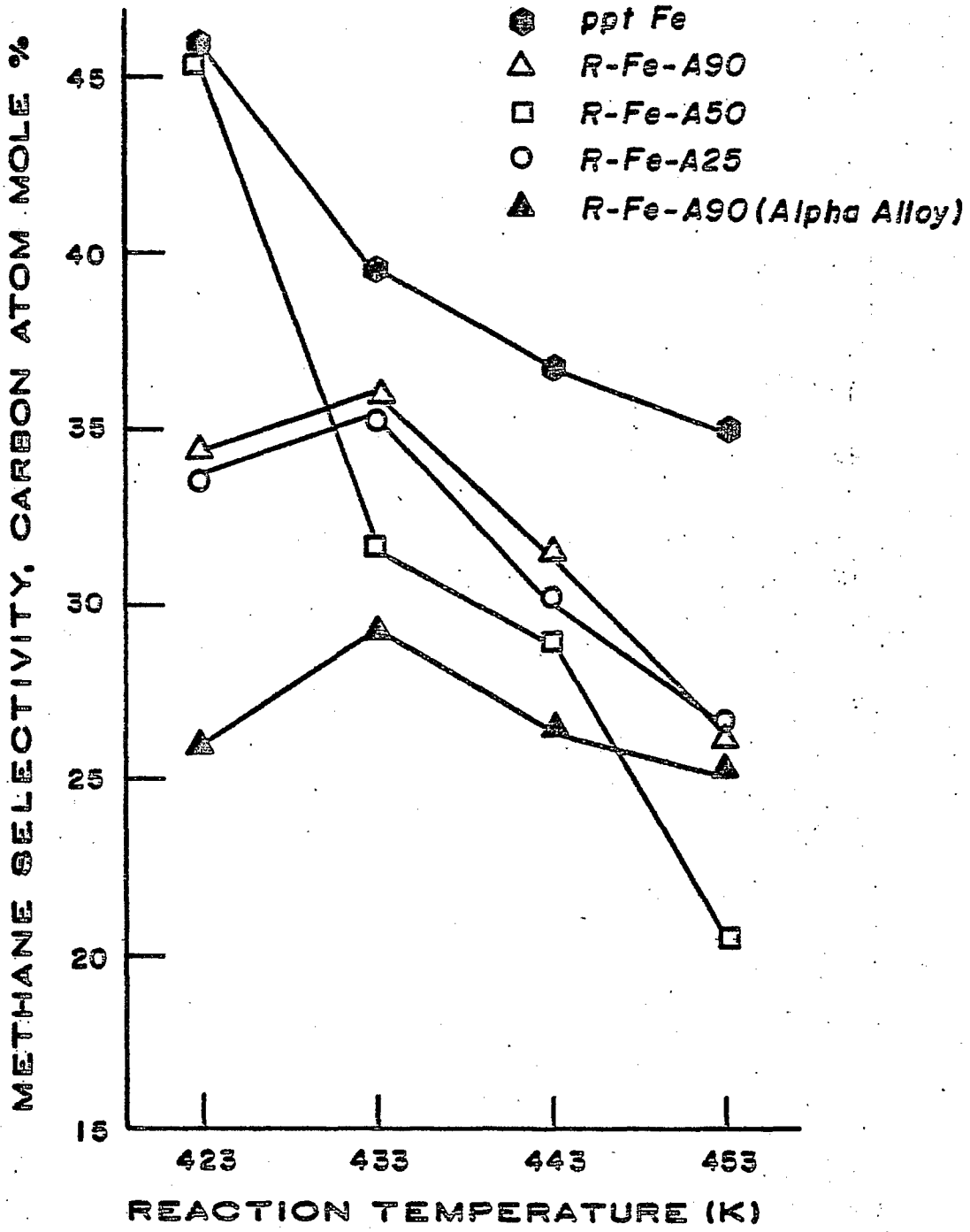
ppt Fe
R-Fe-A90
R-Fe-A50
R-Fe-A25
R-Fe-A90 (Alpha Alloy)
METHANE SELECTIVITY, CARBON ATOM MOLE %
45
40
35
30
25
20
15
423
433
443
453
REACTION TEMPERATURE (K)

Figure 43

Methane Selectivity of Raney Iron Catalyst

Catalyst: Prepared by Caustic Addition Technique

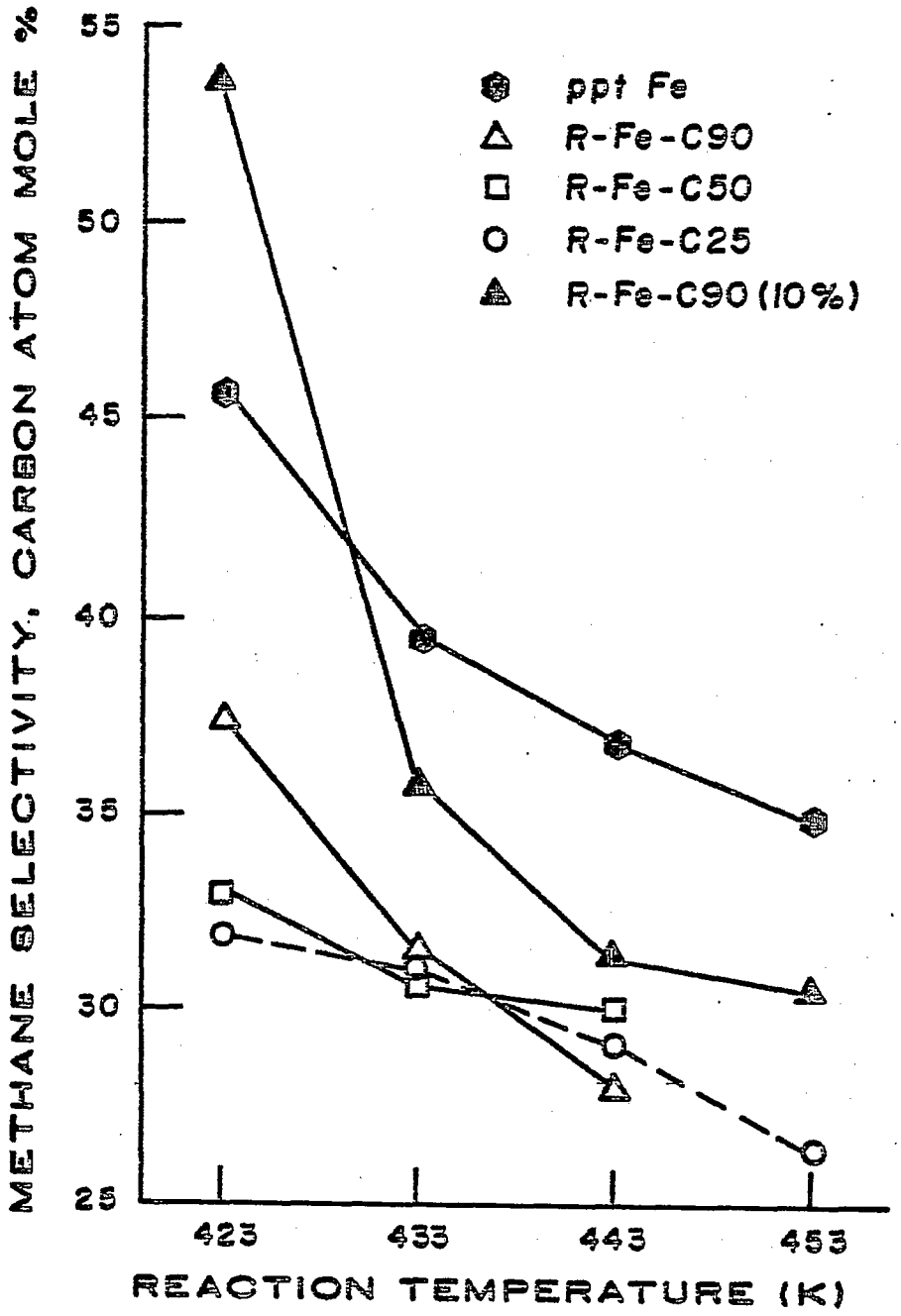
METHANE SELECTIVITY, CARBON ATOM MOLE %
55
50
45
40
35
30
25
423
433
443
453
REACTION TEMPERATURE (K)
ppt Fe
R-Fe-C90
R-Fe-C50
R-Fe-C25
R-Fe-C90 (10%)

Figure 44

C_2-C_4 Hydrocarbon Selectivity of Raney Iron Catalyst

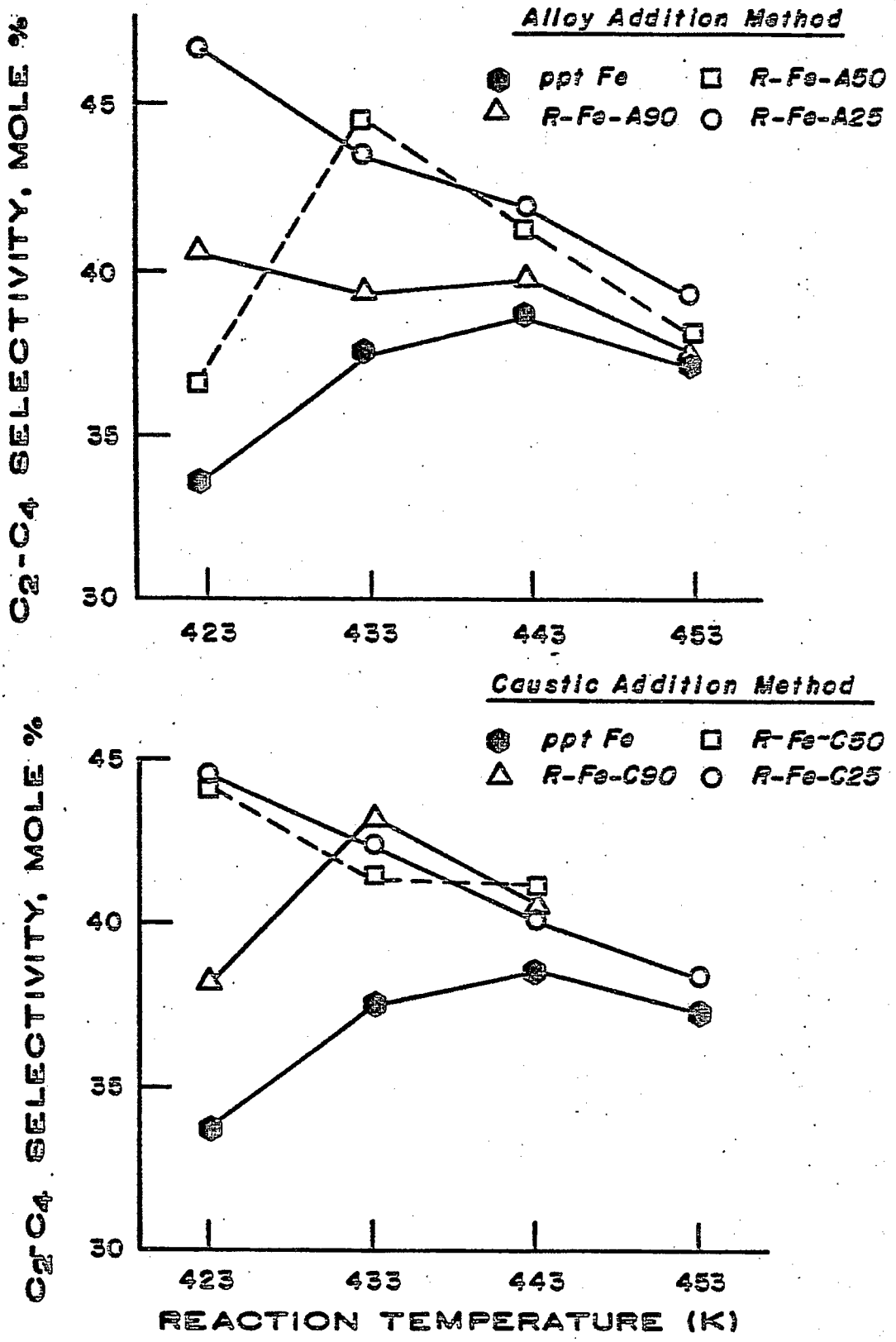
Alloy Addition Method
ppt Fe
R-Fe-A50
R-Fe-A90
R-Fe-A25
C2-C4 SELECTIVITY, MOLE %
45
40
35
30
423
433
443
453
Caustic Addition Method
ppt Fe
R-Fe-C50
R-Fe-C90
R-Fe-C25
C2-C4 SELECTIVITY, MOLE %
45
40
35
30
423
433
443
453
REACTION TEMPERATURE (K)

converged to a narrow range of values, 37 to 43%, at 453 K, irrespective of the different catalyst type or preparation conditions.

The C_5+ selectivities of the Raney iron catalysts at different temperatures are presented in Figure 45. The C_5+ selectivity exhibited a wide variation in the low reaction temperature range, but it converged to about 15% at 453 K, irrespective of the catalyst type or catalyst preparation conditions.

The carbon dioxide selectivities of the Raney iron catalysts prepared by alloy addition and by caustic addition technique are presented in Figures 46 and 47, respectively. The carbon dioxide selectivity increased with increasing temperature for any given catalyst. The precipitated iron catalyst was the least selective for carbon dioxide. The relatively high carbon dioxide selectivity of the Raney iron catalyst compared to the precipitated iron catalyst may be related to the higher level of carbon monoxide conversion achieved at a given temperature with the Raney iron catalyst. It was observed that a high level of carbon monoxide conversion gave a product slate with high carbon dioxide selectivity. Although the catalysts were tested at nearly isothermal conditions, which is true especially at a low level of carbon monoxide conversion, there is a possibility of developing a hot spot at the catalyst surface at the high level of carbon monoxide conversion achieved with a very active catalyst. This is an inherent problem associated with a fixed-bed reactor, especially when a very exothermic reaction, such as carbon monoxide hydrogenation, is taking place in the reactor. The hot spots promote the water-gas-shift reaction, which is favored at high temperatures compared to the hydrocarbon synthesis reaction, resulting in a high carbon dioxide

Figure 45

C_5+ Hydrocarbon Selectivity of Raney Iron Catalyst

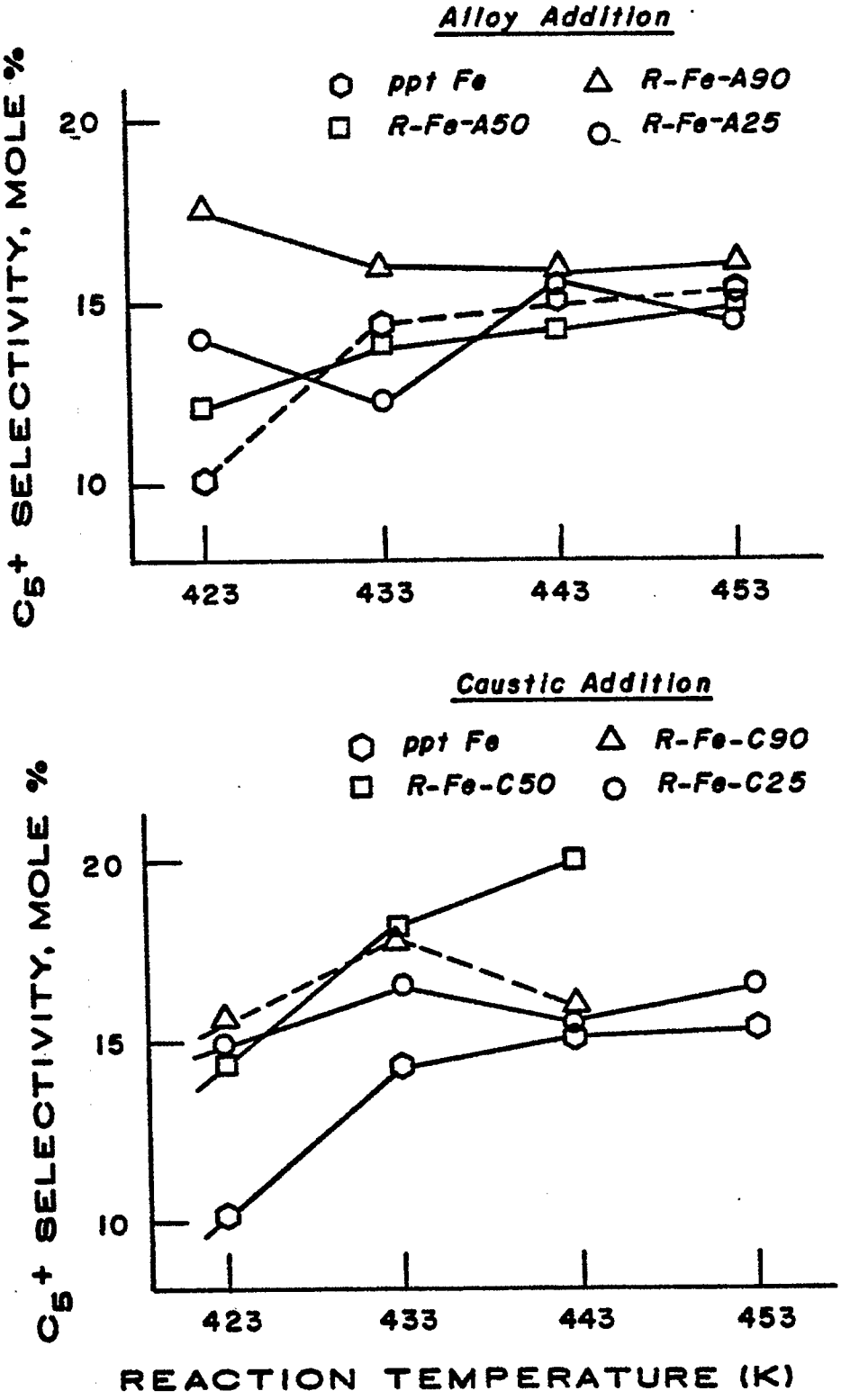
Alloy Addition
ppt Fe
R-Fe-A90
R-Fe-A50
R-Fe-A25
20
15
10
C_5^+ SELECTIVITY, MOLE %
423
433
443
453
Caustic Addition
ppt Fe
R-Fe-C90
R-Fe-C50
R-Fe-C25
20
15
10
C_5^+ SELECTIVITY, MOLE %
423
433
443
453
REACTION TEMPERATURE (K)

Figure 46

Carbon Dioxide Selectivity of Raney Iron Catalyst

Catalyst: Prepared by Alloy Addition Technique

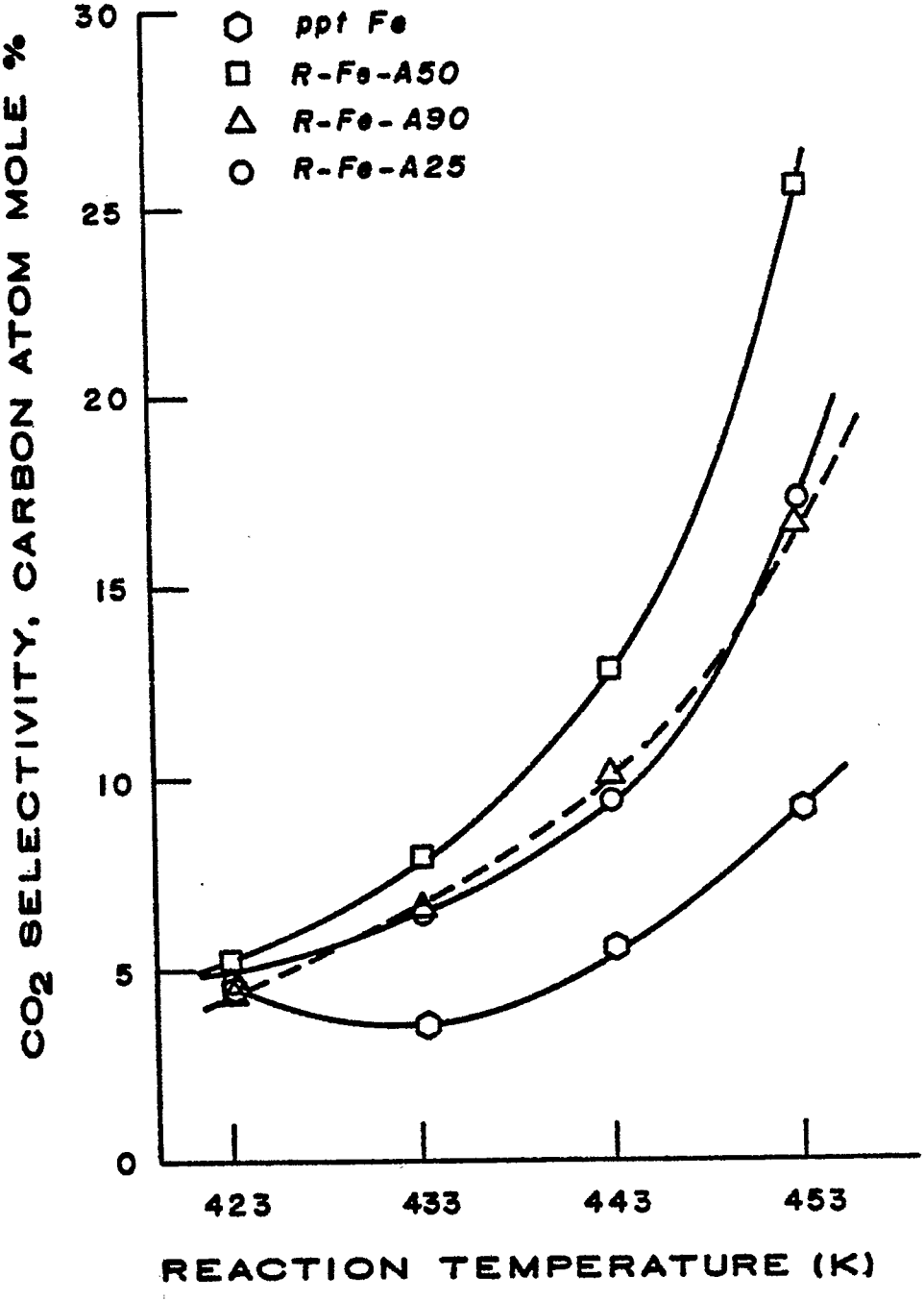
ppt Fe
R-Fe-A50
R-Fe-A90
R-Fe-A25
30
25
20
15
10
5
0
CO2 SELECTIVITY, CARBON ATOM MOLE %
423
433
443
453
REACTION TEMPERATURE (K)

Figure 47

Carbon Dioxide Selectivity of Raney Iron Catalyst

Catalyst: Prepared by Caustic Addition Technique

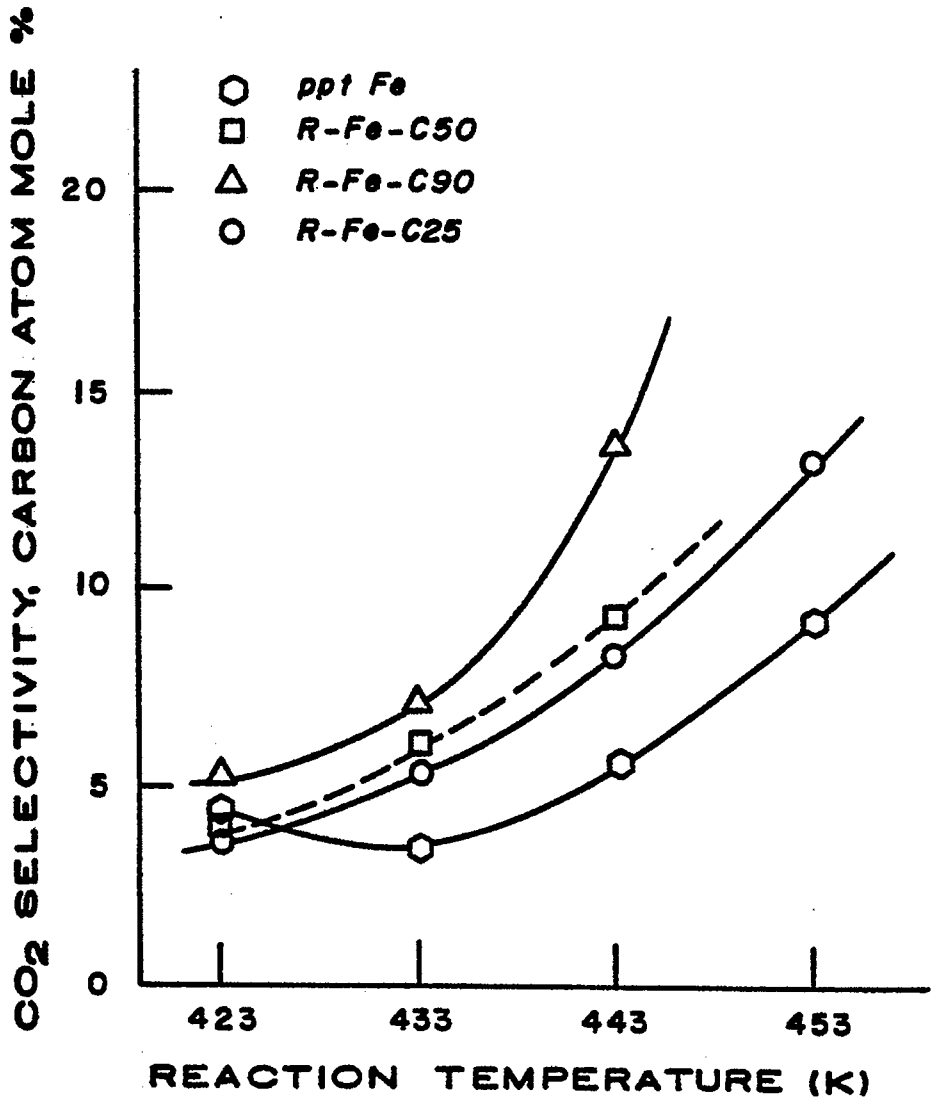
ppt Fe
R-Fe-C50
R-Fe-C90
R-Fe-C25
CO2 SELECTIVITY, CARBON ATOM MOLE %
0
5
10
15
20
423
433
443
453
REACTION TEMPERATURE (K)

selectivity. Thus it may be more meaningful to compare product selectivities between different catalysts at a given conversion rather than at a fixed temperature.

The product carbon atom selectivities for C_2, C_3, and C_4 hydrocarbons, as well as the total C_2-C_4 olefin selectivity at different temperatures, are listed in Table 14. The total C_2-C_4 olefin selectivity decreased with increasing temperature for all the catalysts and ranged from 18 to 26% for the temperature range tested. There were no significant differences in C_2-C_4 selectivity between the different iron catalysts. The ethylene selectivity decreased markedly with increasing temperature for all the catalysts, while the selectivities for other hydrocarbons (olefins or paraffins) were quite insensitive to temperature change as indicated in Table 14.

The olefin-to-paraffin ratios of C_2, C_3, and C_4 hydrocarbons are tabulted in Table 15 as well as the olefin-to-paraffin ratio of the total C_2-C_4 hydrocarbons. The olefin-to-paraffin ratio of the C_2 hydrocarbon (ethylene/ethane) decreased markedly with increasing temperature for all the catalyst while the olefin-to-paraffin ratio of the C_3 (propylene/propane) and C_4 (butene/butane) hydrocarbons remained nearly constant or decreased slightly with increasing temperature. The decrease in the olefin-to-paraffin ratio of C_2 hydrocarbon with increasing temperature is related to the decreasing ethylene selectivity with increasing temperature. Therefore, the C_2-C_4 hydrocarbon olefin-to-paraffin ratio decreased with increasing temperature, due mainly to the decrease in the C_2 hydrocarbon olefin-to-paraffin ratio. The variation of C_2, C_3, C_4, and C_2-C_4 olefin-to-paraffin ratios with temperature is shown for a Raney iron catalyst (R-Fe-A90)

Table 14

C_2-C_4 Olefin Selectivity of Raney Iron Catalysts

Catalyst Type	Temperature (K)	Conversion (%)	Product Carbon Atom Selectivity, %							
			[a] $C_2^=$	C_2	$C_3^=$	C_3	$C_4^=$	C_4	$C_2^= - C_4^=$
R-Fe-A25	423	1.1	6.4	9.0	12.4	6.2	7.4	5.4	26.2
	433	2.4	4.7	9.7	11.5	5.6	7.0	5.1	23.2
	443	4.5	3.8	10.1	11.1	5.3	6.6	4.9	21.5
	453	9.8	2.8	9.7	10.5	5.0	6.3	4.8	19.6
R-Fe-A50	423	1.2	5.2	7.3	9.4	4.8	5.7	4.1	20.3
	433	2.3	4.7	10.4	11.4	5.7	6.9	5.2	22.9
	443	5.1	3.3	10.4	10.6	5.4	6.3	5.0	20.2
	453	14.2	2.4	8.6	9.7	5.9	6.0	5.4	18.1
R-Fe-A90	423	1.3	6.4	6.6	10.5	5.1	6.8	4.8	23.7
	433	3.3	4.5	8.1	10.4	4.9	6.8	4.6	21.6

Table 14 - Continued

Catalyst Type	Temperature (K)	Conversion (%)	Product Carbon Atom Selectivity, %						
			$C_2^=$	C_2	$C_3^=$	C_3	$C_4^=$	C_4	$C_2^= - C_4^=$
R-Fe-A90 (Continued)	443	5.4	3.4	9.1	10.6	5.1	6.6	4.9	20.6
	453	11.5	2.5	8.8	10.2	4.9	6.3	4.9	19.0
R-Fe-A90[b]	423	1.7	6.9	6.7	11.2	4.9	1.7	4.1	24.8
	433	3.5	5.5	7.9	11.5	5.0	7.7	4.9	24.7
	443	6.6	3.9	9.3	11.7	5.0	7.0	4.5	22.6
	453	10.2	3.7	9.3	12.0	5.0	7.3	4.6	23.0
ppt Fe	423	1.0	5.4	5.4	9.1	4.1	5.9	3.8	20.3
	433	2.0	4.7	7.5	10.3	4.5	6.4	4.2	21.4
	443	3.7	3.8	8.5	10.5	4.6	6.7	4.5	21.0
	453	7.4	2.9	8.6	10.2	4.6	6.4	4.5	19.5

Table 14 - Continued

Catalyst Type	Temperature (K)	Conversion (%)	Product Carbon Atom Selectivity, %							
			$C_2^=$	C_2	$C_3^=$	C_3	$C_4^=$	C_4	$C_2^= - C_4^=$
R-Fe-C25	423	1.3	6.8	7.9	11.8	5.8	7.3	5.1	25.9
	433	2.9	5.0	8.9	11.3	5.3	7.0	4.9	23.3
	443	5.8	3.8	9.3	10.7	4.9	6.7	4.7	21.2
	453	10.6	3.1	9.1	10.5	4.7	4.6	6.5	18.1
R-Fe-C50	423	1.3	6.3	8.5	11.7	5.8	7.0	5.1	25.0
	433	3.4	4.4	9.5	10.9	5.2	6.8	4.9	22.1
	443	6.3	3.6	10.1	10.9	5.2	6.7	4.8	21.1
R-Fe-C90	423	1.5	6.2	6.0	10.3	4.7	6.6	4.3	23.2
	433	2.5	5.6	8.3	11.7	5.2	7.6	4.8	24.9
	443	7.4	3.5	9.2	11.1	4.9	7.1	4.8	21.7

Table 14 - Continued

Catalyst Type	Temperature (K)	Conversion (%)	Product Carbon Atom Selectivity, %						
			$C_2^=$	C_2	$C_3^=$	C_3	$C_4^=$	C_4	$C_2^= - C_4^=$
R-Fe-C90 (10%)	423	0.8	6.8	4.8	9.5	4.1	6.1	3.7	22.4
	433	1.4	6.8	7.8	12.5	5.1	7.8	4.6	27.0
	443	3.3	4.8	8.9	11.9	4.8	7.6	4.6	24.2
	453	5.1	4.1	9.5	11.9	4.8	7.5	4.7	23.5

[a]Superscript '=' refers to an olefin.

[b]Alloy from Alpha Products.

Table 15

C_2-C_4 Olefin-to-Paraffin Ratios for Raney Iron Catalysts

Catalyst Type	Temp. (K)	C_2(O/P)	C_3(O/P)	C_4 (O/P)	C_2-C_4 (O/P)
R-Fe-A25	423	0.71	2.00	1.38	1.27
	433	0.48	2.05	1.37	1.13
	443	0.37	2.08	1.34	1.06
	453	0.29	2.09	1.32	1.01
R-Fe-A50	423	0.70	1.98	1.38	1.25
	433	0.45	2.00	1.32	1.07
	443	0.31	1.95	1.26	0.97
	453	0.28	1.66	1.10	0.91
R-Fe-A90	423	0.96	2.07	1.42	1.44
	433	0.55	2.14	1.46	1.23
	443	0.37	2.08	1.36	1.08
	453	0.29	2.06	1.29	1.02
R-Fe-A90[a]	423	1.03	2.28	1.64	1.58
	433	0.70	2.31	1.58	1.39
	443	0.42	2.33	1.55	1.20
	453	0.40	2.41	1.58	1.21
ppt Fe	423	1.00	2.22	1.57	1.54
	433	0.62	2.28	1.53	1.32
	443	0.45	2.27	1.50	1.19
	453	0.34	2.23	1.42	1.10

Table 15 - Continued

Catalyst Type	Temp. (K)	C_2(O/P)	C_3(O/P)	C_4(O/P)	C_2-C_4 (O/P)
R-Fe-C25	423	0.86	2.06	1.42	1.38
	433	0.56	2.14	1.43	1.22
	443	0.41	2.18	1.42	1.12
	453	0.33	2.23	0.71	1.08
R-Fe-C50	423	0.73	2.02	1.39	1.29
	433	0.46	2.09	1.40	1.13
	443	0.35	2.11	1.38	1.05
R-Fe-C90	423	1.03	2.18	1.54	1.53
	433	0.67	2.24	1.59	1.36
	443	0.38	2.26	1.47	1.14
R-Fe-C90 (10%)	423	1.40	2.36	1.65	1.78
	433	0.86	2.42	1.69	1.54
	443	0.54	2.46	1.65	1.32
	453	0.43	2.46	1.62	1.24

[a]Alloy from Alpha Products.

as a typical example in Figure 48. The variation of C_2-C_4 hydrocarbon olefin-to-paraffin ratio with temperature is presented in Figure 49. All catalysts exhibited a narrow range of C_2-C_4 olefin-to-paraffin ratio from 0.9 to 1.2 at 453 K. The C_2-C_4 hydrocarbon olefin-to-paraffin ratio decreased with increasing temperature for all catalysts.

Screening Test with the Raney Iron-Manganese Catalyst

Catalyst activity. The Raney iron-manganese and a coprecipitated iron-manganese (Fe/Mn atomic ratio = 100/5) catalyst have been evaluated in a fixed-bed reactor at the same standard reaction condition as the Raney iron catalysts.

The carbon monoxide conversion and the product selectivity for each of the iron-manganese catalysts are listed in Table 16 at different temperatures. The carbon monoxide conversion at different temperatures for the Raney iron-manganese catalysts prepared by alloy addition and by caustic addition are presented in Figure 50 and 51, respectively. All the Raney iron-manganese catalysts exhibited higher activity, in terms of carbon monoxide conversion, than the coprecipitated catalyst as indicated in Figure 50 and 51. It can be seen that the order of activity changes depending on the temperature, which was also observed with the Raney iron catalysts (see Figure 50 and Figure 51).

The rates of carbon monoxide conversion over the Raney iron-manganese catalysts have been analyzed in the same way as was done for the Raney iron catalysts. The Arrhenius plots for the Raney iron-manganese catalysts and a coprecipitated catalyst are presented in

Figure 48

Low Molecular Weight Hydrocarbon Selectivity

Catalyst: R-Fe-A90

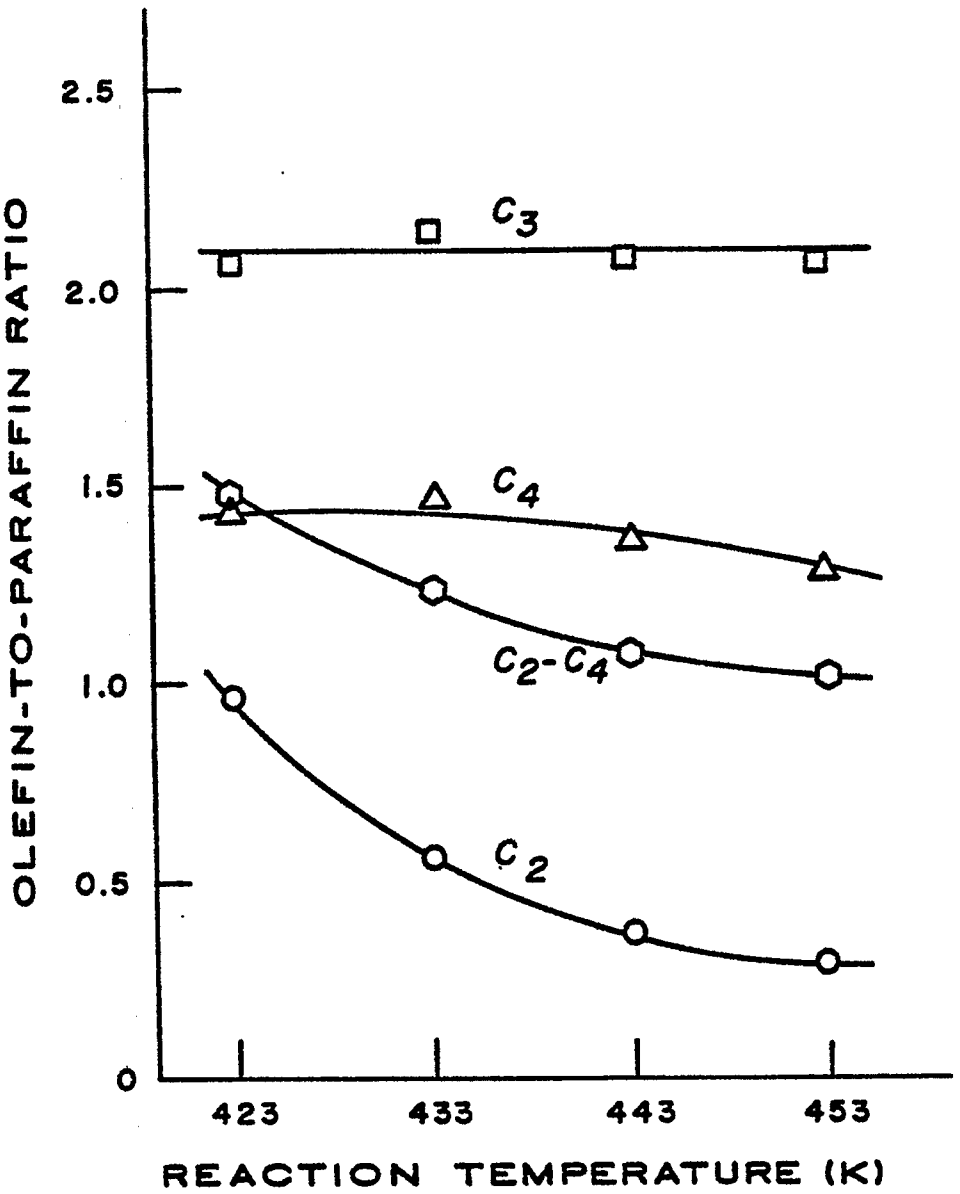
2.5
2.0
1.5
1.0
0.5
0
OLEFIN-TO-PARAFFIN RATIO
C_3
C_4
C_2-C_4
C_2
423
433
443
453
REACTION TEMPERATURE (K)

Figure 49

C_2-C_4 Olefin-to-Paraffin Ratios
for Raney Iron Catalysts

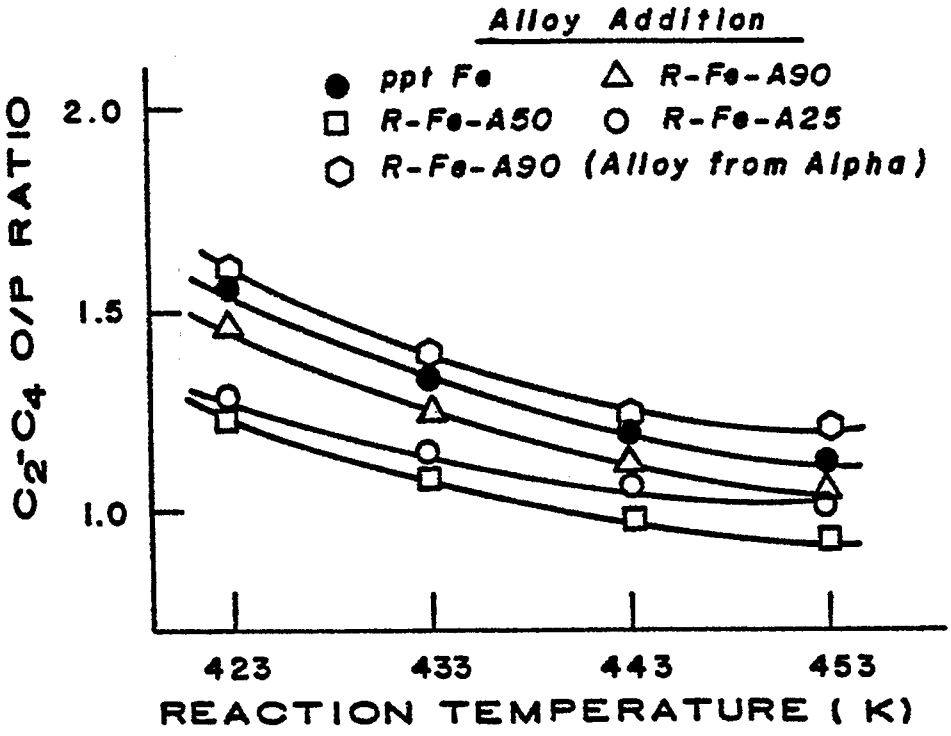
Alloy Addition
ppt Fe
R-Fe-A90
R-Fe-A50
R-Fe-A25
R-Fe-A90 (Alloy from Alpha)
C2-C4 O/P RATIO
2.0
1.5
1.0
423
433
443
453
REACTION TEMPERATURE (K)

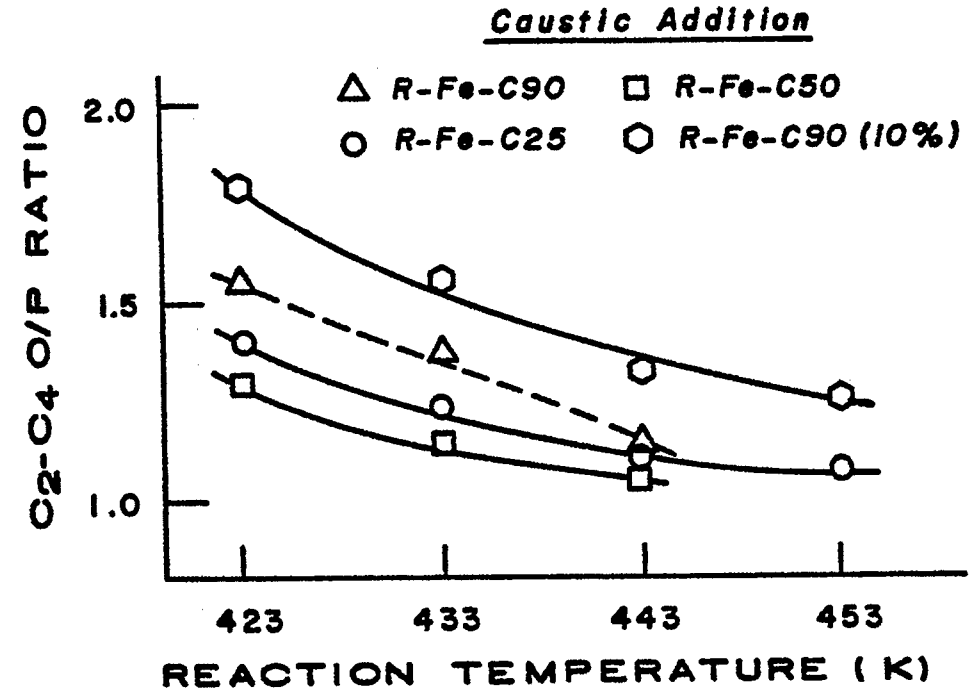
Caustic Addition
R-Fe-C90
R-Fe-C50
R-Fe-C25
R-Fe-C90 (10%)
C2-C4 O/P RATIO
2.0
1.5
1.0
423
433
443
453
REACTION TEMPERATURE (K)

Table 16

Fixed-Bed Evaluation of Iron-Manganese Catalysts

Pressure = 1465 KPa (200 psig); $H_2/CO = 2.0$;

Space Velocity = 3.0 $cm^3 g^{-1} s^{-1}$

Catalyst Type	Temp. (K)	Conversion (%)	Product Carbon Atom Selectivity (%)				
			C_1	$C_{2-}C_4$	C_5^+	ROH[a]	CO_2
Coppt Fe-Mn	423	0.2	40.8	48.4	4.8	0	5.9
	433	0.4	30.6	48.7	10.9	0.8	8.8
	443	1.2	29.6	44.3	17.0	1.2	7.9
	453	2.3	22.8	44.8	20.3	2.2	9.9
	463	4.4	19.5	44.4	20.7	1.3	14.2
R-FeMn-A30	423	0.7	44.4	39.1	10.0	0.7	5.9
	433	1.4	36.6	38.7	16.2	0.8	7.7
	443	2.8	30.3	40.0	17.2	0.6	11.8
	453	4.6	26.2	39.7	16.5	0.4	17.2
	463	8.6	20.5	36.6	16.2	1.0	25.7
	473	12.9	17.0	33.8	15.2	0.7	33.2
R-FeMn-A90	423	1.2	31.1	31.7	29.6	0	7.6
	433	1.6	28.8	38.8	20.3	0	12.0
	443	2.9	22.7	39.4	18.1	0.3	19.5
	453	6.1	19.8	34.7	18.5	0.7	26.3
	463	13.0	15.0	31.7	17.2	0.6	35.4
	473	23.6	12.5	29.7	14.4	0.5	42.9

Table 16 - Continued

Catalyst Type	Temp. (K)	Conversion (%)	Product Carbon Atom Selectivity (%)				
			C_1	C_2-C_4	C_5^+	ROH[a]	CO_2
R-FeMn-A50	423	0.6	38.4	37.1	14.0	0	10.6
	433	1.2	22.1	41.1	20.2	0	16.6
	443	2.7	18.5	36.9	19.7	0.4	24.6
	453	5.0	15.4	33.5	17.3	0.2	33.6
R-FeMn-A50 (10%)	423	0.4	38.0	48.7	10.3	2.9	0
	433	1.0	31.3	44.4	18.2	1.2	4.9
	443	2.2	29.0	42.1	17.6	3.9	7.4
	453	4.9	27.1	41.3	16.7	2.9	12.0
R-FeMn-C90	423	0.8	22.2	42.9	26.2	0	8.8
	433	2.0	19.4	41.7	25.4	0.1	13.4
	443	3.4	18.5	38.6	24.8	0.3	17.8
	453	7.4	16.7	34.7	20.8	1.5	26.3
R-FeMn-C50	423	0.9	29.1	48.0	16.4	0.9	5.5
	433	1.9	26.3	46.5	19.8	0.7	6.7
	443	3.8	24.9	45.1	19.4	0.5	10.1
	453	6.5	22.5	42.7	18.0	2.8	14.0
R-FeMn-C50[b]	423	0.7	25.3	51.4	17.7	0.8	4.9
	433	1.6	24.0	46.8	21.4	1.1	6.7
	443	3.1	23.0	47.1	21.2	1.1	10.0
	453	6.4	25.2	39.8	17.2	3.7	14.2

[a]Alcohols. [b]Duplicate preparation.

Figure 50

Activity of Raney Iron-Manganese Catalyst
for Carbon Monoxide Conversion

Catalyst: Prepared by Alloy Addition Technique

Pressure = 1465 KPa; H_2/CO = 2.0;

Space Velocity = 3.0 $cm^3 g^{-1} s^{-1}$

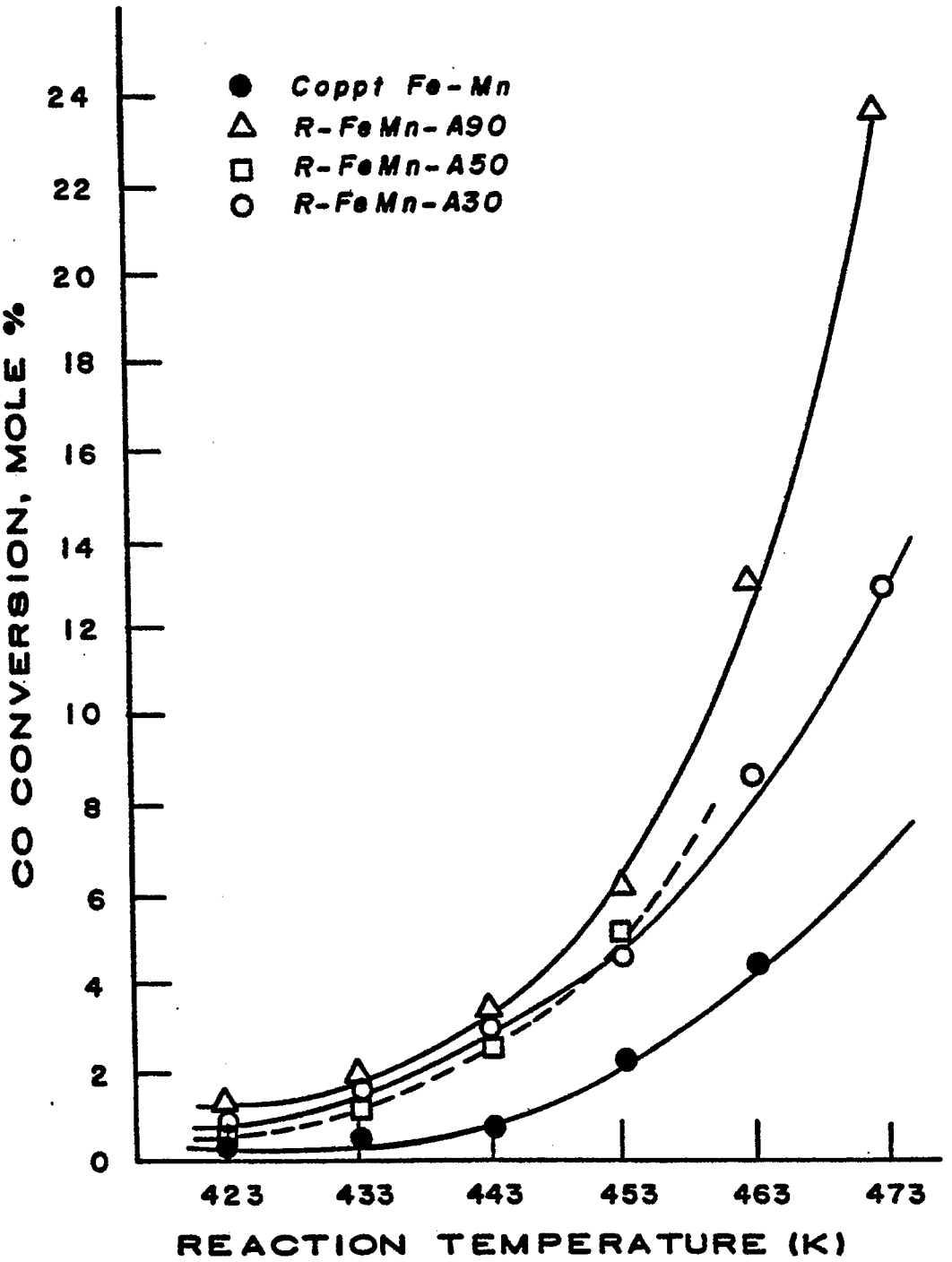
Coppt Fe-Mn
R-FeMn-A90
R-FeMn-A50
R-FeMn-A30
CO CONVERSION, MOLE %
0
2
4
6
8
10
12
14
16
18
20
22
24
423
433
443
453
463
473
REACTION TEMPERATURE (K)

Figure 51

Activity of Raney Iron-Manganese Catalyst for Carbon Monoxide Conversion

Catalyst: Prepared by Caustic Addition Technique

Pressure = 1465 KPa; H_2/CO = 2.0;

Space Velocity = 3.0 $cm^3 g^{-1} s^{-1}$

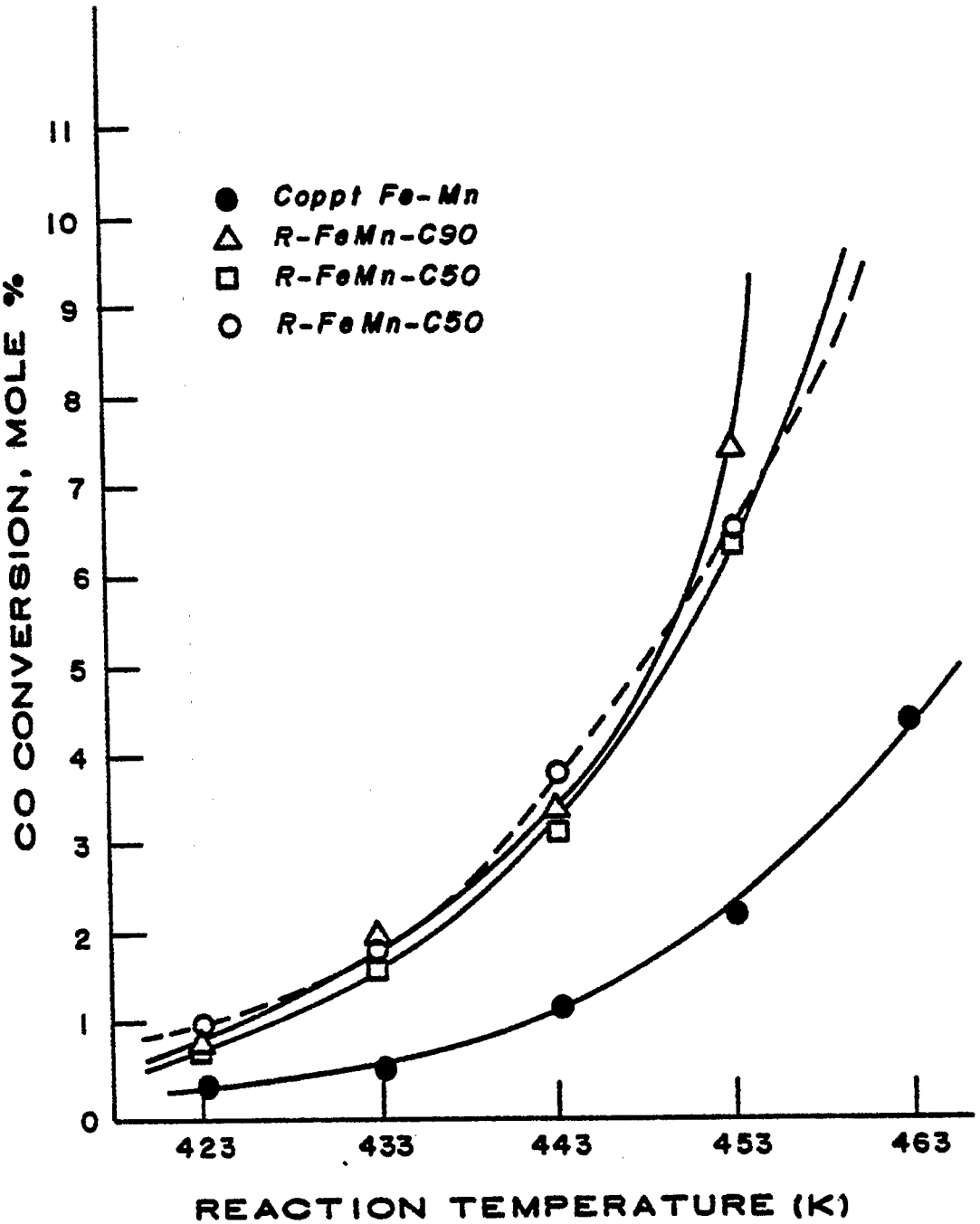
Coppt Fe-Mn
R-FeMn-C90
R-FeMn-C50
R-FeMn-C50
CO CONVERSION, MOLE %
0
1
2
3
4
5
6
7
8
9
10
11
423
433
443
453
463
REACTION TEMPERATURE (K)

Figure 52. The activation energies and the ln (Af) values for carbon monoxide conversion are listed in Table 17. The activation energies ranged from 98 to 133 KJ/mol, which was in the same range as the Raney iron catalysts.

The relative activities were obtained in the same manner as was done for the Raney iron catalysts, that is, the reaction rate of carbon monoxide conversion over a given catalyst was normalized taking the reaction rate over the coprecipitated Fe-Mn catalyst at each temperature as 1.0. The relative activity of a given catalyst increased with increasing temperature, when the activation energy of the catalyst was higher than that of the coprecipitated iron-manganese catalyst, 129.7 KJ/mol.

The relative activities of the Raney iron-manganese catalysts prepared by the alloy addition technique indicated that the catalyst leached at 363 K yielded a catalyst (R-FeMn-A90) with higher activity than the catalyst leached at 323 K (R-FeMn-A50) and at 303 K (R-FeMn-A30). The order of activity for the R-FeMn-A50 and R-FeMn-A30 catalysts changed, depending on the temperature, that is, in the high temperature range above 443 K, the R-FeMn-A50 catalyst exhibited higher activity, while below 443 K the R-FeMn-A30 exhibited higher activity.

The Raney iron-manganese catalyst prepared by caustic addition and leached at 363 K (R-FeMn-C90) exhibited a higher activity than that of the catalyst leached at 323 K (R-FeMn-C50).

The Raney iron-manganese prepared by alloy addition with a low concentration of the NaOH solution [(R-FeMn-A50 (10%)] exhibited an activity for carbon monoxide conversion similar to that of the

Figure 52

Arrhenius Plots for Carbon Monoxide Conversion
over Iron-Manganese Catalysts

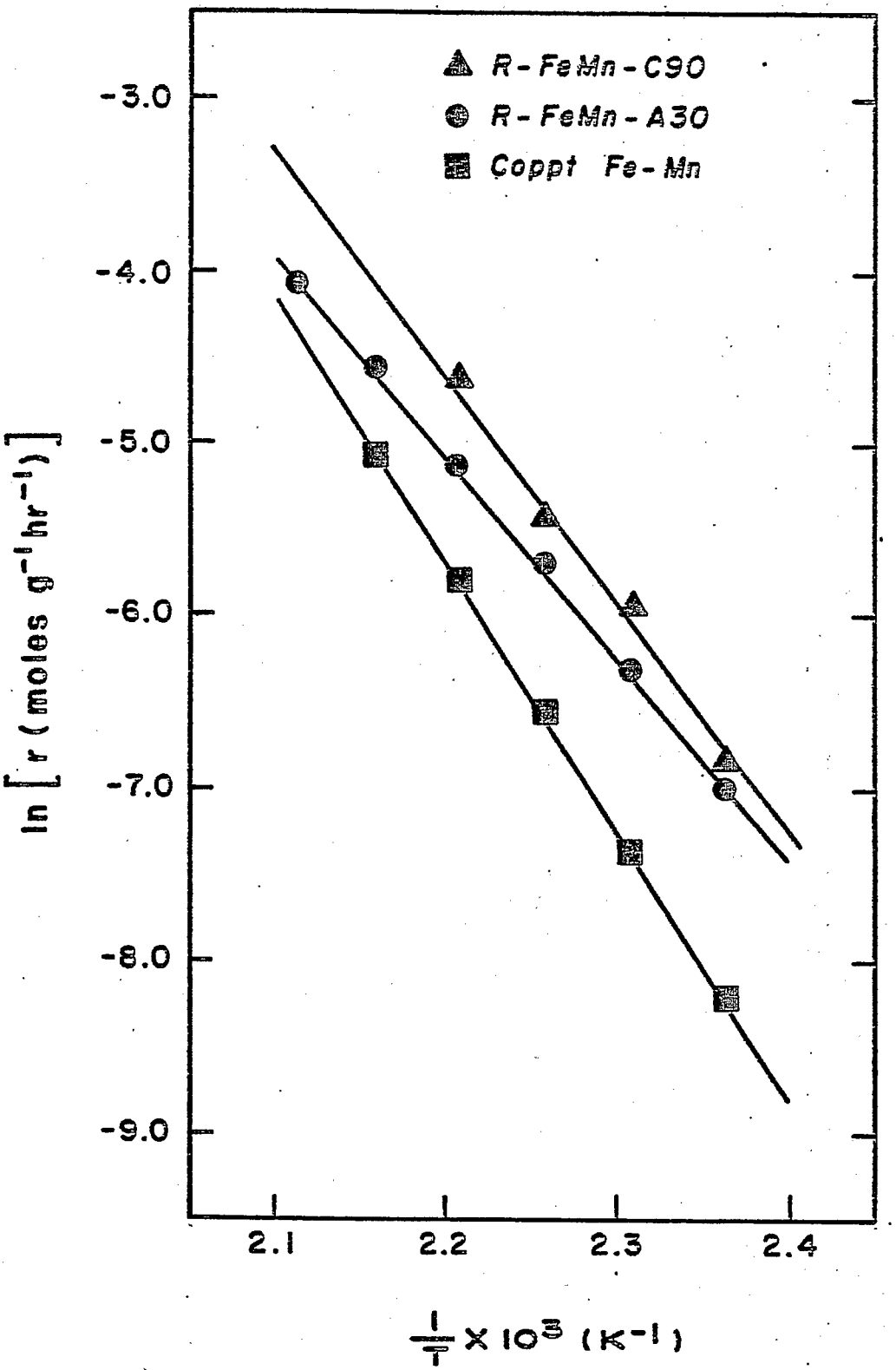
R-FeMn-C90
R-FeMn-A30
Coppt Fe-Mn
-3.0
-4.0
-5.0
-6.0
-7.0
-8.0
-9.0
2.1
2.2
2.3
2.4
ln [r (moles g⁻¹ hr⁻¹)]
1/T X 10³ (K⁻¹)

Table 17

Activation Energy and Relative Activity of Raney Iron-Manganese Catalysts

Catalyst Type	E (KJ/mol)	ln (Af)	Relative Activity					
			Temperature (K)					
			423	433	443	453	463	473
			(1.0)	(2.36)	(5.31)	(11.49)	(24.12)	(49.44)
Coppt Fe-Mn	129.7	28.7	1.0	1.0	1.0	1.0	1.0	1.0
R-FeMn-A90	103.8	22.8	4.53	3.82	3.25	2.79	2.41	2.09
R-FeMn-A50	114.2	25.3	2.86	2.59	2.35	2.14	1.96	1.80
R-FeMn-A30	97.9	20.8	3.57	2.89	2.37	1.96	1.63	1.37
R-FeMn-A50 (10%)	132.6	30.1	1.97	2.00	2.04	2.07	2.10	2.13
R-FeMn-C90	115.1	25.9	4.06	3.69	3.36	3.07	2.83	2.60
R-FeMn-C50	105.9	23.3	4.49	3.83	3.30	2.86	2.49	2.18
R-FeMn-C50[a]	116.3	26.1	3.45	3.16	2.91	2.69	2.49	2.31

[a]Duplicate preparation

catalyst prepared with a 20% NaOH solution (R-FeMn-A50) in the reaction temperature range of 423 to 473 K, even though there was a considerable difference in BET surface areas. No reasonable correlation could be made between the BET surface area and the order of activity. The catalytic activity for carbon monoxide conversion converged to similar values as the reaction temperature was increased for two R-FeMn-C50 catalysts, which were duplicate preparations from different batches of alloy.

The reaction rate data for carbon monoxide conversion could also be correlated reasonably well by a first-order kinetic equation as was done previously for the Raney iron catalyst data. The activation energy obtained from the first-order equation agreed to within $\pm$ 4 KJ/mol with the activation energies listed in Table 17.

The rate of product (C_1-C_4 and CO_2) formation has been analyzed in the same manner as was done for carbon monoxide conversion. The Arrhenius plots for hydrocarbon synthesis reactions over Raney iron-manganese catalysts and a coprecipitated iron-manganese catalyst are presented in Figure 53. As indicated in the Arrhenius plots, the rate of the hydrocarbon formation decreased in the following order: $CH_4 > C_2H_4 > C_3H_6 > C_2H_6 > C_4H_8 > C_3H_8 \sim C_4H_{10}$. The order of the reaction rate indicated that ethylene was favored over ethane with the Raney iron-manganese catalysts. However, the trend was the opposite with the Raney iron catalysts.

The activation energies and the ln (Af) values obtained from the Arrhenius plots for each product are listed in Table 18. The activation energy for each product was in the following range: CH_4 = 66 - 116 KJ/mol, C_2H_4 = 82 - 118 KJ/mol, C_2H_6 = 98 - 146 KJ/mol, C_3H_6 =

Figure 53

Arrhenius Plots for Hydrocarbon Formation over Iron-Manganese Catalysts

C_1: Methane

C_2: Ethane

C_3: Propane

C_4: Butane

CO: Carbon Monoxide

$C_2^=$: Ethylene

$C_3^=$: Propylene

$C_4^=$: Butene

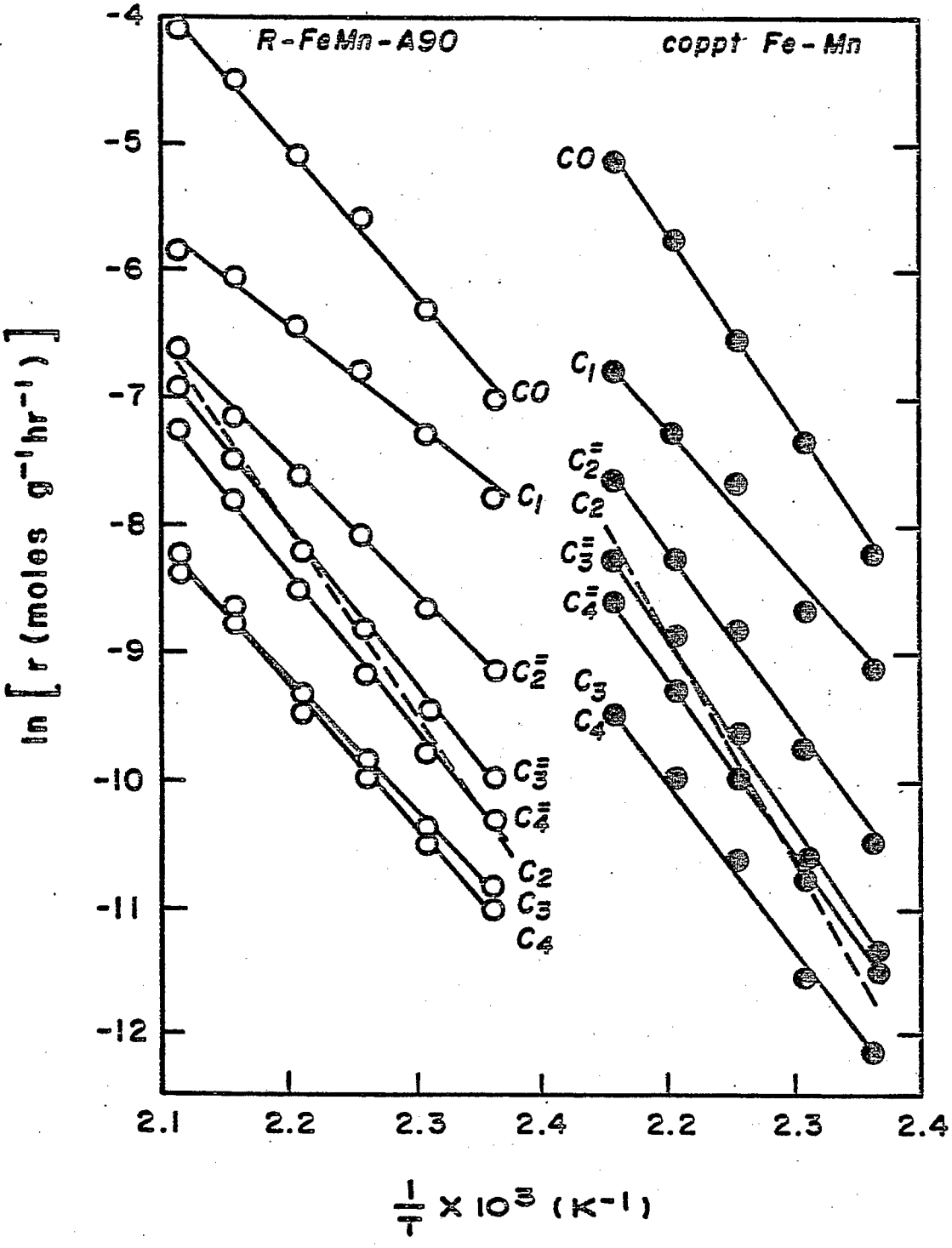
R-FeMn-A90
coppt Fe-Mn
CO
C1
C2=
C3=
C4=
C2
C3
C4
ln [r (moles g-1hr-1)]
-4
-5
-6
-7
-8
-9
-10
-11
-12
2.1
2.2
2.3
2.4
2.2
2.3
2.4
1/T x 10^3 (K-1)

Table 18

Kinetic Parameters for Product Formation over Raney Iron-Manganese Catalysts

Catalyst Type	Methane		Ethylene		Ethane		Propylene	
	E[b]	ln Af	E	ln Af	E	ln Af	E	ln Af
Coppt Fe-Mn	100.8	19.4	118.0	22.3	141.4	27.9	130.1	25.6
R-FeMn-A90	72.4	12.8	82.4	13.6	120.5	23.2	103.8	19.4
R-FeMn-A50	67.8	11.0	84.1	13.5	128.4	25.4	114.6	22.0
R-FeMn-A30	66.1	11.0	83.7	13.4	98.3	17.4	99.2	17.9
R-FeMn-A50 (10%)	115.1	24.2	97.1	17.0	145.6	30.2	127.2	25.5
R-FeMn-C90	100.8	20.3	115.1	22.7	129.7	25.8	110.9	21.4
R-FeMn-C50	92.9	18.4	81.6	13.3	114.2	22.2	103.8	19.6
R-FeMn-C50[a]	115.9	24.5	82.4	13.6	128.4	25.9	108.4	20.8

Table 18 - Continued

Catalyst Type	Propane		1-Butene		Butane		Carbon Dioxide	
	E[b]	ln Af	E	ln Af	E	ln Af	E	ln Af
Coppt Fe-Mn	114.6	20.4	120.9	22.6	114.2	20.0	160.2	34.5
R-FeMn-A90	86.6	13.7	103.8	18.8	93.7	15.3	162.3	36.9
R-FeMn-A50	97.1	16.3	118.0	22.4	100.8	17.1	176.6	40.8
R-FeMn-A30	82.8	12.5	98.7	17.1	83.7	12.4	157.7	35.1
R-FeMn-A50 (10%)	118.0	22.1	121.8	23.3	121.8	22.8	204.6	47.1
R-FeMn-C90	95.8	16.3	110.9	20.8	81.6	12.4	172.4	39.8
R-FeMn-C50	90.4	15.1	101.3	18.2	96.2	16.3	157.3	35.0
R-FeMn-C50[a]	95.0	16.1	110.0	20.5	100.4	17.3	174.1	39.5

[a]Duplicate preparation

[b]KJ/mol.

99 - 130 KJ/mol, C_3H_8 = 83 - 115 KJ/mol, 1-C_4H_8 = 99 - 122 KJ/mol, C_4H_{10} = 82 - 122 KJ/mol and CO_2 = 157 - 205 KJ/mol. The range of activation energy for carbon dioxide formation was much higher than that for hydrocarbon formation as was observed with the Raney iron catalysts.

The activation energy for propylene and butene formation was always higher than the activation energy for propane and butane formation, respectively, for each catalyst evaluated. The activation energy for ethane formation was always higher than that for ethylene formation.

Product selectivity. The product selectivities of the Raney iron-manganese catalysts are listed in Table 16. When comparing the product selectivities of two catalysts prepared at the same condition, but with different concentrations of NaOH solution [R-FeMn-A50 and R-FeMn-A50 (10%)], the catalyst leached with a low concentration of NaOH solution was more selective for methane, C_2-C_4 hydrocarbons and alcohols and was less selective for C_5+ hydrocarbons and carbon dioxide.

The product selectivities were almost the same for two duplicate catalysts (R-FeMn-C50) which were prepared at the same conditions, but from different batches of alloy.

The methane selectivities of Raney iron-manganese catalysts prepared by the alloy addition and by the caustic addition method are presented in Figure 54 and Figure 55, respectively. The methane selectivity decreased with increasing temperature for each type of catalyst as was observed with the Raney iron catalysts. The methane

Figure 54

Methane Selectivity of Raney Iron-Manganese Catalyst

Catalyst: Prepared by Alloy Addition Technique

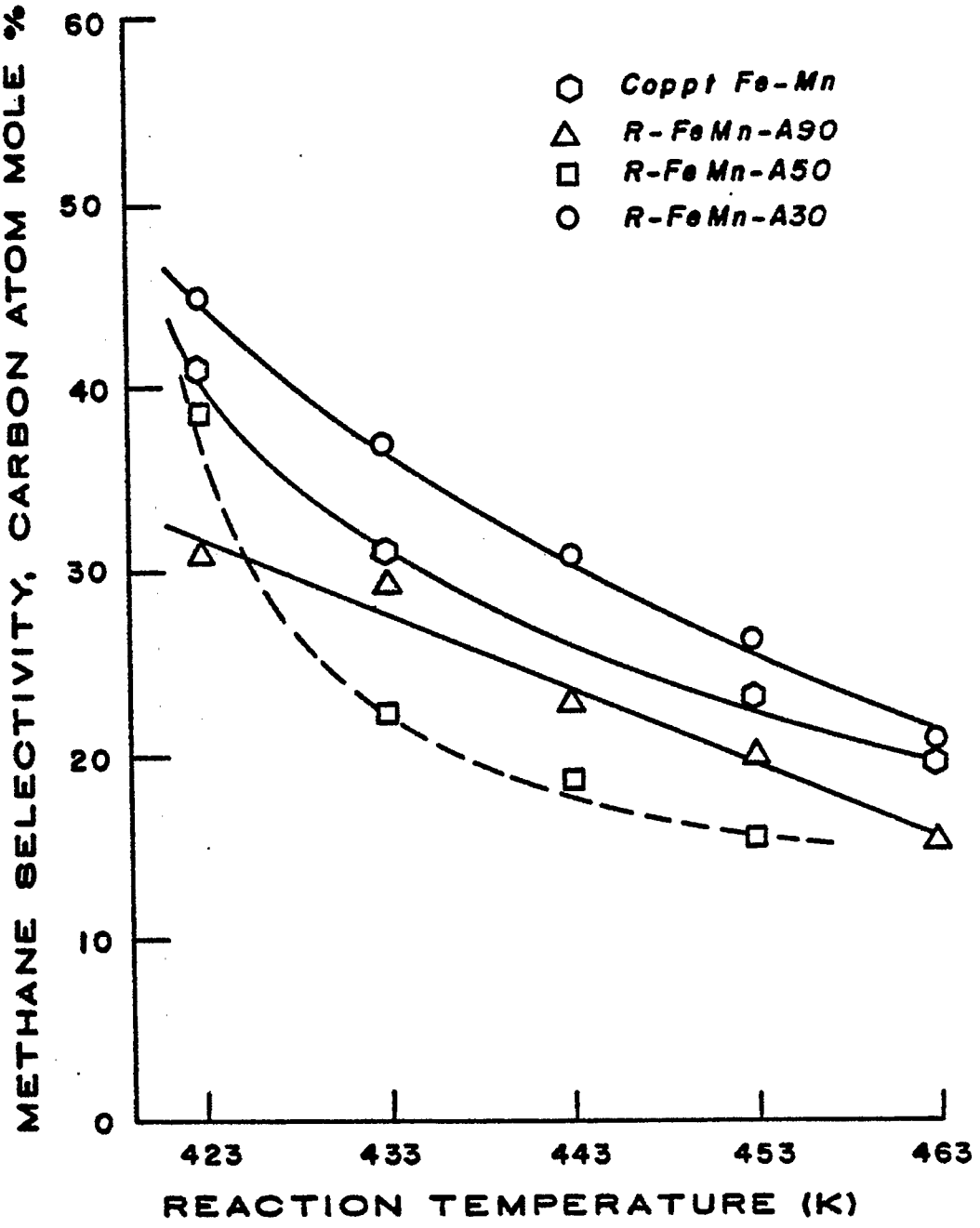
METHANE SELECTIVITY, CARBON ATOM MOLE %
60
50
40
30
20
10
0
423
433
443
453
463
REACTION TEMPERATURE (K)
Coppt Fe-Mn
R-FeMn-A90
R-FeMn-A50
R-FeMn-A30

Figure 55

Methane Selectivity of Raney Iron-Manganese Catalyst

Catalyst: Prepared by Caustic Addition Technique

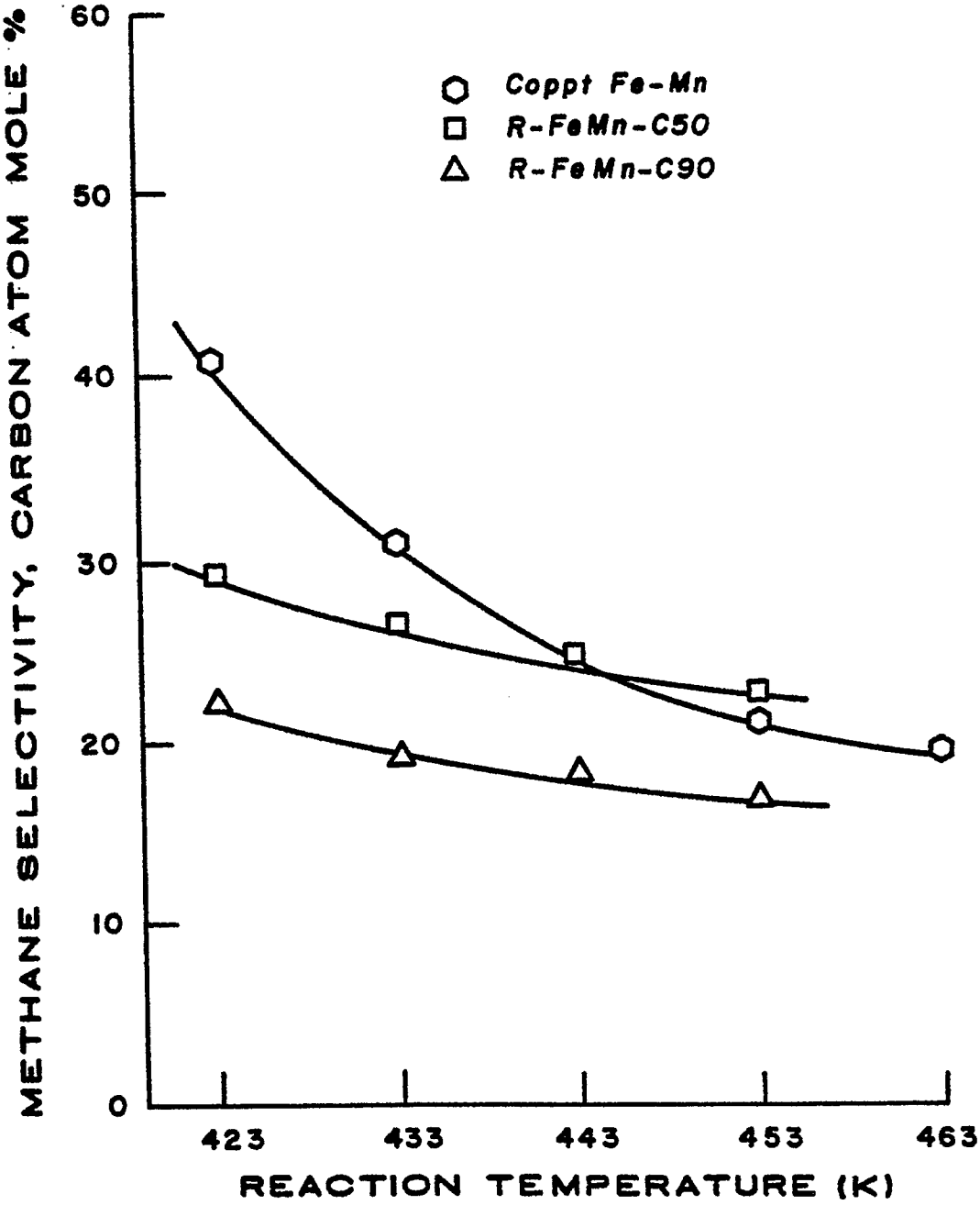
Coppt Fe-Mn
R-FeMn-C50
R-FeMn-C90
METHANE SELECTIVITY, CARBON ATOM MOLE %
60
50
40
30
20
10
0
423
433
443
453
463
REACTION TEMPERATURE (K)

selectivity of the Raney iron-manganese catalysts ranged from 15 to 27% at 453 K, which was lower than that of the Raney iron catalysts at the same temperature.

The C_2-C_4 hydrocarbon selectivities of the Raney iron-manganese catalysts prepared by alloy addition technique and by the caustic addition technique are presented in Figure 56 and 57, respectively. The C_2-C_4 hydrocarbon selectivity generally decreased with increasing temperature. The coprecipitated iron-manganese and the R-FeMn-C50 catalyst showed the highest C_2-C_4 hydrocarbon selectivity. At 453 K the C_2-C_4 hydrocarbon selectivity ranged from 34 to 45%. This range of C_2-C_4 hydrocarbon selectivity was quite similar to 35 to 45% obtained with the Raney iron catalysts at the same temperature. The C_5+ hydrocarbon selectivities of the Raney iron-manganese catalysts prepared by the alloy addition technique and by the caustic addition technique are presented in Figure 58 and 59, respectively.

The C_5+ hydrocarbon selectivity generally decreased with increasing temperature except for the coprecipitated iron-manganese, for which the C_5+ hydrocarbon selectivity increased with increasing temperature. The C_5+ hydrocarbon selectivity was quite different for different catalysts in the low temperature range, however, it converged to a narrow range as the reaction temperature increased. At 453 K it ranged from 16 to 20%.

The carbon dioxide selectivities of the Raney iron-manganese catalysts are presented in Figure 60 and 61. The carbon dioxide selectivity increased with increasing temperature. The carbon dioxide selectivity of the coprecipitated Fe-Mn was the lowest. A high carbon

Figure 56

C_2-C_4 Hydrocarbon Selectivity of Raney Iron-Manganese Catalyst

Catalyst: Prepared by Alloy Addition Technique

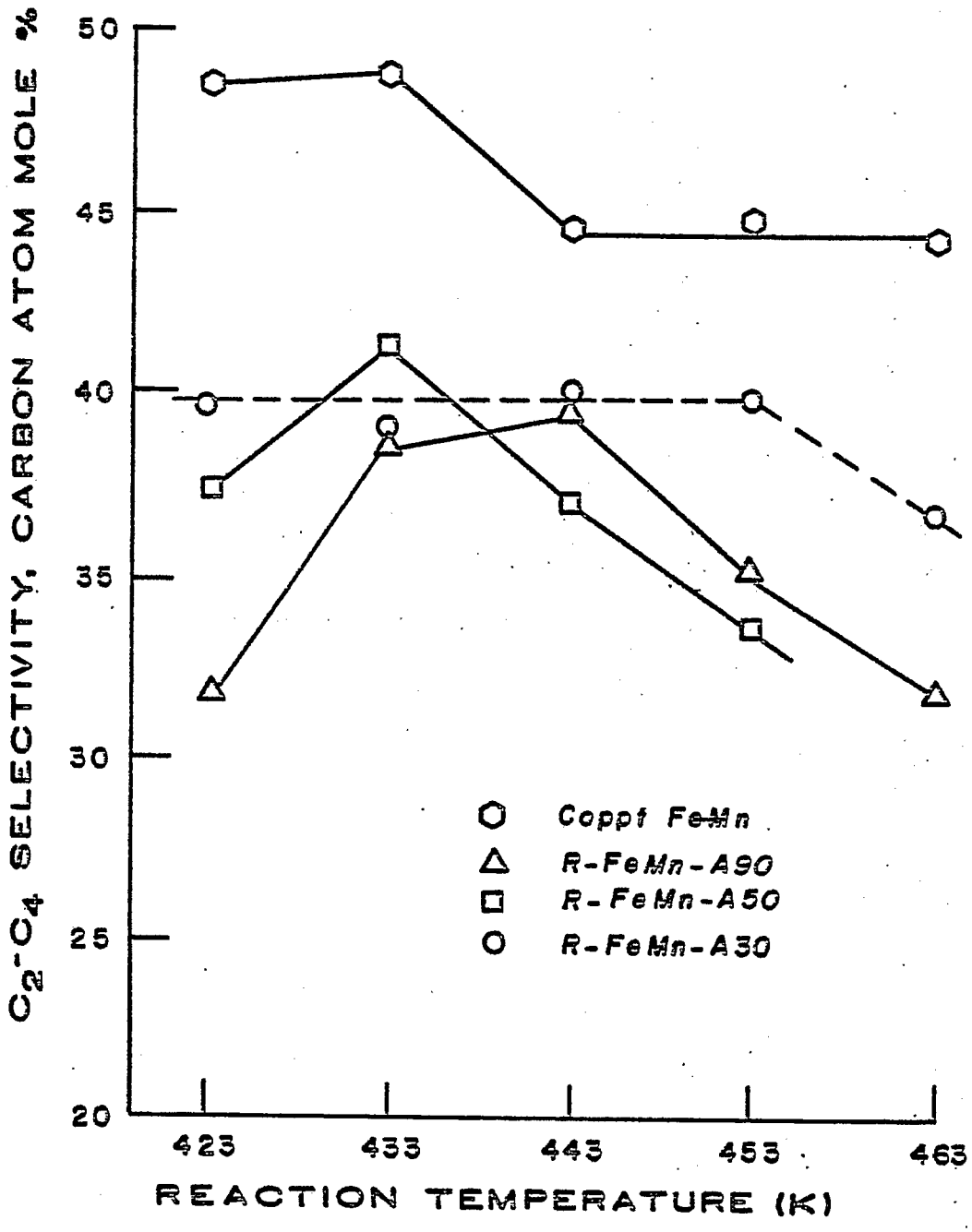
C_2-C_4 SELECTIVITY, CARBON ATOM MOLE %
50
45
40
35
30
25
20
423
433
443
453
463
REACTION TEMPERATURE (K)
Coppt Fe-Mn
R-FeMn-A90
R-FeMn-A50
R-FeMn-A30

Figure 57

C_2-C_4 Hydrocarbon Selectivity of Raney Iron-Manganese Catalyst

Catalyst: Prepared by Caustic Addition Technique

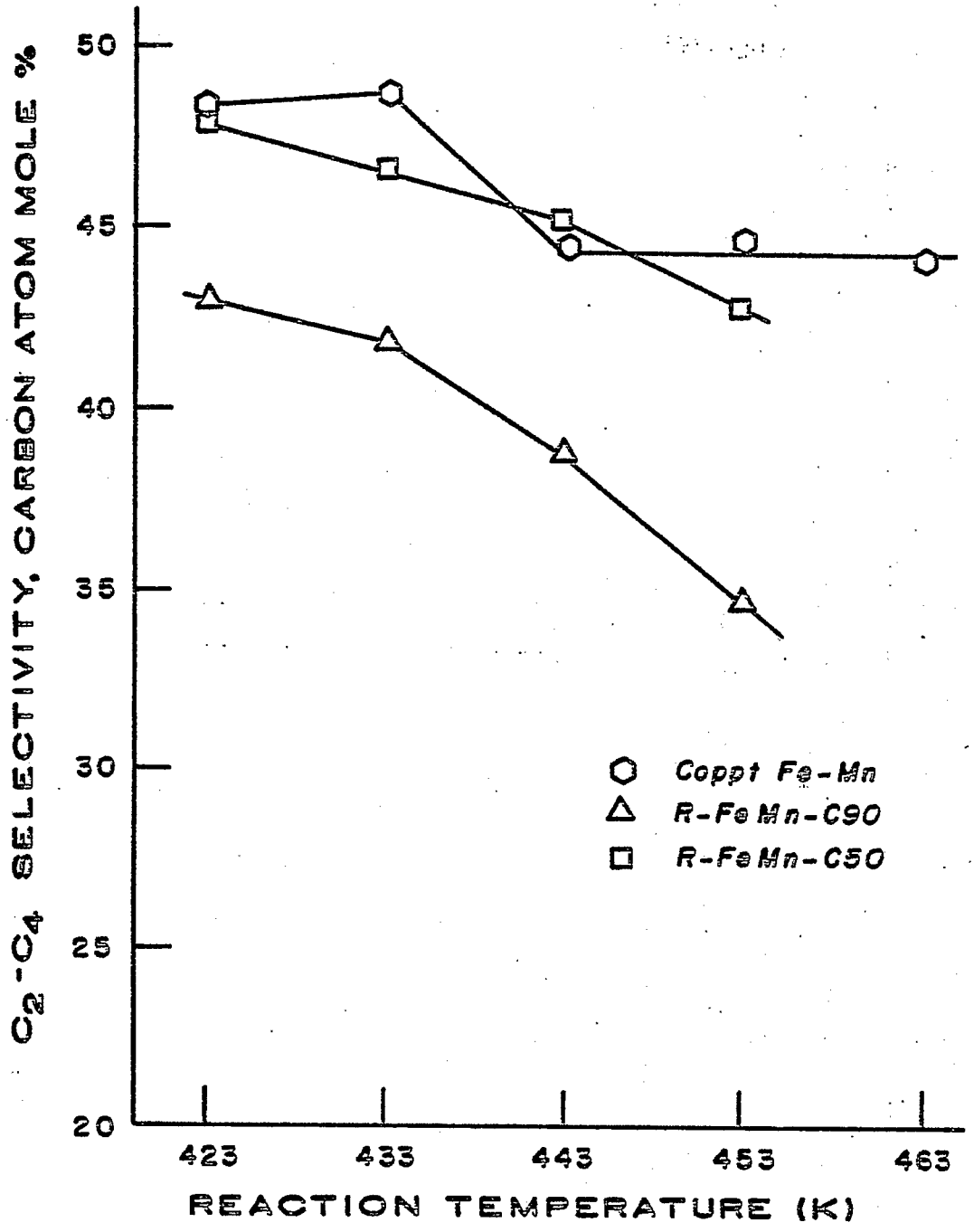
C_2-C_4 SELECTIVITY, CARBON ATOM MOLE %
50
45
40
35
30
25
20
423
433
443
453
463
REACTION TEMPERATURE (K)
Coppt Fe-Mn
R-Fe Mn-C90
R-Fe Mn-C50

Figure 58

C_5^+ Hydrocarbon Selectivity of Raney Iron-Manganese Catalyst

Catalyst: Prepared by Alloy Addition Technique

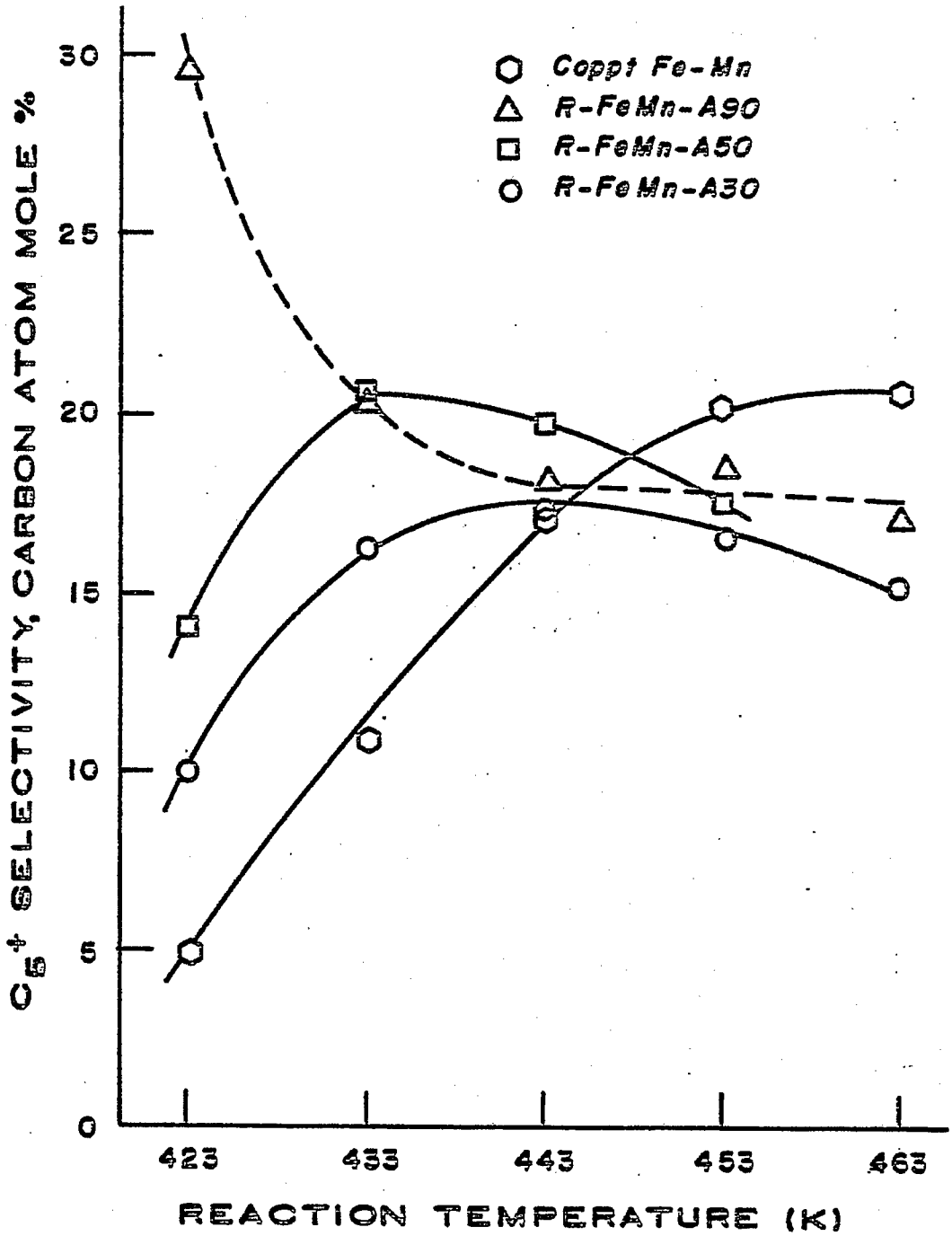
Coppt Fe-Mn
R-FeMn-A90
R-FeMn-A50
R-FeMn-A30
C_5^+ SELECTIVITY, CARBON ATOM MOLE %
0
5
10
15
20
25
30
423
433
443
453
463
REACTION TEMPERATURE (K)

Figure 59

C_5+ Hydrocarbon Selectivity of Raney Iron-Manganese Catalyst

Catalyst: Prepared by Caustic Addition Technique

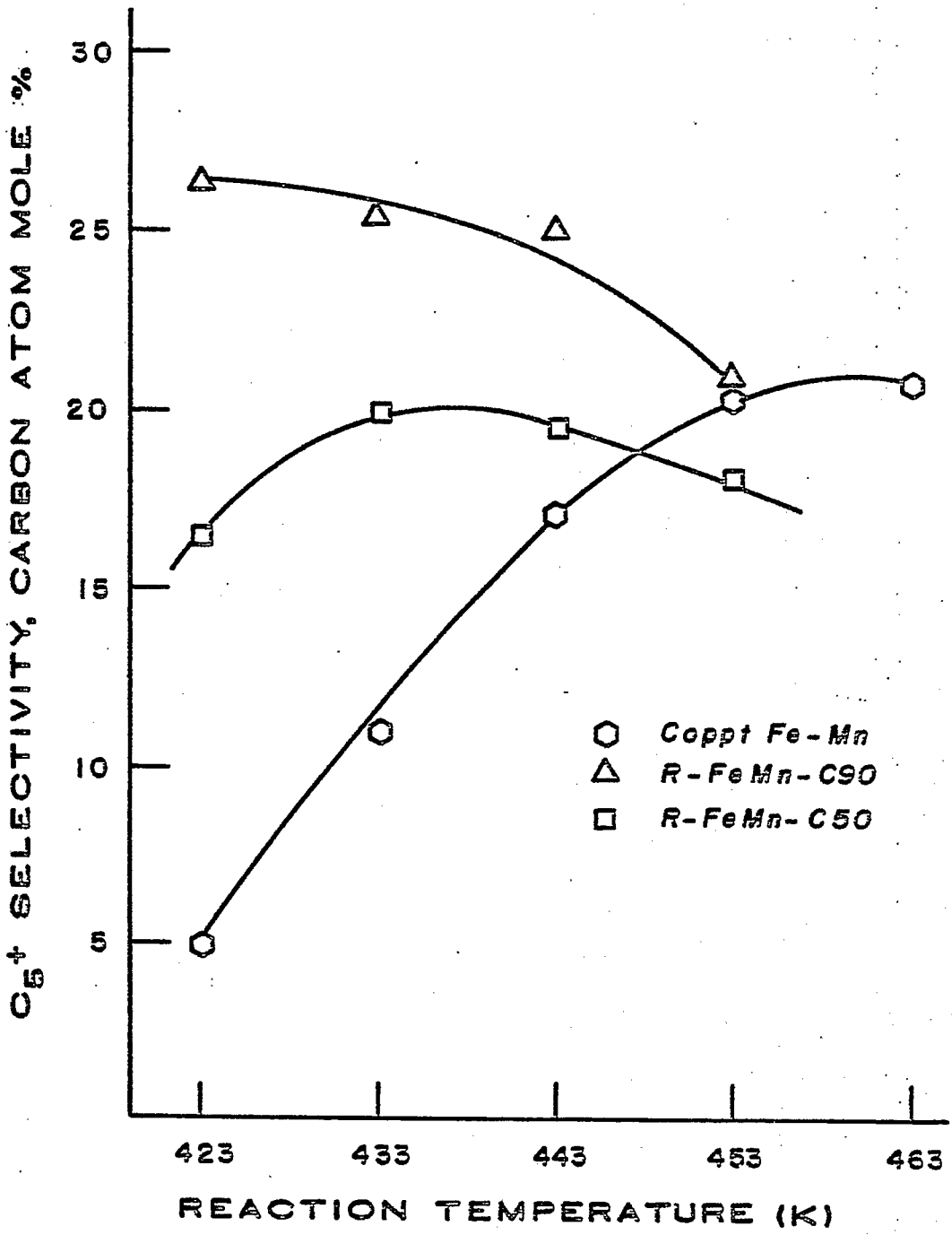
30
25
20
15
10
5
C_5^+ SELECTIVITY, CARBON ATOM MOLE %
Coppt Fe-Mn
R-FeMn-C90
R-FeMn-C50
423
433
443
453
463
REACTION TEMPERATURE (K)

Figure 60

Carbon Dioxide Selectivity of Raney
Iron-Manganese Catalyst

Catalyst: Prepared by Alloy Addition Technique

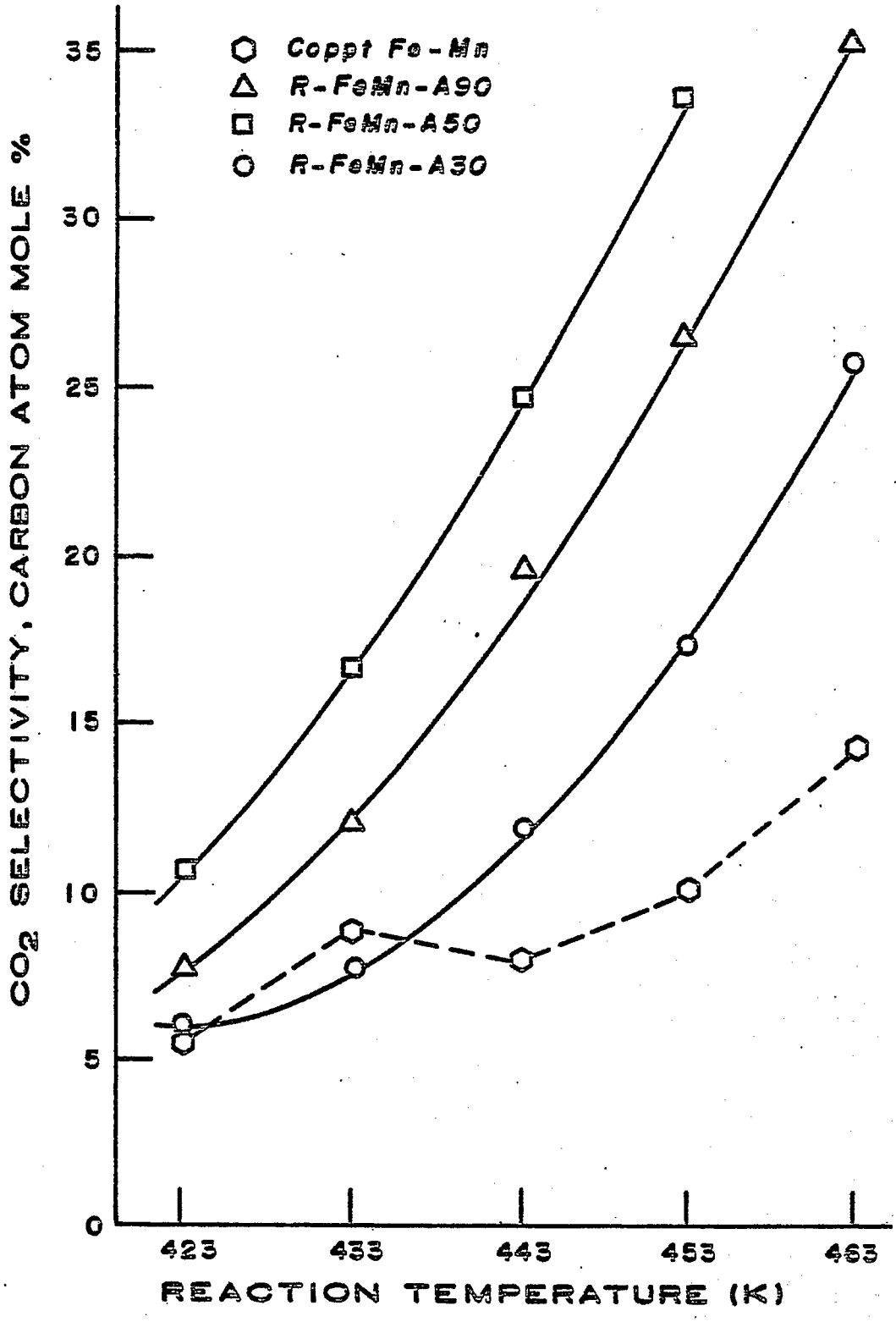
Coppt Fe-Mn
R-FeMn-A90
R-FeMn-A50
R-FeMn-A30
CO2 SELECTIVITY, CARBON ATOM MOLE %
0
5
10
15
20
25
30
35
423
433
443
453
463
REACTION TEMPERATURE (K)

Figure 61

Carbon Dioxide Selectivity of Raney
Iron-Manganese Catalyst

Catalyst: Prepared by Caustic Addition Technique

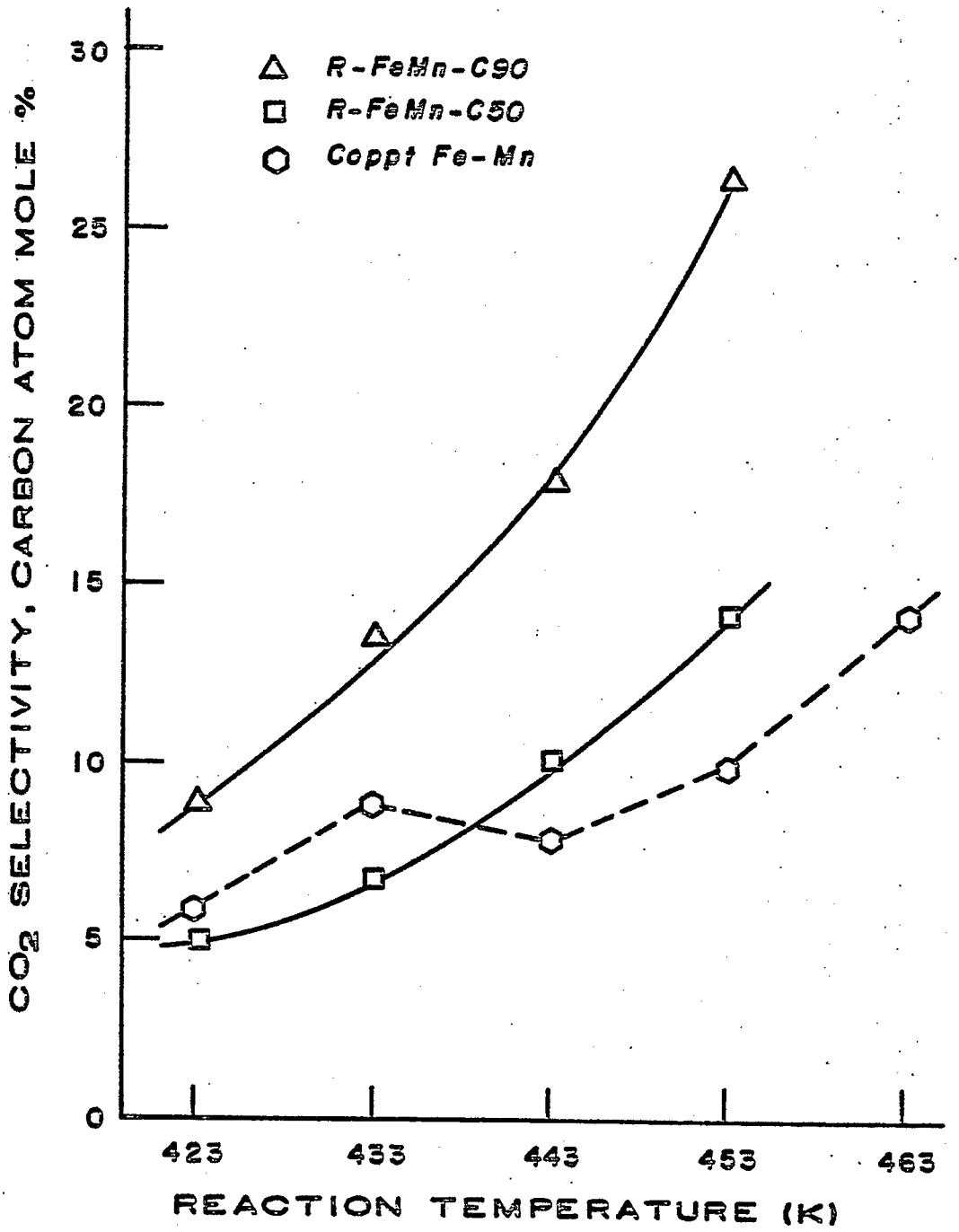
R-FeMn-C90
R-FeMn-C50
Coppt Fe-Mn
CO_2 SELECTIVITY, CARBON ATOM MOLE %
0
5
10
15
20
25
30
423
433
443
453
463
REACTION TEMPERATURE (K)

dioxide selectivity occurs at a high level of carbon monoxide conversion for the Raney iron-manganese catalysts, which was also the same case for the Raney iron catalysts.

The selectivity for C_2, C_3, C_4 hydrocarbon (olefin and paraffin) and C_2-C_4 olefins of the Raney iron-manganese catalysts are listed in Table 19. The C_2-C_4 olefin selectivity decreased slightly with increasing temperature and it ranged from 22 to 34% between 423 and 453 K. The C_2-C_4 olefin selectivity of the Raney iron-manganese catalysts was higher than that of the Raney iron catalysts in the same temperature range (18 - 26%). The selectivity for ethylene decreased slightly with increasing temperature, while the selectivity for ethane increased for a given catalyst (Table 19). The C_3 and C_4 olefin and paraffin selectivities remained constant or decreased slightly with increasing temperature.

The olefin-to-paraffin ratios of the C_2, C_3, and C_4 hydrocarbons as well as the olefin-to-paraffin ratios of the total C_2-C_4 hydrocarbons are presented in Table 20. The olefin-to-paraffin ratio of the C_2 hydrocarbon decreased markedly with increasing temperature, while the olefin-to-paraffin ratios of the C_3 and C_4 hydrocarbons increased. This increase in the olefin-to-paraffin ratio of the C_3 and C_4 hydrocarbons was in contrast to the decrease in the olefin-to-paraffin ratios of the C_3 and C_4 hydrocarbons observed with the Raney iron catalysts. The resultant C_2-C_4 hydrocarbon olefin-to-paraffin ratio remained quite constant or increased slightly with increasing temperature.

Table 19

C_2-C_4 Olefin Selectivity of Raney Iron-Manganese Catalysts

Catalyst Type	Temperature (K)	Conversion (%)	Product Carbon Atom Selectivity (%)						
			[a]$C_2^=$	C_2	$C_3^=$	C_3	$C_4^=$	C_4	$C_2^= - C_4^=$
R-FeMn-A30	423	0.7	7.0	4.8	10.7	4.8	7.3	4.5	25.0
	433	1.4	6.0	5.7	10.8	4.5	7.5	4.3	24.2
	443	2.8	5.4	6.4	11.5	4.4	8.0	4.2	24.9
	453	4.6	5.0	6.5	11.8	4.1	8.2	3.9	25.0
	463	8.6	4.6	5.7	11.4	3.5	7.9	3.4	23.9
	473	12.9	4.6	4.8	10.8	3.0	7.7	2.9	23.1
R-FeMn-A50	423	0.6	7.4	3.5	9.9	4.6	7.1	4.6	24.4
	433	1.2	7.2	4.7	11.2	4.9	8.3	4.8	26.7
	443	2.7	5.4	4.8	10.6	4.0	8.0	4.2	24.0
	453	5.0	4.3	4.6	10.0	3.4	7.7	3.6	22.0

Table 19 - Continued

Catalyst Type	Temperature (K)	Conversion (%)	Product Carbon Atom Selectivity (%)						
			$C_2^=$	C_2	$C_3^=$	C_3	$C_4^=$	C_4	$C_2^= - C_4^=$
R-FeMn-A90	423	1.2	6.9	2.3	9.0	3.8	6.5	3.3	22.3
	433	1.6	8.5	2.9	11.2	4.3	8.0	3.8	27.7
	443	2.9	8.3	3.3	11.6	3.9	8.6	3.5	28.5
	453	6.1	6.2	3.7	10.5	3.2	7.9	3.0	24.6
	463	13.0	4.5	4.0	9.8	2.9	7.5	3.1	23.8
	473	23.6	4.3	3.7	9.7	2.4	7.2	2.5	21.1
R-FeMn-A50 (10%)	423	0.4	9.5	5.9	13.4	5.8	8.8	5.4	31.7
	433	1.0	8.0	5.5	12.5	5.0	8.6	4.8	29.1
	443	2.2	6.2	6.5	12.1	4.6	8.3	4.3	26.6
	453	4.9	4.7	7.3	12.1	4.4	8.1	4.4	25.1

Table 19 - Continued

Catalyst Type	Temperature (K)	Conversion (%)	Product Carbon Atom Selectivity (%)							
			$C_2^=$	C_2	$C_3^=$	C_3	$C_4^=$	C_4	$C_2^= - C_4^=$
Coppt Fe-Mn	423	0.2	10.4	3.3	13.2	5.7	9.7	6.0	33.3
	433	0.4	10.9	3.9	13.8	5.6	9.4	5.2	34.1
	443	1.2	9.4	4.2	12.8	4.8	8.9	4.4	31.1
	453	2.3	8.5	4.7	13.3	4.5	9.5	4.4	21.3
	463	4.4	8.2	4.3	13.7	4.0	10.0	4.1	31.9
R-FeMn-C90	423	0.8	9.2	2.7	10.9	5.1	8.0	7.0	28.0
	433	2.0	8.6	3.0	10.8	4.5	8.2	6.5	27.6
	443	3.4	7.6	3.4	10.5	4.1	8.1	4.9	26.2
	453	7.4	6.1	3.5	10.0	3.5	7.9	3.8	24.0

Table 19 - Continued

Catalyst Type	Temperature (K)	Conversion (%)	Product Carbon Atom Selectivity (%)					
			$C_2^=$	C_2	$C_3^=$	C_3	$C_4^=$	C_4	$C_2^= - C_4^=$
R-FeMn-C50	423	0.9	9.3	5.8	13.2	5.9	8.6	5.3	31.1
	433	1.9	7.8	6.6	12.9	5.4	8.7	5.1	29.4
	443	3.8	6.7	7.0	12.8	4.9	8.9	4.8	28.4
	453	6.5	5.9	6.7	12.6	4.4	8.6	4.4	27.1
R-FeMn-C50[b]	423	0.7	11.4	4.9	13.9	6.1	9.3	5.5	34.6
	433	1.6	9.3	5.4	13.0	5.3	8.9	5.0	31.2
	443	3.1	7.8	6.1	12.9	4.8	9.0	4.7	29.7
	453	6.4	5.9	6.0	11.7	4.0	8.1	4.0	25.7

[a]Superscript '=' refers to an olefin.

[b]Duplicate preparation.

Table 20

C_2-C_4 Olefin-to-Paraffin Ratios for Raney Iron-Manganese Catalysts

Catalyst Type	Temp. (K)	C_2(O/P)[a]	C_3(O/P)	C_4 (O/P)	C_2-C_4 (O/P)
R-FeMn-A30	423	1.47	2.24	1.62	1.78
	433	1.06	2.38	1.75	1.68
	443	0.83	2.61	1.93	1.64
	453	0.77	2.84	2.09	1.69
	463	0.81	3.23	2.35	1.87
	473	0.96	3.65	2.68	2.14
R-FeMn-A50	423	2.11	2.17	1.55	1.93
	433	1.54	2.31	1.73	1.87
	443	1.11	2.65	1.92	1.85
	453	0.94	2.95	2.14	1.90
R-FeMn-A90	423	3.05	2.40	1.94	2.39
	433	2.94	2.64	2.13	2.51
	443	2.49	2.94	2.45	2.58
	453	1.66	3.25	2.63	2.42
	463	1.12	3.38	2.41	2.17
	473	1.18	4.09	2.90	2.49
Coppt Fe-Mn	423	3.12	2.32	1.61	2.21
	433	2.79	2.46	1.82	2.32
	443	2.25	2.68	2.04	2.34
	453	1.85	2.94	2.15	2.30
	463	1.91	3.38	2.46	2.57
R-FeMn-A50 (10%)	423	1.63	2.32	1.62	1.86
	433	1.44	2.48	1.78	1.88
	443	0.94	2.63	1.82	1.69
	453	0.67	2.76	1.84	1.56

Table 20 - Continued

Catalyst Type	Temp. (K)	C_2 (O/P)[a]	C_3 (O/P)	C_4 (O/P)	C_2-C_4 (O/P)
R-FeMn-C50	423	1.60	2.24	1.64	1.83
	433	1.18	2.41	1.70	1.72
	443	0.96	2.60	1.84	1.69
	453	0.87	2.86	1.98	1.75
R-FeMn-C50[b]	423	2.33	2.30	1.71	2.11
	433	1.72	2.47	1.78	2.00
	443	1.29	2.66	1.91	1.90
	453	0.99	2.92	2.03	1.84
R-FeMn-C90	423	3.36	2.13	1.14	1.89
	433	2.83	2.38	1.27	1.97
	443	2.27	2.54	1.67	2.12
	453	1.73	2.91	2.09	2.23

[a] O/P : Olefin-to-paraffin ratio.

[b] Duplicate preparation.

The variation of the olefin-to-paraffin ratios of the C_2, C_3, C_4 and C_2-C_4 hydrocarbons with temperature is presented for the Raney iron-manganese catalyst (R-FeMn-C90) in Figure 62.

The dependence of C_2-C_4 hydrocarbon olefin-to-paraffin ratio on the reaction temperature is shown in Figure 63. The C_2-C_4 hydrocarbon olefin-to-paraffin ratio ranged from 1.6 to 2.6, which was in a higher range than that of the Raney iron, 1.0 to 1.5. The C_2-C_4 olefin-to-paraffin ratios for the Raney iron-manganese catalysts remained constant or increased slightly with increasing temperature in contrast to the marked decrease of C_2-C_4 olefin-to-paraffin ratios for the Raney iron catalysts as shown in Figure 49.

Product Distribution

The distribution of hydrocarbon products from the Fischer-Tropsch synthesis is often correlated by the Schulz-Flory equation:

$$\ln (m_p/p) = \ln \frac{(1-\alpha)^2}{\alpha} + p \ln \alpha \qquad (36)$$

where m_p is the mass fraction of a hydrocarbon (olefin plus paraffin) with a carbon number p and α is the chain propagation probability.

Since all the Raney catalysts were tested at a differential condition for a relatively short period of time, no sizable amount of liquid and/or solid high molecular weight hydrocarbons could be collected for gas chromatographic product analysis. In all cases hydrocarbon products up to C_7 have been analyzed. Equation (36) was used to determine the chain propagation probability.

Another equation (77), developed by Zein El Deen, et al.,[162] was also used to analyze the product distribution data and to

Figure 62

Low Molecular Weight Hydrocarbon Selectivity

Catalyst: R-FeMn-C90

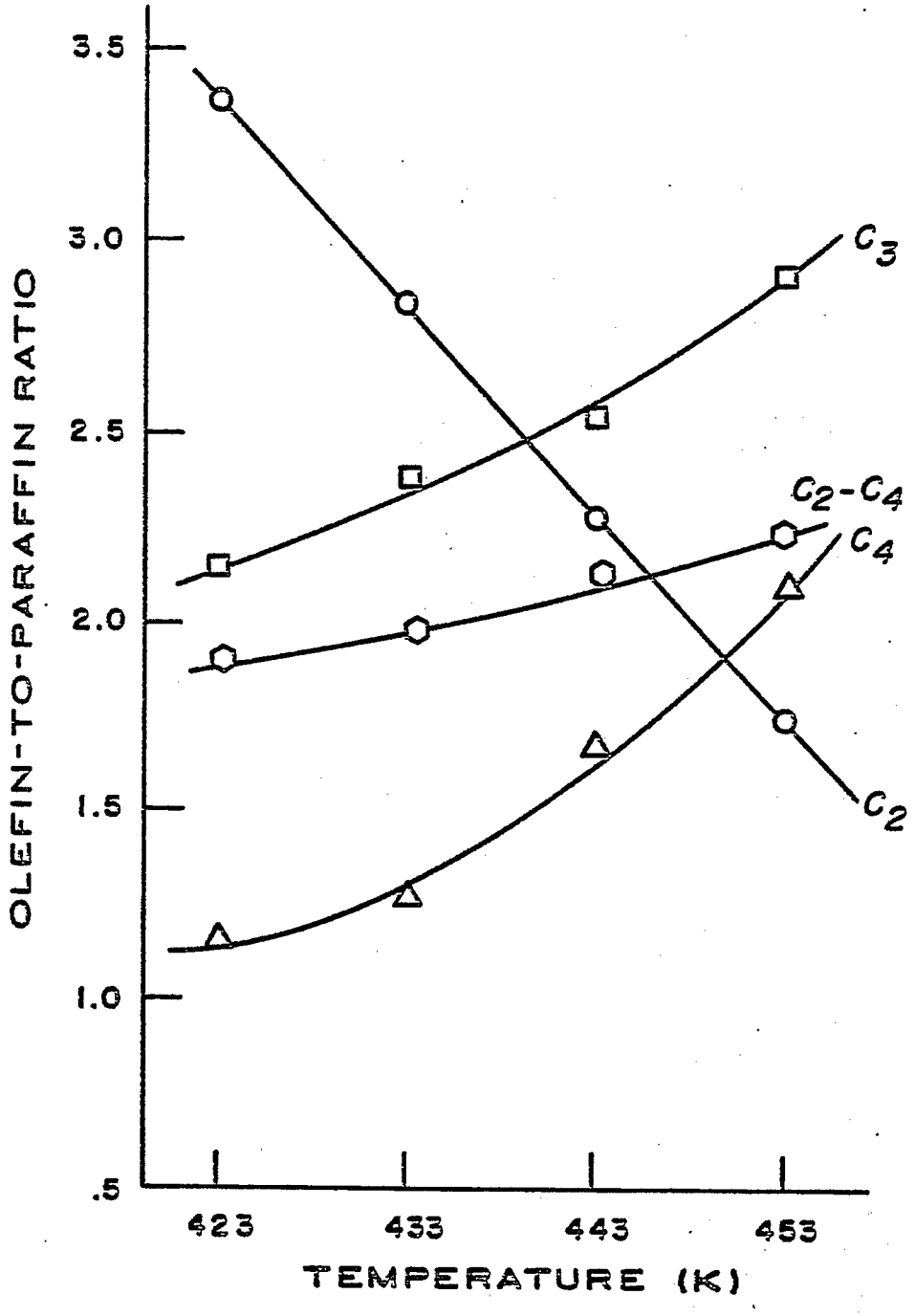
OLEFIN-TO-PARAFFIN RATIO
3.5
3.0
2.5
2.0
1.5
1.0
.5
423
433
443
453
TEMPERATURE (K)
C_3
C_2-C_4
C_4
C_2

Figure 63

C_2-C_4 Olefin-to-Paraffin Ratios for
Raney Iron-Manganese Catalysts

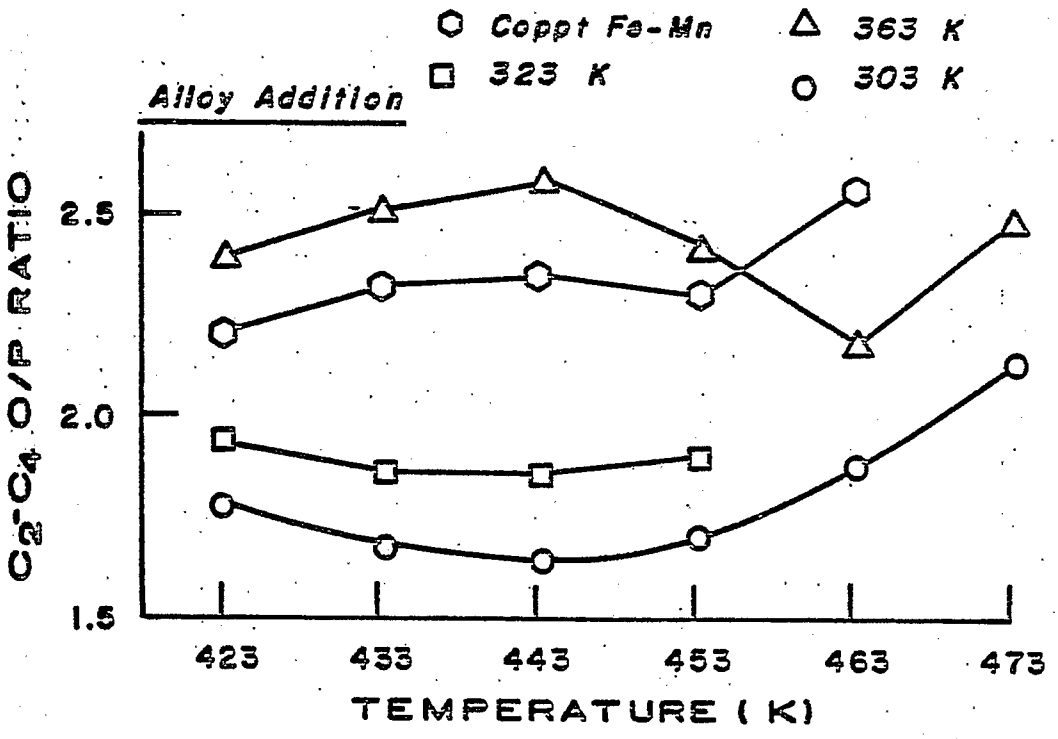
Coppt Fe-Mn
323 K
363 K
303 K
Alloy Addition
C2-C4 O/P RATIO
2.5
2.0
1.5
423
433
443
453
463
473
TEMPERATURE (K)

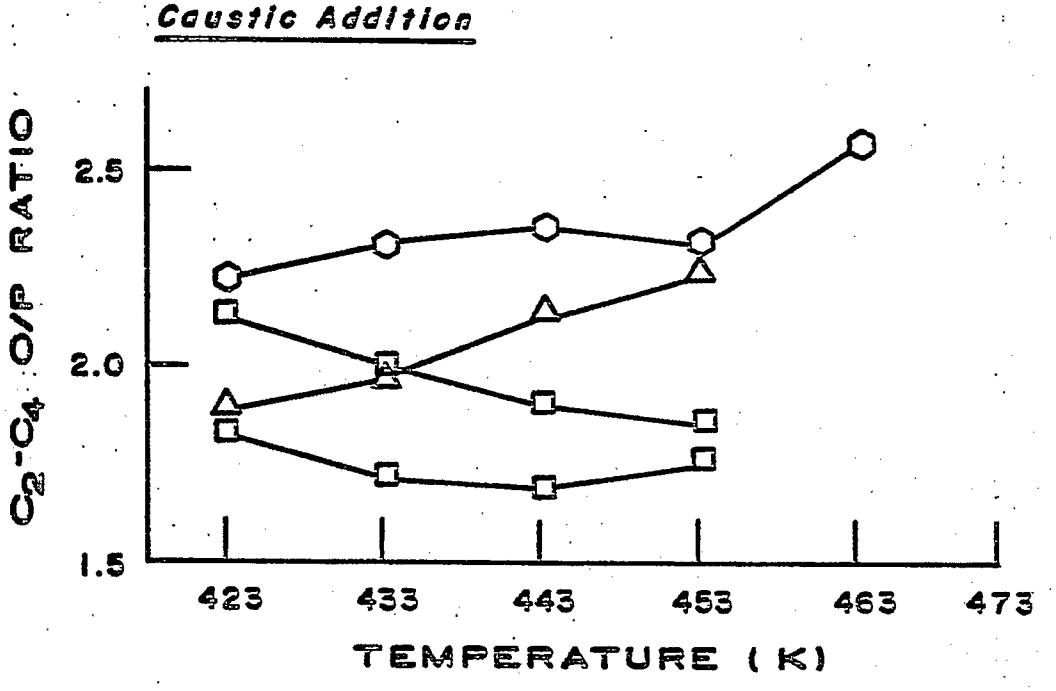
Caustic Addition
C2-C4 O/P RATIO
2.5
2.0
1.5
423
433
443
453
463
473
TEMPERATURE (K)

determine the α values:

$$r_P/r_{CO} = A\alpha^P \qquad (77)$$

where r is the rate of formation of hydrocarbons (paraffin plus olefin) with a carbon number P (mol/sec), r_{CO} is the rate of carbon monoxide conversion (mol/sec), α is the chain propagation probability, and A is a constant. This equation was derived based on an assumption that the carbon chain is built up by the stepwise addition of one carbon atom to an adsorbed growing chain and that the probability of chain growth is independent of chain length. This assumption is essentially the same as the one made in the derivation of Equation (36). However, Equation (77) has a different aspect from Equation (36). Equation (77) not only correlates the product distribution of hydrocarbons (olefin plus paraffin), but it also predicts the product carbon atom mole percent of other carbon products such as carbon dioxide and branched or oxygenated hydrocarbons. The fraction of total carbon atom in all hydrocarbons, olefins and paraffins, is obtained from Equation (77) as follows:

$$\Sigma S_P = \Sigma P \frac{r_P}{r_{CO}} = \int_{P=0}^{P=\infty} P A\alpha^P dP = \frac{A}{(\ln \alpha)^2} \qquad (78)$$

where S_P is the mole fraction of carbon atom in hydrocarbons (olefin plus paraffin) with a carbon number P. The mole fraction of carbon atoms in carbon dioxide, branched, and oxygenated hydrocarbons is obtained by difference between 1.0 and the value obtained from Equation (78).

The plots of Equation (36) and (77) for a Raney iron-manganese catalyst (R-FeMn-A90) are found in Figure 64. It can be seen that the two plots are essentially the same type, yielding the same α value. The methane selectivity was higher and the C_2 hydrocarbon selectivity was lower than the predicted value by Equation (36). This trend was as typical and is one often observed in the product distribution from the Fischer-Tropsch synthesis reaction.[60]

The α values for the Raney iron and the Raney iron-manganese catalysts obtained from the above two equations using linear regressions are listed in Table 21. According to Equation (36), α value can be obtained from either the slope or the intercept of the plot, $\ln (m_p/p)$ versus p. The two values from the slope and the intercept of the plot were in close agreement (Table 21). The α values for the Raney iron catalysts were in a narrow range of 0.52 - 0.55 from Equation (77) [0.51 - 0.54 from Equation (36)], while α values for the Raney iron-manganese catalysts were in a slightly higher range than the α values for the Raney iron, that is, 0.54 - 0.62 from Equation (77) [0.53 - 0.59 from Equation (36)].

The mole fraction of carbon atoms in all hydrocarbons, olefin plus paraffin, was estimated for each catalyst by Equation (77) using α values obtained from the r_p/r_{CO} versus p plots. The estimated values were always lower than the actual total mole fraction of carbon atom in all hydrocarbons determined experimentally. This discrepancy seemed to be due to the incomplete collection of oxygenated or higher molecular weight hydrocarbons, which led to an overestimation for the total mole fraction of carbon atoms in all hydrocarbons (olefin plus paraffin).

Figure 64

Correlation of Hydrocarbon Product Distribution

Catalyst: R-FeMn-A90

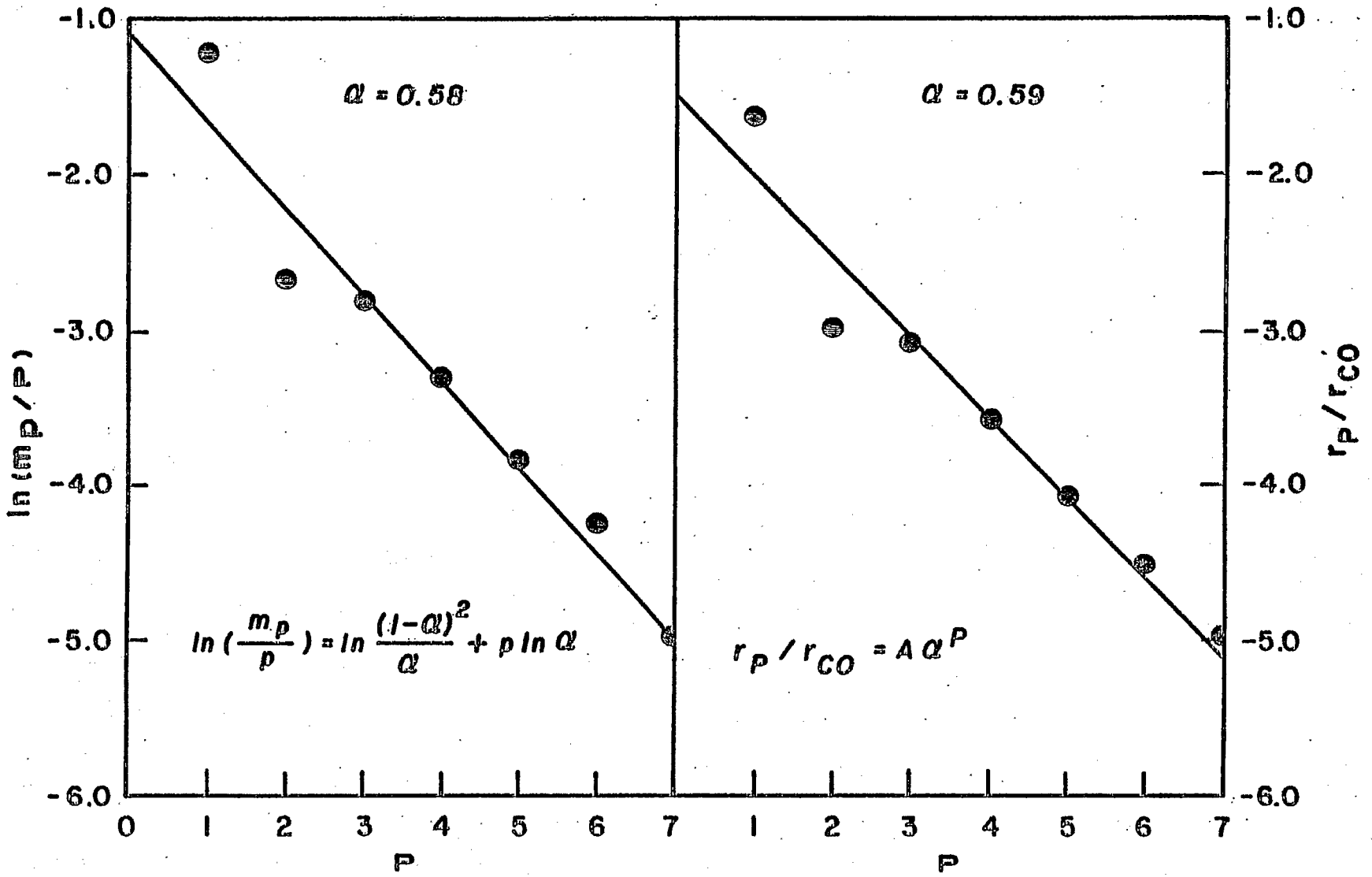
α = 0.58
α = 0.59
$\ln\left(\frac{m_p}{p}\right) = \ln\frac{(1-\alpha)^2}{\alpha} + p\ln\alpha$
$r_P / r_{CO} = A\,\alpha^P$
ln (mp / P)
rp / rco
P
P
-1.0
-2.0
-3.0
-4.0
-5.0
-6.0
0
1
2
3
4
5
6
7

Table 21

Chain Propagation Probability at 453 K

Catalyst Type	Chain Propagation Probability	
	Equation (36)	Equation (79)
ppt Fe	0.51 (0.51)[c]	0.52
R-Fe-A25	0.51 (0.51)	0.53
R-Fe-A50	0.53 (0.53)	0.54
R-Fe-A90	0.51 (0.51)	0.55
R-Fe-A90[a]	0.54 (0.53)	0.52
R-Fe-C25	0.53 (0.53)	0.54
R-Fe-C50[b]	0.51 (0.51)	0.52
R-Fe-C90[b]	0.51 (0.51)	0.52
R-Fe-C90 (10%)	0.52 (0.51)	0.52
Coppt Fe-Mn	0.56 (0.55)	0.57
R-FeMn-A30	0.53 (0.53)	0.58
R-FeMn-A50	0.59 (0.58)	0.60
R-FeMn-A90	0.58 (0.57)	0.59
R-FeMn-A50 (10%)	0.53 (0.53)	0.54
R-FeMn-C90	0.57 (0.56)	0.62
R-FeMn-C50	0.55 (0.54)	0.56
R-FeMn-C50	0.54 (0.54)	0.55

[a]Alloy from Alpha Products.

[b]Chain propagation probability at 443 K.

[c]α values obtained from the intercept of the plots.

Conclusions

1. The aluminum-iron (50/50 wt %) alloy consisted of ζ-$FeAl_2$ and η-Fe_2Al_5 phases, while the aluminum-iron-manganese (59/38/3 wt %) alloy contained only a single phase, $(Fe,Mn)Al_3$.

2. The extent of aluminum leached from the aluminum-iron and the aluminum-iron-manganese alloys increased with increasing leaching temperature in the range of 298 to 363 K and with increasing sodium hydroxide concentration in the range of 2 to 20 wt % for both the alloy and the caustic addition method. The extent of leaching estimated by hydrogen gas evolution was in reasonable agreement with the value obtained by elemental analysis.

3. The BET surface area of Raney iron catalyst ranged from 26 to 54 m^2/g. The BET surface area of Raney iron-manganese ranged from 64 to 116 m^2/g. At a given leaching temperature, leaching with a low concentration of sodium hydroxide solution yielded a catalyst with low surface area.

4. The major metal phase in all the Raney catalysts (iron and iron-manganese) was α-Fe. Unreacted aluminum alloy phases were found from a catalyst leached at a low temperature (< 323 K) or with a dilute NaOH solution (< 20 wt %). Magnetite was found from a

catalyst prepared at a high leaching temperature, 363 K, by caustic addition method.

5. The crystallite size of α-Fe in the Raney catalysts, measured by x-ray line broadening, increased with increasing leaching temperature. There was a linear relationship between the BET surface area and the reciprocal of the crystallite size of α-Fe.

6. Optimum catalyst reduction temperature was 673 K for precipitated and 648 K for Raney-type catalysts, respectively. Both types of catalysts underwent essentially complete reduction at the appropriate reduction temperature within 5 hours.

7. Interphase and intra-particle heat and mass transfer limitations were negligible at the standard reaction conditions.

8. The activity of Raney iron and iron-manganese catalysts, in terms of carbon monoxide conversion, was higher than the precipitated iron and the coprecipitated iron-manganese catalyst, respectively.

9. A Raney catalyst, iron and iron-manganese, prepared at a higher leaching temperature or with higher concentration of sodium hydroxide solution, was more active for carbon monoxide conversion.

10. The activation energy for carbon monoxide conversion over Raney iron and iron-manganese ranged from 96 to 139 KJ/mol.

11. No significant differences in product selectivity were observed for the Raney catalysts prepared at different conditions for both Raney iron and iron-manganese catalysts.

12. Raney iron-manganese catalysts were more selective for C_2-C_4 light olefins than the Raney iron. The C_2-C_4 hydrocarbon

olefin-to-paraffin ratio for Raney iron-manganese ranged from 1.7 to 2.5, while it ranged from 0.9 to 1.3 for Raney iron.

13. The selectivity of Raney iron-manganese catalysts for C_2-C_4 olefins was in the same range as that of the coprecipitated iron-manganese catalyst. The C_2-C_4 hydrocarbon olefin-to-paraffin ratios for Raney iron-manganese catalysts ranged from 1.6 to 2.4 at 453 K, while it was 2.3 for the coprecipitated catalyst at the same temperature.

14. The hydrocarbon product distribution could be correlated by the Schulz-Flory equation. The chain propagation probability for the Raney catalysts ranged from 0.51 to 0.60.

REFERENCES

1. Waddams, A. L., Chemicals from Petroleum, 3rd ed., Wiley, New York (1973).

2. Kölbel, H., and Tillmetz, K. D., Ger. Pat. 2,507,647 (1975).

3. Büssemeier, B., Frohning, C. D., Horn, G., and Klug, W., Ger. Pat. 2,518,964 (1975).

4. Yang, C. H., "Catalytic Synthesis of Light Hydrocarbons from Carbon Monoxide/Hydrogen over Metal Catalysts," Ph.D. Thesis, Dept. of Mining and Fuels Engineering, University of Utah (1979).

5. Zaman Khan, M. K., Yang, C. H., and Oblad, A. G., "The Synthesis of Light Hydrocarbons from CO and H_2 Mixtures over Selected Metal Catalysts," ACS Fuels Div. Preprints 22 (2) 138 (1977).

6. Yang, C. H., Zaman Khan, M. K., Massoth, F. E., and Oblad, A. G., "Studies on the Co-Cu-Al_2O_3 Catalyst System for Conversion of CO and H_2 to Light Hydrocarbon Products," ACS Fuel Div. Preprints 22 (2) 148 (1977).

7. Yang, C. H., and Oblad, A. G., "Catalytic Synthesis of Light Olefinic Hydrocarbons from CO and H_2 over Some Iron Catalysts," ACS Pet. Chem. Div. Preprints 23 (2) 513 (1978).

8. Tsai, Y. S., "Production of Low Molecular Weight Olefins over Unsupported Iron-Manganese Catalysts," M.S. Thesis, Dept. of Mining and Fuels Engineering, Universtity of Utah (1980).

9. Tsai, Y. S., Hanson, F. V., Oblad, A. G., and Yang, C. H., "The Hydrogenation of Carbon Monoxide over Unsupported Iron-Manganese Catalysts for the Production of Low Molecular Weight Olefins," ACS Fuel Div. Preprints 25 (2) 127 (1980).

10. Dent, A. L., and Lin, M., "Cobalt-Based Catalysts for the Production of C_2-C_4 Hydrocarbons from Syn-Gas," ACS Pet. Chem. Div. Preprints 23 (2) 502 (1978).

11. Diaz, G. C., "Production of Olefins with Nickel-Zeolite Catalyst," ACS Pet. Chem. Div. Preprints 23 (2) 765 (1978).

12. Ellgen, P. C., Bartley, W. J., Bhasin, M. M., and Wilson, T. P., "Rhodium-Based Catalyst for the Conversion of Synthesis Gas to Two-Carbon Chemicals," ACS Pet. Chem. Div. Preprints 23 (2) 616 (1978).

13. Murchinson, C. G., and Murdick, B. A., "Use Syngas for Olefin Feedstock," Hydrocarbon Proc. 60 (1) 159 (1981).

14. Haynes, W. P., Baird, M. J., Schehl, R. R., and Zarochak, M. F., "Fischer-Tropsch Studies in a Bench-Scale Tube Wall Reactor Using Magnetite, Raney Iron and Taconite Catalysts," ACS Pet. Chem. Div. Preprints 23 (2) 559 (1978).

15. Russel, J. H., Oden, L. L., and Henry, J. L., "Effects of Additives on Methanation Activity of Raney Nickel Catalysts," Bur. Mines Rep. Invest. 8487 (1980).

16. Pennline, H. W., Schehl, R. R., Haynes, W. P., and Forney, A. J., "Methanation in Catalyst-Sprayed Tube Wall Reactors: A Review," DOE/PETC/TR-80/7 (1980).

17. Dirksen, H. A., and Linden, H. R., "Pipeline Gas from Coal by Methanation of Synthesis Gas," Inst. Gas Technol. Res. Bull. 31 (1963).

18. Sabatier, P., and Senderens, J. B., C. R. Acad. Sci., Paris 134, 514 (1902), quoted in ref. 49.

19. Badische Aniline und Soda Fabrik, Ger. Pat. 295,202 and 295,203 (1916).

20. Fischer, F., and Tropsch, H., Brennst.-Chem. 4, 276 (1923), quoted in ref. 49.

21. Frohning, C. D., "Fischer-Tropsch Synthese," Chemierohstoffe Aus Kohle, Falbe, J. ed. Thieme, Stuttgart (1977).

22. Pichler, H., "Twenty-five Years of Synthesis of Gasoline by Catalytic Conversion of Carbon Monoxide and Hydrogen," Advan. Catal., vol. 4, p. 284, Frankenburg, W. G., Rideal, E. K., and Komarewsky, V. I., eds., Academic Press, New York (1952).

23. Pichler, H., and Hector, A., "Carbon Monoxide-Hydrogen Reactions," Kirk-Othmer Encyclopedia of Chemical Technology, Vol. 4, p. 446, 2nd ed., Wiley, New York (1964).

24. Bienstock, D., Field, J. H., Forney, A. J., Meyers, J. G., and Benson, H. E., "The Fischer-Tropsch Synthesis in the Oil Circulation Process: Experiments with a Nitrided Fused-Irion Catalyst," Bur. Mines Rep. Invest. 5603 (1960).

25. Bienstock, D., Forney, A. J., and Field, J. H., "Fischer-Tropsch Oil Circulation Process: Experiments with a Massive-Iron Catalyst," Bur. Mines Rep. Invest. 6194 (1963).

26. Schlesinger, M. D., Benson, H. E., Murphy, E. M., and Storch, H. H., "Chemicals from the Fischer-Tropsch Synthesis," Ind. Eng. Chem. 46, 1322 (1954).

27. Schlesinger, M. D., Crowell, J. H., Leva, M., and Storch, H. H., "Fischer-Tropsch Synthesis in Slurry Phase," Ind. Eng. Chem. 43, 1474 (1951).

28. Schlesinger, M. D., and Benson, H. E., "Upgrading Fischer-Tropsch Products," Ind. Eng. Chem. 47 2104 (1955).

29. Karn, F. S., Schultz, J. F., Kelly, R. E., and Anderson, R. B., "Hydrogen Sulfide Poisoning of Nitrided and Carbided Iron Catalysts in the Fischer-Tropsch Synthesis," Ind. Eng. Chem. Prod. Res. Dev. 3, 33 (1964).

30. Schultz, J. F., Seligman, B., Shaw, L., and Anderson, R. B., "Effect of Nitriding on Three Types of Iron Catalysts," Ind. Eng. Chem., 44, 397 (1952).

31. Baird, M. J., and Steffgen, F. W., "Methanation Studies on Nickel-Aluminum Flame-Sprayed Catalysts," Ind. Eng. Chem. Prod. Res. Dev. 16, 142 (1977).

32. Elliot, J. J., Haynes, W. P., and Forney, A. J., "Gasoline via the Fischer-Tropsch Reaction Using the Hot Gas Recycle System," ACS Fuel Div. Preprints 16 (1) 44 (1972).

33. Field, J. H., Bienstock, D., Forney, A. J., and Demski, R. J., "Further Studies of the Fischer-Tropsch Synthesis Using Gas Recycle Cooling (Hot-Gas-Recycle Process)," Bur. Mines Rep. Invest. 5871 (1961).

34. Bussemeier, B., Frohning, C. D., and Cornils, B., "Low Olefins via Fischer-Tropsch," Hydrocarbon Proc. 55 (11) 105 (1976).

35. Anderson, R. B., "The Thermodynamics of the Hydrogenation of Carbon Monoxide and Related Reaction," Catalysis, Vol. 4, Chapter 1, Emmett, P. H., ed., Reinhold, New York (1956).

36. Rossini, F. D., Pitzer, K. S., Taylor, W. J., Ebert, J. P., Kilpatrick, J. E., Beckett, C. W., Williams, M. G., and Werner, H. G., "Selected Values of Properties of Hydrocarobns," Nat. Bur. Stand. Circular C461 (1947).

37. Anderson, R. B., Lee, C. B., and Mahiels, J. C., "The Thermodynamics of the Hydrogenation of Oxides of Carbon, J. Can. Chem. Eng. 54, 590 (1976).

38. Vannice, M. A., "The Catalytic Synthesis of Hydrocarbons from Carbon Monxoide and Hydrogen," Catal. Rev.-Sci. Eng., 14 (2) 153 (1976).

39. Karn, F. S., Schultz, J. F., and Anderson, R. B., "Hydrogenation of Carbon Monoxide and Carbon Dioxide on Supported Ruthenium Catalysts at Moderate Pressures," Ind. Eng. Chem. Prod. Res. Develop. 4, 265 (1965).

40. Dry, M. E., Shingles, T., and Boshoff, L. J., "Rate of Fischer-Tropsch Reaction over Iron Catalysts," J. Catal. 25, 99 (1972).

41. Anderson, R. B., Seligman, B., Schultz, J. F., Kelly, R. E., and Elliott, M. A., "Some Important Variables of the Synthesis on Iron Catalysts," Ind. Eng. Chem. 44, 391 (1952).

42. Kölbel, H., and Engelhardt, F., Erdöl u Kohle 3, 529 (1950), quoted in ref. 45.

43. Pichler, H., "Synthesis of Hydrocarbons from Carbon Monoxide and Hydrogen," Bur. Mines Special Rept. (1947), quoted in ref. 45.

44. Anderson, R. B., Karn, F. S., and Schultz, J. F., "Kinetics of the Fischer-Tropsch Synthesis on Iron Catalysts," Bur. Mines Bull. 614 (1964).

45. Anderson, R. B., "Kinetics and Reaction Mechanism of the Fischer-Tropsch Synthesis," Catalysis, Vol. 4, Chap. 3, Emmett, P. H., ed., Reinhold, New York (1956).

46. Atwood, H. E., and Bennett, C. O., "Kinetics of the Fischer-Tropsch Reaction over Iron," Ind. Eng. Chem. Proc. Des. Develop. 18 (1) 163 (1979).

47. Vannice, M. A., "The Catalytic Synthesis of Hydrocarbons from H_2/CO Mixtures over the Group VIII Metals. I. The Specific Activities and Product Distributions of Supported Metals," J. Catal. 37, 449 (1975).

48. Vannice, M. A., "The Catalytic Synthesis of Hydrocarbons from H_2/CO Mixtures over the Group VIII Metals. II. The Kinetics of the Methanation Reaction over Supported Metals," J. Catal. 37, 462 (1975).

49. Dry, M. E., "The Fischer-Tropsch Synthesis," Catalysis, Science and Technology, Chap. 4, Anderson, J. R., and Boudart, M., eds., Springer-Verlag, New York (1981).

50. Kölbel, H., and Hanus, D., "Zum Reaktionsmechanismus der Fischer-Tropsch-Synthese. X. Mitteilung," Chem. Ing. Techn. 46, 1042 (1974).

51. Kölbel, H., Ralek, M., and Jiru, P., "Infrarotspektren der Adsorptionskomplexe der Kohlenmonoxids und des Wasserstoffs auf eineum Eisen-Magnesiumoxid-Mischkatalysator," Erdol u Kohle, 23 580 (1970).

52. Blyholder, G., and Goodsel, A. J., "Infrared Spectra of C_2H_4 Adsorption and CO insertion Reactions on an Fe Surface," J. Catal. 23, 374 (1971).

53. Blyholder, G., "Structures of Some C_xH_yO Compounds Adsorbed on Iron," J. Phys. Chem. 70, 893 (1966).

54. Kölbel, H., and Roberg, H., "Chemisorption Wärmer der Simultanadsorption an Eisen-Katalysatoren der Fischer-Tropsch-Synthese. XI. Mitteilung zum Reaktionsmechanismus der Fischer-Tropsch-Synthese," Ber. Bunsenges. Phys. Chem. 81, 634 (1977).

55. Kölbel, H., Patzschke, G., and Hammer, H., "Zum Reaktions-mechanismus der Fischer-Tropsch-Synthese. IX. Mitteilung: Stöchiometrische Chemisorptionskomplexe an Eisenkatalysatoren," Brennst.-Chem. 47, 4 (1966).

56. Anderson, R. B., Hofer, L. E., and Storch, H. H., "Der Reaktionsmechanismus der Fischer-Tropsch-Synthese," Chem. Ing. Techn. 30, 560 (1958).

57. Della Betta, R. A., and Shelef, M., "Heterogeneous Methanation: In Situ Infrared Spectroscopic Study of Ru/Al_2O_3 during the Hydrogenation of CO," J. Catal. 48, 111 (1977).

58. Rofer-DePoorter, C. K., "A Comprehensive Mechanism for the Fischer-Tropsch Synthesis," Chem. Rev. 81, 447 (1981).

59. Pichler, H., and Schulz, H., "Neuere Erkenntnisse auf dem Gebiet der Synthese von Kohlenwasserstoffen aus CO und H_2," Chem. Ing. Techn. 42, 1162 (1970).

60. Henrici-Olivé, G., and Olivé, S., "The Fischer-Tropsch Synthesis: Molecular Weight Distribution of Primary Products and Reaction Mechanism," Angew. Chem. Int. Ed. 15, 136 (1976).

61. Fischer, F., and Tropsch, H., Chem. Ber. 59, p. 830, p. 832 (1926) quoted in ref. 58.

62. Raupp, G. B., and Delgass, W. N., "Mössbauer Investigation of Supported Fe Catalysts. III. In Situ Kinetics and Spectroscopy during Fischer-Tropsch Synthesis," J. Catal. 58, 361 (1977).

63. Galwey, A. K., "A Kinetic Investigation of the Reaction of Nickel Carbide with Hydrogen," J. Catal. 1, 227 (1962).

64. Kummer, J. T., Dewitt, T. W., and Emmett, P. H., "Some Mechanism Studies on the Fischer-Tropsch Synthesis Using C^{14}," J. Am. Chem. Soc. 70, 3632 (1948).

65. Ekerdt, J. G., and Bell, A. T., "Synthesis of Hydrocarbons from CO and H_2 over Silica-Supported Ru: Reaction Rate Measurements and Infrared Spectra of Adsorbed Species," J. Catal. 58, 170 (1979).

66. Rabo, J. A., Risch, A. P., and Poutsma, M. L., "Reactions of Carbon Monoxide and Hydrogen on Co, Ni, Ru, and Pd Metals," J. Catal. 53, 295 (1978).

67. Biloen, P., Helle, J. N., and Sachtler, W. M. H., "Incorporation of Surface Carbon into Hydrocarbons during Fischer-Tropsch Synthesis: Mechanistic Implications," J. Catal. 58, 95 (1979).

68. Flory, P. J., "Molecular Size Distribution in Linear Condensation Polymers," J. Am. Chem. Soc. 58, 1877 (1936).

69. Schulz, G. V., Z. Phys. Chem. B43, 25 (1939), quoted in ref. 49.

70. Storch, H. H., Golumbic, N., and Anderson, R. B., The Fischer-Tropsch and Related Syntheses, Wiley, New York (1951).

71. Anderson, R. B., Friedel, R. A., and Storch, H. H., "Fischer-Tropsch Reaction Mechanism Involving Stepwise Growth of Carbon Chain," J. Chem. Phys. 19, 313 (1951).

72. Weller, S. W., and Friedel, R. A., "Isomer Distribution in Hydrocarbons from the Fischer-Tropsch Process," J. Chem. Phys. 17, 801 (1949).

73. Manes, M., "The Distribution of Liquid and Solid Fischer-Tropsch Hydrocarbons by Carbon Number," J. Am. Chem. Soc. 74, 3148 (1949).

74. Cady, W. E., Launer, P. J., and Weitkamp, A. W., "Products of Hydrogenation of Carbon Monoxide," Ind. Eng. Chem. 45, 343, 350, 363 (1953).

75. Madon, R. J., "On the Growth of Hydrocarbon Chains in the Fischer-Tropsch Synthesis," J. Catal. 57, 183 (1979).

76. Haddeland, G. E., "Process Economics Reviews - Ethylene from Carbon Monoxide and Hydrogen," Stanford Research Institute, Report No. PEP 76-3-3 (1977).

77. Rao, V. U. S., Gormley, R. J., Pennline, H. W., Schneider, L. C., and Obermeyer, R., "Synthesis Gas Conversion to Gasoline Range Hydrocarbons over Medium Pore Zeolite Catalysts Containing 3d-Metals and Bimetallics," ACS Fuel Div. Preprints 25 (2) 119 (1980).

78. "New Route Produces Ethylene from Synthesis Gas," Chem. Eng. News, Nov. 15 (1982).

79. Raney, M., U.S. Pat. 1,563,787 (1925).

80. Raney, M., U.S. Pat. 1,628,191 (1927).

81. Lieber, E., and Morritz, F. L., "The Uses of Raney Nickel," Advan. Catal., Vol. 5, p. 417, Frankenburg, W. G., Rideal, E. K., and Komarewsky, V. I., eds., Academic Press, New York (1953).

82. Schröter, R., "Neur Methoden der Präparativen Organischen Chemie," Angew. Chem., Vol. 54, p. 229, p. 252 (1941), trans. in English, Newer Methods of Preparative Organic Chemistry, p. 61, Foerst, W., and Kirchner, F. K., eds., Academic Press, New York (1948).

83. Metals Handbook, Vol. 8, p. 260, p. 392, 8th ed., Am. Soc. Metals, Metals Park, Ohio (1973).

84. Reed-Hill, R. E., Physical Metallurgy Principles, p. 524, 2nd ed., Van Nostrand, New York (1973).

85. Covert, L. W., and Adkins, H., "Nickel by the Raney Process as a Catalyst of Hydrogenation," J. Am. Chem. Soc. 54, 4116 (1932).

86. Mozingo, R., "Catalyst, Raney Nickel," Organic Synthesis, Vol. 21, p. 15, Drake, N. L., ed., Wiley, New York (1941).

87. Pavlic, A. A., and Adkins, H., "Preparation of a Raney Nickel Catalyst," J. Am. Chem. Soc. 68, 1471 (1946).

88. Adkins, H., and Billica, H. R., "The Preparation of Raney Nickel Catalysts and Their Use under Conditions Comparable with Those for Platinum and Palladium Catalysts," J. Am. Chem. Soc. 70, 695 (1948).

89. Smith, H. A., Bedoit, W. C., Jr., and Fuzek, J. F., "The Preparation and Aging of Raney Nickel Catalysts," J. Am. Chem. Soc. 71, 3769 (1949).

90. Adkins, H., and Kresek, G., "Comparison of Nickel Catalysts in the Hydrogenation of β-Naphthol," J. Am. Chem. Soc. 70, 412 (1948).

91. Pattison, J. N. and Degering, E. F., "Some Factors Influencing the Activity of Raney Nickel Catalyst. I. Preparation of Raney Nickel from Nickel-Magnesium Alloy," J. Am. Chem. Soc. 72, 5756 (1950).

92. Dominguez, N. A., Lopez, I. C., and Franco, R., "Simple Preparation of a Very Active Raney Nickel Catalyst," J. Org. Chem. 26, 1625 (1961).

93. Nishimura, S., and Urushibara, Y., "A Method for the Preparation of the Raney Nickel Catalyst with a Greater Activity," J. Chem. Soc. Jap. 20, 199 (1957).

94. Yasumura, J., and Yoshino, T., "Laminated Raney Nickel Catalyst," Ind. Eng. Chem. Prod. Res. Develop. 11 (3) 290 (1972).

95. Veijola, V., Keränen, T. and Härkönen, M., "Raney Iron Prepared from Metal Powders as a Catalyst in Ammonia Synthesis," Kemia-Kemi 1, 43 (1976).

96. Betz, E. C., Can. Pat. 983,001 (1976).

97. McMaster, R. C., U.S. Pat. 2,608,469 (1952).

98. Hart, R. K., "A Study of Boehmite Formation on Aluminum Surfaces by Electron Diffraction," Trans. Farad. Soc. 50, 269 (1954).

99. Hart, R. K., "The Formation of Films on Aluminum Immersed in Water," Trans. Farad. Soc. 53, 1020 (1957).

100. Bernard, W. J., and Randall, J. J., Jr., "An Investigation of the Reaction Between Aluminum and Water," J. Electrochem. Soc. 107, 483 (1960).

101. Vedder, W., and Vermilyea, D. A., "Aluminum Water Reaction," Trans. Farad. Soc. 65, 561 (1969).

102. Kalecinski, J., "The Hydrated Electron in Reaction of Aluminum with Aqueous Solution of Alkali Hydroxides," Bull. Acad. Polon. Sci. Ser. Sci. Chem. 18, 262 (1970).

103. Streicher, M. A., "The Dissolution of Aluminum in Sodium Hydroxide Solutions," Trans. Electrochem. Soc. 93, 285 (1948).

104. Lure, B. A., Chernyshov, A. N., Perova, N. N., and Svetlov, B. S., "Kinetics of the Reaction of Aluminum with Water and Aqueous Alkalis," Kinetika i Kataliz 17 (6) 1453 (1976).

105. Fasman, A. B., Almashev, B. K., and Rechkin, V. N., "Physico-chemical Characteristics of Skeletal Catalysts Made from Binary Nickel Aluminides," Zh. Prikl. Khim. 46 (2), 282 (1973).

106. Presnyakov, A. A., Chernousova, K. T., Kabiev, T., Fasman, A. B., and Bocharova, T. T., "Mechanism of Catalyst Formation during the Leaching Process," Zh. Prikl. Khim. 45 (5) 985 (1967).

107. Robertson, S. D., and Anderson, R. B., "The Structure of Raney Nickel. IV. X-Ray Diffraction Studies," J. Catal. 23, 286 (1971).

108. Kokes, R. J., and Emmett, P. H., "The Role of Hydrogen in Raney Nickel Catalysts," J. Am. Chem. Soc. 81, 5032 (1959).

109. Swartzendruber, L. J., and Evans, B. J., "Nuclear Gamma Ray Resonance Observation of the Activation Process in Raney Iron and Urushibara Iron Catalysts," J. Catal. 43 , 207 (1976).

110. Freel, J., Pieters, W. J. M., and Anderson, R. B., "The Structure of Raney Nickel. II. Electron Microprobe Studies," J. Catal. 16, 281 (1970).

111. Robertson, S. D., Freel, J., and Anderson, R. B., "The Structure of Raney Nickel. VI. Transmission and Scanning Electron Microscopy Studies," J. Catal. 24, 130 (1972).

112. Sato, M., and Ohta, N., "Decrease of the Surface Area of Raney-Type Catalysts in the Aluminum Dissolution Process," Bull. Chem. Soc. Jap. 28, 182 (1955).

113. Mars, P., Scholten, J. J. F., and Zwietering, P., "On the Absence of Specially-Bound Hydrogen in Raney Nickel Catalysts," 2nd Intern. Cong. Catal., p. 1245, Paris (1960).

114. Fouilloux, P., Martin, G. A., Renouprez, A. J., Morawack, B., Imelik, B., and Prettre, M., "A Study of the Texture and Structure of Raney Nickel," J. Catal. 25, 212 (1972).

115. Freel, J., Pieters, W. J. M., and Anderson, R. B., "The Structure of Raney Nickel. I. Pore Structure," J. Catal. 14, 247 (1969).

116. Robertson, S. D., and Anderson, R. B., "The Structure of Raney Nickel. V. Partial Activation of the Catalyst," J. Catal. 41, 405 (1976).

117. Wainwright, M. S., and Anderson, R. B., "Raney Nickel-Copper Catalysts. II. Surface and Pore Structures," J. Catal. 64, 124 (1980).

118. Fasman, A. B., Sokolsky, D. V., Timofeeva, V. F., Bazhakov, D. K., and Pushkaryova, G. A., "The Influence of the Formation Mechanism and of the Chemical Composition on the Pore Structure of Raney Catalysts," Proc. Int. Symp. Pore Struct. Prop. Mater. RILEM/IUPAL 3B, 85 (1973).

119. Kokes, R. J., and Emmett, P. H., "Chemisorption of Carbon Monoxide, Carbon Dioxide and Nitrogen on Nickel Catalysts," J. Am. Chem. Soc. 82, 1037 (1960).

120. Kokes, R. J., and Emmett, P. H., "Adsorption Studies on Raney Nickel," J. Am. Chem. Soc. 83, 29 (1961).

121. Huff, J. R., Jasinski, R. J., and Parthasarathy, R., "Adsorption of Gases on Raney Nickel," Ind. Eng. Chem. Proc. Des. Develop. 3, 159 (1964).

122. Freel, J., Robertson, S. D., and Anderson, R. B., "The Structure of Raney Nickel. III. The Chemisorption of Hydrogen and Carbon Monoxide," J. Catal. 18, 243 (1970).

123. Kagan, A. S., Kagan, N. M. K., Ul'yanova, G. D., and Dmitrenko, V. E., "Shape of Crystals of Nickel Skeletal Catalysts," Soviet Physics - Crystallography 15 (6) 1057 (1971).

124. Pearce, C. E., and Lewis, D., "X-ray Diffraction Line Broadening Studies of Raney Copper and Nickel," J. Catal. 26, 318 (1972).

125. Williamson, G. K., and Hall, W. H., "X-Ray Line Broadening from Filed Aluminum and Wolfram," Acta. Met. 1, 22 (1953).

126. Warren, B. E., "X-Ray Studies of Reformed Metals," Prog. Metal Phys. 8, 147 (1959).

127. Kagan, A. S., Kagan, N. M., Ul'yanova, G. D., and Mironov, L. G., "Relation Between Structure and Activity of Raney Catalysts," Zh. Prikl. Khim. 47 (7), 978 (1973).

128. MacNab, J. I., and Anderson, R. B., "The Structure of Raney Nickel. VIII. Magnetic Properties Related to Particle Size and Hydrogen Evolution," J. Catal. 29, 338 (1973).

129. Tungler, A., Petro, J., Mathé, T., Heiszman, J., Békássy, S., and Csuros, Z., "Complex Study of Raney Nickel Skeleton Catalysts, VII," Acta Chim. Acad. Sci. Hung. 89 (1), 31 (1976).

130. Raney, M., "Catalysts from Alloys," Ind. Eng. Chem. 32, 1199 (1940).

131. Janko, A., and Pielaszek, J., "Lattice Spacing Determination for the α- and β-phases of Nickel-Hydrogen and Nickel-Deuterium Synthesis," Bull. Acad. Pol. Sci. Ser. Sci. Chim. 15 (11), 569 (1967).

132. Martin, G. A., and Fouilloux, P., "Influence of Aluminum and Hydrogen Contents on Magnetic Properties of Raney Nickel Catalysts," J. Catal. 38, 231 (1975).

133. Nicolau, I., and Anderson, R. B., "Hydrogen in a Commercial Raney Nickel," J. Catal. 68, 339 (1981).

134. Zavorin, V. A., Yakavleva, T. I., Toibaev, K. K., Fasman, A. B., and Sokol'skii, D. V., "State of Hydrogen in a Raney Nickel Catalyst," Zh. Prikl. Khim. 48 (1), 95 (1974).

135. Popov, N. I., Sokol'skii, D. V., Schvets, I. S., Kolomytsev, L. A., and Kan, S. I., "Thermal Desorption of Hydrogen from Reduced Raney Catalysts," Zh. Prikl. Khim. 47 (7), 976 (1973).

136. Nakabayashi, I., Hisano, T., and Terazawa, T., "Activity and Hydrogen Content of a Plate-Type Raney Nickel Catalyst," J. Catal. 58, 74 (1979).

137. MacNab, J. I., and Anderson, R. B., "The Structure of Raney Nickel. VII. Ferromagnetic Properties," J. Catal. 29, 328 (1973).

138. Renouprez, A. J., Fouilloux, P., and Coudurier, G., "Different Species of Hydrogen Chemisorbed on Raney Nickel Studied by Neutron Inelastic Spectroscopy," J. Chem. Soc., London, 73 (1) 1 (1977).

139. Shil'shtein, S. Sh., Vishnevetskii, E. A., Somenkov, V. A., and Fasman, A. B., "Low-Temperature Transfer of Hydrogen from the Surface to the Bulk of Dispersed Nickel," Izv. Akad. Nauk SSSR, Neorg. Mater. 16 (12), 2144 (1980).

140. Powder Diffraction File, Inorg. Sets, Berry, L. G., ed., Joint Committee on Powder Diffraction Standards, Swarthmore, Pa (1972).

141. Scherrer, P., Göttinger Nachr. 2, 98 (1918), quoted in ref.

142. Warren, B. E., "X-Ray Diffraction Methods," J. Appl. Phys. 12, 375 (1941).

143. Cullity, B. D., Elements of X-Ray Diffraction, 2nd ed., Addison-Wesley, Reading, Ma (1978).

144. Bartram, S. F., "Crystallite-Size Determination from Line Broadening and Spotty Patterns," Handbook of X-Rays, Chapter 17, Kaelble, E. F., ed., McGraw-Hill, Reading, Ma (1967).

145. Brunauer, S., Emmett, P. H., and Teller, E., "Adsorption of Gases in Multimolecular Layers," J. Am. Chem. Soc. 60, 309 (1938).

146. Gregg, S. J., and Sing, K. S. W., Adsorption, Surface Area and Porosity, Academic Press, New York (1967).

147. Willard, H. H., Merritt, L. L., Jr., and Dean, J. A., Instrumental Methods of Analysis, 5th ed., Van Nostrand, Princeton, N.J., (1974).

148. Purdy, G. R., and Anderson, R. B., "The Use of the Electron Probe Microanalyzer in Catalysis," Experimental Methods in Catalytic Research, Vol. 2, Chap. 3, Anderson, R. B., and Dawson, P. T., eds., Academic Press, New York (1976).

149. Duncumb, P., and Reed, S. J. B., "Quantitative Electron Probe Microanalysis," Nat. Bur. Stand. Spec. Publ. No. 298, p. 133 (1968).

150. Philibert, J., 3rd International Symposium on X-Ray Optics and X-Ray Microanalysis, Pattel, H. H., Costett, V. E., and Engstrom, E., eds., Academic Press, New York (1963).

151. Reed, S. J. B., "Characteristic Fluorescence Corrections in Electron-Probe Microanalysis," Brit. J. Appl. Phys. 16, 913 (1965).

152. The Kanthal Super Handbook, Bulten-Kanthal AB, Hallstahammar, Sweden (1972).

153. Metals Handbook, Vol. 7, p. 120, 8th ed., Am. Soc. Metals, Metals Park. Oh (1973).

154. Mondolfo, L. F., Metallography of Aluminum Alloys, Wiley, New York (1973).

155. Metals Handbook, Vol. 8, 8th ed., Am. Soc. Metals, Metals Park, Oh (1973).

156. Sorum, C. H., and Legowski, J. J., Introduction to Semimicro Qualitative Analysis, p. 275, 5th ed., Prentice-Hall, Englewood Cliffs, N. J. (1977).

157. Instruction Manual for Accusorb 2100, Micromeritics, Norcross, Ga (1979).

158. Operator's Manual 351 AA/AE Spectrophotometer, Instrumentation Laboratories, Wilmington, Ma (1975).

159. Allred, V. D., Buxton, S. R., and McBride, J. P., "Characteristic Properties of Thorium Oxide Particles," J. Phys. Chem. 61, 117 (1957).

160. Satterfield, C. N., Mass Transfer in Heterogenous Catalysis, M.I.T. Press, Cambridge, Ma (1970).

161. Butt, J. B., and Weekman, V. W., Jr., "Characterization of the Activity, Selectivity and Aging Properties of the Heterogeneous Catalysts," Standardization of Catalyst Test Methods, Weller, S. W., ed., AIChE Symp. Ser., Vol. 70, No. 143, Am. Inst. Chem. Eng., New York (1974).

162. Zein El Deen, A., Jacobs, J., and Baerns, M., "Kinetic Measurements of the Hydrogenation of Carbon Monoxide (Fischer-Tropsch Synthesis) Using an Internal Recycle Reactor, ACS Symp. Ser. 65, Weekman, V. W., Jr., and Luss, D., eds., Am. Chem. Soc., Washington, D.C. (1978).

163. Dietz, W. A., "Response Factors for Gas Chromatographic Analyses," J. Gas Chrom., p. 68, Feb. (1967).

164. Supelco Bulletin 770, "Quantitative Gas Chromatography," Supelco, Inc., Bellefonte, Pa.

165. Bird, R. B., Stewart, W. E., and Lightfoot, E. N., Transport Phenomena, Wiley, New York (1960).

166. Mears, D. E., "Tests for Transport Limitations in Experimental Catalytic Reactors," Ind. Eng. Chem. Proc. Des. Develop. 10 (4) 541 (1971).

☆U.S. GOVERNMENT PRINTING OFFICE: 1986-631-076/20065